UNIVERSITÀ DEGLI STUDI DI SASSARI

SCUOLA DI DOTTORATO IN SCIENZE

BIOMOLECOLARI E BIOTECNOLOGICHE

INDIRIZZO BIOCHIMICA E BIOLOGIA MOLECOLARE

XXVI CICLO

DIRETTORE: PROF.SSA CLAUDIA CROSIO

LRRK2

– AN IMPORTANT PLAYER IN PARKINSON'S DISEASE –

ROLE IN VESICLE AND RECEPTOR TRAFFICKING

Dottorando:

Dott.ssa Del Giudice Maria Grazia

Tutor:

Dott. Ciro Iaccarino

La presente tesi è stata prodotta nell'ambito della Scuola di Dottorato in Scienze Biomolecolari e Biotecnologiche dell'Università degli Studi di Sassari, a.a. 2010/2011 – XXVI ciclo, con il supporto di una borsa di studio finanziata con le risorse del P.O.R. SARDEGNA F.S.E. 2007-2013 - Obiettivo competitività regionale e occupazione, Asse IV Capitale umano, Linea di Attività l.3.1.

INDEX

	Page
SUMMARY	1
1. INTRODUCTION	5
1.1 PARKINSON DISEASE	6
1.2 DOPAMINE AND DOPAMINE RECEPTORS	9
1.2.1 Dopamine Synthesis and Metabolism	10
1.2.2 Dopamine Receptors trafficking	11
1.3 TREATMENT	14
1.3.1 Drug Therapy	14
1.3.2 Surgical Therapy	16
1.4 ETIOLOGY	16
1.4.1 Environmental Factors	17
1.4.2 Genetic Factors	19
1.5 LEUCINE RICH REPEAT KINASE 2 (LRRK2)	26
1.5.1 Physio-Pathological role of LRRK2 (PARK8)	26
1.6 LEUCINE RICH REPEAT KINASE 2 AND LEUCINE RICH REPAT KINASE 1	44

2. MAERIALS AND METHODS 48

2.1Materials 49

2.2 Methods 52

3. RESULTS 61

3.1 Characterization of PC12 Cells Stably Expressing Doxycycline-inducible LRRK2 WT or Pathological Mutants 62

3.2 LRRK2 Influences the Basal and Nicotine-induced secretion of DA in PC12 Cells 64

3.3 Vesicle Distribution in PC12 Cells Expressing LRRK2 G2019S Pathological Mutant 69

3.4 LRRK2 Increases Growth Hormone Extracellular Level in Neuronal Cells 71

3.5 LRRK2 Affects the Localization of Dopamine Receptor D1 both in Neuronal Cells and Transgenic Mouse Tissues 73

3.6 LRRK1 and LRRK2 functional redundancy in receptors trafficking 76

4. DISCUSSION 87

5. REFERENCES 108

- **ABBREVIATION LIST** 120

LRRK2 – an important player in Parkinson's Disease – role in vesicle and receptor trafficking

Del Giudice Maria Grazia: "LRRK2 – an important player in Parkinson's Disease – role in vesicle and receptor trafficking". Scuola di Dottorato in Scienze Biotecnologiche e Biomeolecolari – Università degli Studi di Sassari

SUMMARY

State of the art: PD (Parkinson's disease) is the second most common neurodegenerative disease affecting 4 million people worldwide. It is characterized by loss of pigmented neurons in the SNpc (*substantia nigra pars compacta*) and presence of cytoplasmic inclusion bodies (called Lewy bodies). In particular, the loss of dopaminergic neurons is responsible for both depletion of dopamine in the caudate putamen and motor dysfunction.

Although the majority of cases are sporadic, mutations in the leucine-rich repeat kinase 2 (LRRK2) gene (PARK8; OMIM #609007) are linked to late-onset autosomal dominant PD, accounting for up to 6-7% of familial PD cases compatible with dominant inheritance and 1–2% of sporadic PD cases. LRRK2 linked PD patients show clinical and neurochemical indistinguishable phenotype from sporadic affected ones. Up to date, LRRK2 protein is the most significant identified player in PD pathogenesis. Despite its predominance in PD, the physiological function of LRRK2 is not known, and therefore its precise role in the etiology of PD is far from being understood. Recent studies suggest a potential role of LRRK2 in vesicle trafficking. Subcellular fractionation and confocal analysis demonstrate the presence of LRRK2 in microsomal, synaptic vesicle–enriched and synaptosomal cytosolic fractions from animal brain, as well as the mitochondrial outer membrane. Moreover perturbations of LRRK2 expression have been shown to influence neurite extension and vesicle endocytosis. Finally, LRRK1 (Leucine Rich Repeat Kinase 1), the LRRK2 closest homologue, affects the EGF receptor (EGFR) endosmal trafficking. LRRK1 and 2 share protein domain organization and enzymatic activity typology although LRRK1 is not reported to be involved in PD pathogenesis. The assessment of a contingent crosstalk between these two proteins is still a gap in the field.

Objectives and models: My research focuses on studying LRRK2 role in the secretion process, neurotransmitter release and receptors trafficking. In order to study these aspects I used the following models: i) to study dopamine (DA) release, PC12 cells expressing LRRK2 WT or bearing pathological mutations under inducible promoter control. These cells are a

good model to investigate neurotransmitter release mechanisms since they share the same secretion system with dopaminergic neurons; ii) SH-SY5Y or HEK-293 cells transiently co-transfected with murine growth hormone (mGH) expressing construct as a secretion reporter and LRRK2 WT or mutant; iii) HEK-293 or SH-SY5Y, transiently co-transfected with construct coding for Dopamine Receptor D1 (DRD1) and LRRK2 WT or mutant; iv) Striatum and hippocampus from WT or transgenic G2019S LRRK2 mice. Finally, I conducted a functional redundancy study between LRRK2 and its closest homologue LRRK1, in respect to EGFR trafficking. EGFR and dopamine receptors (DAR) are members respectively of tyrosine kinase receptors family and G protein coupled receptors family. For this study I developed a confocal microscopy assay making use of different SH-SY5Y cell lines: LRRK2 Knock-Down (KD) stably expressing GFP-LRRK1, LRRK1 KD SH-SY5Y stably expressing GFP-LRRK2, or stable SH-SY5Y co-expressing a KD control construct and GFP-LRRK1 or 2 .

Experimental approach and results: LRRK2 is reported to interact with a broad range of proteins involved in synaptic functions, cytoskeleton dynamics, and vesicular trafficking, moreover previous work done in the laboratories have provided different hints of a potential role of LRRK2 in vesiscle trafficking . However, up to date, the physiological function of LRRK2 is elusive. The main topic of my PhD thesis was to figure out which role has LRRK2 in the vesicle trafficking using the following secretion reporter assays: SH-SY5Y were transiently co-transfected with mGH and WT or mutant LRRK2 both pathological and kinase dead. After 24 hours of protein expression, growth medium and cell lysates were collected and the mGH secretion level was measured in presence of WT or mutant LRRK2. The results demonstrate that expression of WT or pathological mutant LRRK2 determines an increase in basal GH extracellular level, moreover this increase is greater in presence of the pathological G2019S mutation. Furthermore the LRRK2 effect on mGH secretion is absent when a LRRK2 kinase dead mutant is co-transfected. To further elucidate LRRK2 kinase activity contribution in the observed mGH reporter secretion changes, the same assay was performed treating SH-SY5Y cells co-transfected with mGH and G2019S with the LRRK2 kinase inhibitor GSK2578215A. The presence of LRRK2 inhibitor significantly reduces the increase in GH extracellular level due to LRRK2 G2019S expression.

Neurotransmitter release has been studied in collaboration with a pharmacology research group of Department of Clinical and Experimental Medicine - University of Sassari - that has performed all the microdialysis experiments. To control LRRK2 expression in PC12, the Tet-ON system was used. Upon induction with doxycycline to obtain LRRK2 expression, cells were treated with nicotine to induce dopamine release. Direct measuring of dopamine released was performed by microdialysis. Main result of this set of experiments is that the pathological mutant G2019S determines a significant DA extracellular level increase compared to WT in both basal and nicotine induced condition. The same PC12 model was utilized to study vesicle distribution by Electron Microscopy (EM). Resultant images play up a significant increase of the electron-dense vesicles in the proximity of the plasma membrane in presence of G2019S mutant. These vesicles are probably recruited for docking phase of exocytosis process.

Vesicle trafficking regulates different cellular functions, including neurotransmitter or protein release and localization of membrane receptors. The previous results prompted me to analyze the possible effect of LRRK2 on membrane receptor localization using the membrane levels of DRD1 as a read-out. SH-SY5Y cells were transfected with plasmid coding for DRD1 in absence or in presence of LRKK2 G2019S, LRKK2 D1994A (kinase dead mutant), LRRK2 R1441G, or LRRK2 completely lacking the kinase domain (ΔKIN LRRK2). 48 hours after transfection, the sub-cellular distribution of D1DR receptors from cell lysates was analyzed by purification of different cell components. The presence of LRRK2 G2019S or R1441G and, to a lesser extent, LRRK2 D1994A or WT determines a significant increase in the level of membrane-associated DRD1 compared to DRD1 alone, while the effect is completely abolished in presence of the ΔKIN mutant. Interestingly all these results seem to be evident only in neuronal cells since they are not displayed in non-neuronal cell lines such as HEK-293.

To extend the analysis to a more physiological system I analyzed the distribution of two neurotransmitter receptors in the striatum of transgenic LRRK2 G2019S mice compared to non-transgenic ones. In particular, I analyzed the NMDA-NR1 receptor (NR1) and DRD1 distribution in total, membrane or vesicle fractions obtained from the striatum of 5

different animals of the two genotypes. LRRK2 G2019S expression leads to a significant increase of DRD1 in membrane fraction paralleling a significant decrease in vesicle fraction, with no significant differences in total protein extracts between the two genotypes. No significant differences among the different fractions were observed for NR1, clathrin or sec8, a member of the exocyst complex.

In line with these results on vesicle trafficking, I developed a confocal microscopy assay to assess functional redundancy between LRRK2 and LRRK1 in respect to EGFR trafficking. SHSY5Y KD for one of the two proteins but expressing a GFP fusion of the homologue one are treated with EGF-Rhodamine conjugate to track the receptor internalization. GFP-LRRK1 is co-localizing with EGFR in both LRRK2 KD or control conditions. On the opposite, LRRK2 does not co-localize with EGFR in control condition as well as in LRRK1 KD background. Thus LRRK2 seems not able to compensate for LRRK1 function in EGFR internalization process. This result has been validated by two-way ANOVA analysis. At the moment I am developing a similar assay to investigate the role of LRRK1 or 2 on dopamine receptor trafficking.

CHAPTER 1

INTRODUCTION

1.1 PARKINSON DISEASE

Parkinson Disease (PD) is a chronic, neurodegenerative, progressive disease. The main neuropathological features are the extensive and selective loss of neurons in the Substantia Nigra pars compacta (SNpc) and the presence of intraneuronal proteinacious cytoplasmic inclusions, termed "Lewy Bodies" (LBs). The cell bodies of nigrostriatal neurons are in the SNpc, and they project primarily to the putamen (in the striatum). The loss of these neurons, which normally contain conspicuous amounts of neuromelanin, produces the classic gross neuropathological finding of SNpc depigmentation (Figure 1B)(2). Dopamine (DA) depletion in the striatum and neuron loss in SNpc are also responsible of the characteristic motor symptoms of PD: tremor at rest, rigidity, postural instability and bradykinesia. At the onset of symptoms, striatal DA is depleted of ≈80%, and ≈60% of SNpc

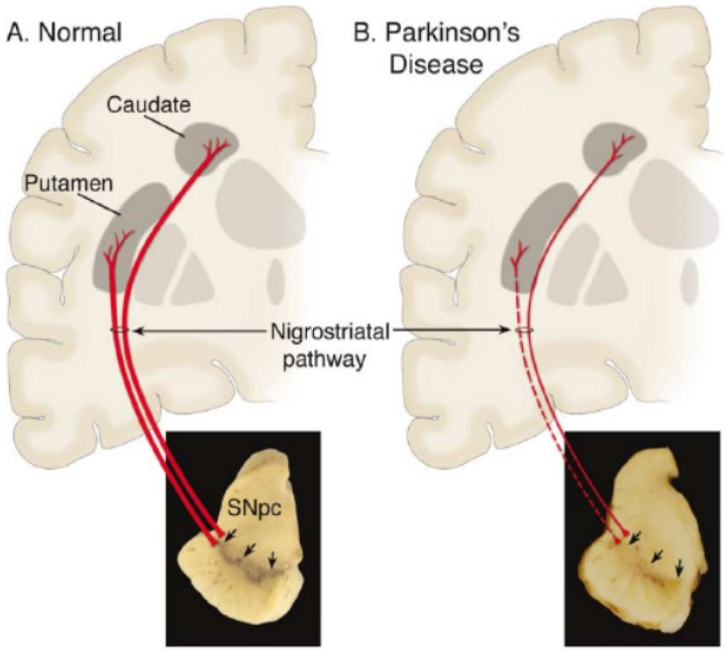

Figure 1: (A)Schematic representation of the normal nigrostriatal pathway (in red). It is composed of dopaminergic neurons whose cell bodies are located in the SNpc; (arrows). These neurons project (thick solid red lines) to the striatum (i.e., putamen and caudate nucleus). (B) The diseased nigrostriatal pathway (in red) in PD. There is a marked loss of dopaminergic neurons that project to the putamen (dashed line) The photograph demonstrates depigmentation (i.e., loss of dark-brown pigment neuromelanin; (Arrows)(1)

dopaminergic neurons have already been lost. Nevertheless, the neurodegeneration is not limited to the SNpc but extends to other encephalic sub regions including noradrenergic neurons in the locus coeruleus and serotoninergic neurons in the nucleus basalis (2).

Incidence of PD is estimated in about 20/100000 cases per year in the population over 50 years, up to 120/100000 new cases per year among the over 70 years old (2). Sometimes, differences in incidence are observed between different ethnic groups probably due to disease etiology namely linked to environmental risk factors exposure or genetic susceptibility. The average age onset is about 60 years, even if 4% of patients display an early disease development (before 50 years). Furthermore, since the clinical features of PD emerge only when a high percentage of SNpc neurons is compromised and the striatal DA levels are strongly reduced, it is plausible that epidemiology studies underestimate the disease incidence.

Parkinson Disease has an heterogeneous nature, there are slow and fast progression forms; relatively simple symptomatology beside clinically complex forms.

Indeed Parkinson forms are classified into: Primary Parkinson, Parkinson Plus and secondary parkinsonism (see table 1) (3)

Idiopathic PD, also known as Primary Parkinson, is characterized by rigidity, resting tremor, slowness of movement, rigidity and balance loss. This form of pathology has slow progress rate and at present there are no external causes ascribable to the symptomatology.

In life, the diagnosis of PD is made on clinical features, but definite diagnosis requires the identification of both LB and SNpc dopaminergic neuron loss. LBs are not specific for PD, however, and are also found in AD, in a condition called "dementia with LB disease" and as an incidental pathologic finding in people of advanced age at a greater frequency than the prevalence of PD (3). LBs are spherical eosinophilic cytoplasmic protein aggregates composed of numerous proteins, including α-synuclein, parkin, ubiquitin, and neurofilaments, and they are found in dopaminergic neurons in all affected brain regions (4, 5). LBs are more than 15 μm in diameter and have an organized structure containing a dense hyaline core surrounded by a clear halo. Electron microscopy reveals a dense granulovesicular core surrounded by a ring of radiating 8–10 nm fibrils (6).

Category	Features
Primary Parkinson	Parkinson Disease (sporadic – familial) Monogenic Parkinsonism
Secondary Parkinsonism	Vascular: multi-infarct state Trauma Infectious: post encephalitic Toxin: Mn, CO, MPTP, Cyanide Drug induced: dopamine antagonist and depletors
Parkinson Plus	Progressive sopranuclear palsy Multiple System Atrophy Syndromes Diffuse Lewy Bodies Disease

Table 1. Parkinson forms.

Another parkinsonism form is "Parkinson Plus". In this category are grouped some neurodegenerative disorders showing a strict clinical similarity with PD, but characterized by concurrent presence of other neurological aspects (cerebellar, pyramidal, vegetative, cognitive). The most important among the Parkinson Plus manifestations are: Progressive sopranuclear palsy, Multiple System Atrophy Syndrome and the corticobasal degeneration (7).

The last parkinsonism category is Secondary Parkinsonism. These forms display similar characteristics to PD, have known etiology, variable progress and a very low prevalence. Secondary Parkinsonisms can be induced by toxins (Manganese, carbon monoxide, cyanide), drugs (neuroleptics, antiemetics, calcium blockers), or traumatic brain damages (i.e. Pugilistic Parkinson). Drug-induced parkinsonism are marked out by the lack of neuronal loss and are subject to remission after drug assumption interruption. On the contrary, neurotoxins damage to the SNpc is irreversible (8). All Secondary Parkinsonisms

are characterized of a very fast clinical development, lacking or reduced drug response and no Lewy Bodies presence in respect to the Primary Parkinson forms.

For years, diagnostic criteria for idiopathic Parkinson Disease have been developed. Recently Gelb and colleagues have reviewed them highlighting how clinical diagnosis of PD is established on the presence of cardinal motor symptoms in combination with the exclusion of specific uncharacteristic symptoms. Among motor cardinal signs:

- Resting tremor
- Rigidity
- Bradykinesia
- Asymmetric onset
- Postural instability.

Lastly, also the responsiveness to levodopa (L-Dopa) is considered. This is, with sporadic exceptions, a necessary but not exclusive requisite for PD diagnosis, inasmuch is observed also in atypical forms of the disease (9, 10).

1.2 DOPAMINE AND DOPAMINE RECEPTORS

As mentioned before, a progressive demise of the dopaminergic cells in the SNpc is observed in post-mortem brains of PD patients. From SNpc the dopaminergic neurons form synapses mainly with neurons of the *striatum* (another nucleus of the *basal ganglia)*. This system constitutes the nigrostriatal pathway, which regulates the *extrapyramidal system* designated to the movement, posture and balance minding control (11).

Dopamine is synthetized by dopaminergic cells in SNpc (pre-synaptic level) (12, 13), thus, in the parkinsonian patient, SNpc cells degeneration dramatically drops dopamine production and dopamine levels in the *striatum* producing all the motor symptoms which characterize the pathology.

.

1.2.1 Dopamine synthesis and metabolism

Dopamine, together with adrenaline and noradrenaline, constitutes the catecholamine neurotransmitter class. They are all synthetized starting from tyrosine through a shared pathway including five enzymes: the tyrosine-hydroxylase, an aromatic amino acid decarboxylase; the dopamine β-hydroxylase; the pteridine-reductase and the feniletanolamina-N-methyltransferase. The first enzyme in the pathway, the tyrosine-hydroxylase, converts the amino acid tyrosine to L- dihydroxiphenilalanine (L-DOPA). At the next step of the pathway, the L-DOPA is decarboxylated by the DOPA-decaroxylase obtaining dopamine and CO_2. The dopamine β-hydroxylase converts dopamine in norepinephrine.

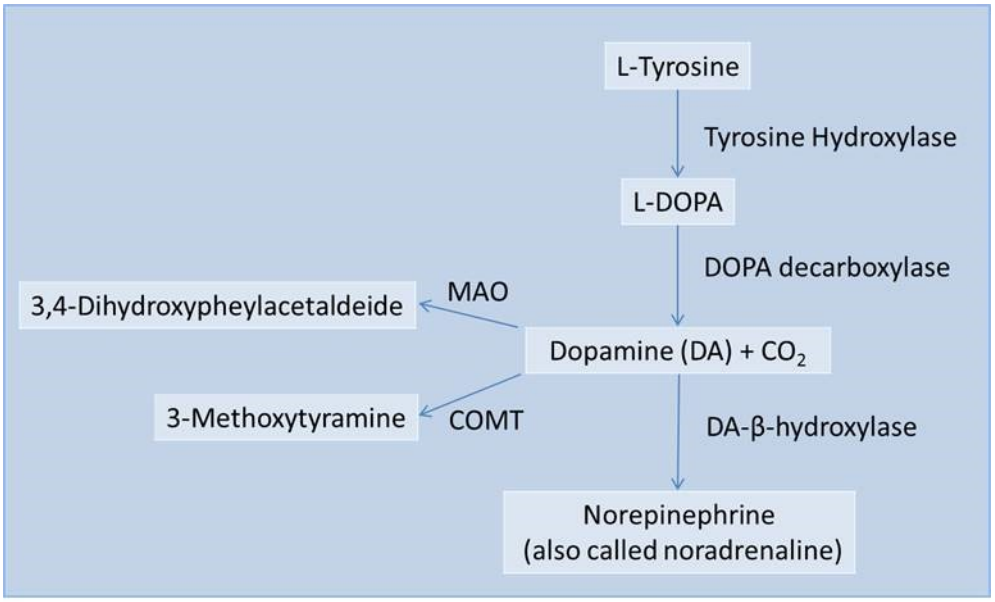

Figure 2: Synthesis and metabolism of Dopamine (DA)

Once synthesized in the SNpc neurons, dopamine is stored in vesicles and released in the inter-synaptic space, where is free to interact with DA receptors (both at pre and postsynaptic level) and exert its action. Dopamine activity is terminated with a process called "re-uptake" at the presynaptic terminal. In this process dopamine is transported in the presynaptic neuron by the dopamine transporter (DAT), and, is degradated by two enzymes: the monoamine-oxidase (MAO) and the catechyl-O-metyl-transferase (COMT). The MAOs are localized in the external mitochondrial membrane, albeit other MAOs are

also present outside the dopaminergic neuron, respectively MAO A and MAO B; whereas the COMT are extraneuronal enzymes that inactivate catecholamines by methylation of the hydroxyls on the catechol ring (Figure 2).

1.2.2 Dopamine receptors trafficking

Dopamine receptors belong to the large family of heptahelical transmembrane spanning G protein-coupled receptors (GPCRs). Five mammalian dopamine receptor subtypes have been identified and are classified into two major groups, the D1- (D1 and D5) and D2- (D2, D3, D4) like receptors (14, 15).

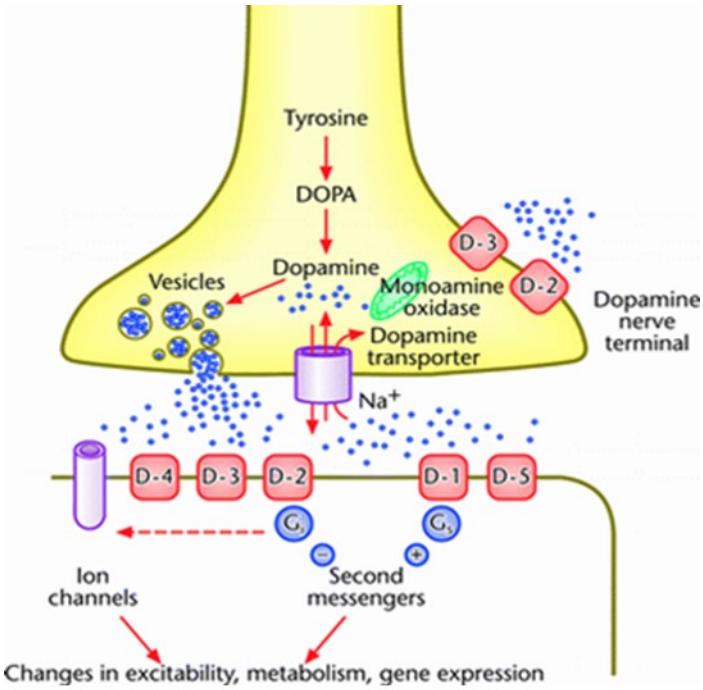

Figure 3: Dopaminergic Synapsis.

Although dopamine receptors are similar in structure, receptor subtypes differ by their affinity for dopamine and coupling to downstream effectors, including heterotrimeric guanine nucleotide-binding proteins (G proteins) (14, 16). Dopamine receptor subtypes are expressed differentially throughout the brain. Among the D1-like receptors, D1 receptors are the most abundant, with mRNA transcripts found in the *neostriatum, nucleus accumbens, and olfactory tubercle*. Lower levels of D1 receptor mRNA are found in the cerebral cortex, hypothalamus, and thalamus (14). Among the D2-like receptors, D2 receptors are the most abundant, with mRNA transcripts found in the *neostriatum, nucleus accumbens, and olfactory tubercle*, as well as the midbrain, including the s*ubstantia nigra and ventral tegmental area* (14).

The canonical mechanisms for GPCRs signaling, reviewed in (17) can be extended to dopamine receptors D1 and D2.

Binding of ligands (such as hormones, neurotransmitters or sensory stimuli) induces conformational changes in the transmembrane and intracellular domains of the receptor thereby allowing interactions with heterotrimeric G proteins. Activated GPCRs act a guanine nucleotide exchange factors (GEFs) for the α subunits of heterotrimeric G proteins, catalyzing the release of GDP and the binding of GTP for G protein activation. The activated G protein subunits (α•GTP and βγ) can then associate with downstream effectors (17) including second messengers like adnylate cyclase and ion channels, to modulate various aspects of cellular physiology. A distinguishing feature of D1- and D2-like receptors is their differential coupling to heterotrimeric G proteins. In many cell types D1-like receptors couple to Gαs, which activates adenylate cyclase (52, 53) while D2-like receptors couple to the pertussis toxin-sensitive Gαi or Gαo, which inhibit adenylate cyclase (48, 54)

G protein-mediated signaling by agonist-activated GPCRs can be terminated through GPCR phosphorylation by GPCR kinases (GRKs) and concomitant GPCR association with arrestins, which interact with clathrin and the clathrin adaptor AP2 to drive GPCR internalization into endosomes (see figure 4 from (17)) Finally, G protein activity is terminated by GTP hydrolysis and the re-formation of the G protein heterotrimer. GPCR internalization regulates the functional process of receptor desensitization (17), a process that determines the end of the GPCR signaling.

Following internalization after association with arrestins, GPCRs can be trafficked to lysosomes, where they are ultimately degraded, or to recycling endosomes for recycling back to the cell surface in the functional process of re-sensitization — whereby the cell is re-sensitized for another round of signaling.

GPCR internalization is heavily influenced by two of the canonical families of GPCR-interacting proteins, the GRKs and the arrestins. However, certain other GPCR-interacting proteins can also regulate the endocytic trafficking of GPCRs in a more receptor selective manner. For example, the GPCR-associated sorting proteins (GASPs) promotes D2R trafficking to lysosomes following agonist stimulated endocytosis (17).

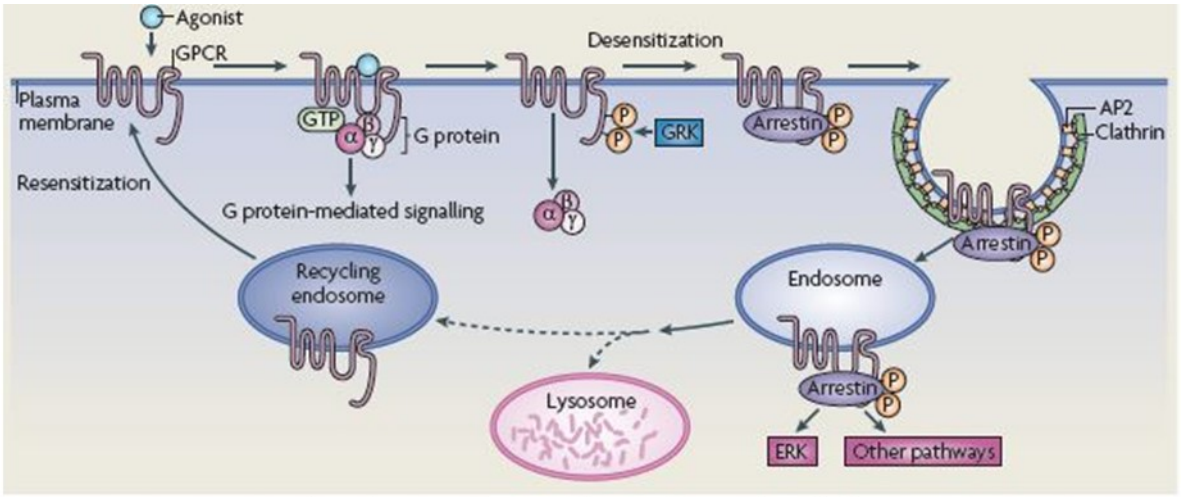

Figure 4: Canonical mechanisms for GPCR's signalling and trafficking. Nature Review .

Dopamine receptor-mediated signaling is a tightly regulated process that is highly dependent on the accessibility of receptors to agonist binding at the cell surface. This availability of functional surface receptors is governed by a strict balance of the various intracellular receptor trafficking pathways that, in association with receptor sensitivity, work in concert to regulate the amplitude of agonist-mediated cellular responsiveness (14).

It has been demonstrated that GPCRs are not static within the plasma membrane but can move in the plane of the membrane by the passive process of lateral diffusion (18-20). One of the key factors that govern the dynamics of lateral diffusion of GPCRs is their association with other cellular proteins. The formation of these protein complexes can serve to restrict the movements of the GPCRs, effectively stabilizing the receptors in specific microdomains within the membrane, such as the synapses for example. Movement by lateral diffusion has been reported for several GPCRs including dopamine D1 receptors. In cultured neurons, approximately 65% of D1 receptors are mobile with the remaining receptor anchored within the membrane. This ratio of mobile *vs* anchored receptors is not fixed, but fluctuating. Scaffolding proteins have a role in this process, either stabilizing DA receptors at the membrane or decreasing their stability.

1.3 TREATMENT

Current PD medication treat symptoms none halt or retard dopaminergic neuron degeneration. The main obstacle to developing neuroprotective therapies is a limited understanding of the key molecular events that provoke neurodegeneration (2).

1.3.1 Drug Therapy

As mentioned above, to date, no defined neuroprotective treatment for PD influencing the natural progressive course of the disease has been established. Therefore current treatments aim at correcting the dopaminergic deficit in the S*ubstantia Nigra* either through (i) the substitution of dopamine via its precursor levodopa, or (ii) the prolongation of the synaptic availability of dopamine via inhibitors of enzymes of the dopamine metabolism: COMT (catechyl-O-metyl-transferase) and MAO B (monoamine-oxidase B), or (iii) the activation of functional relevant receptors via dopamine-agonists (21).

Levodopa

Levodopa (L-dopa) is the most effective drug in the treatment of PD and virtually all patients benefit from this treatment (21). L-dopa is the natural parent for dopamine, it enters in the dopaminergic neurons that convert it into dopamine. Direct administration of

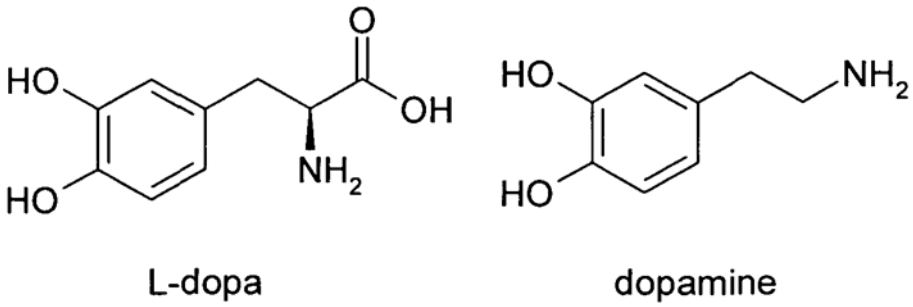

Figure 5: Levodopa and Dopamine (3 4 dihydroxyphenylalanine) structures.

dopamine as a drug is not possible as it is not able to pass the hematoencephalic barrier and thus reach the dopaminergic neurons. The L-dopa is orally administered and absorbed in the bowel, and finally enters the systemic circulation. The L-dopa decarboxylase, outside of CNS, catalyzes the transformation of L-dopa into dopamine by removing its carboxylic

group. Since dopamine has no therapeutic effect at peripheral level rather unpleasant side effects, L-dopa is routinely administered in combination with a decarboxylase inhibitor to avoid peripheral L-dopa decarboxylase activity. Once in the brain, L-dopa is converted in dopamine by neuronal L-dopa decarboxylase in the cytoplasm, here is actively transported in the synaptic vesicles. Dopamine storing in vesicles avoids its enzymatic degradation by MAO and it is essential for the following release of the neurotransmitter in the inter-synaptic space upon neuronal stimulation. When the impulse reach the dopaminergic neurons, the vesicles fuse their membrane with the neuronal plasma membrane releasing dopamine in the synaptic space, where it can reach the receptors on the post-synaptic neurons and complete its therapeutic activity.

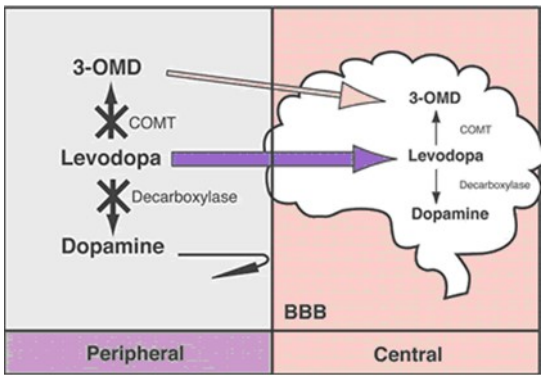

Figure 6: Levodopa action mechanism

Although levodopa represents the gold standard in PD therapy, chronic levodopa treatment is known to result in motor complications (dyskinesia, dystonia) or neuropsychiatric problems in later stage of disease (21).

Dopamine agonists

Dopamine agonists are a class of drugs that share the capacity to directly stimulate dopamine receptors. This class of therapeutics compounds offers some advantages over levodopa therapy as the reduced incidence of levodopa-related adverse effects, no requirement of metabolic conversion and potential neuro-protective benefits. However, the anti-Parkinson efficacy is limited and motor complications are not completely prevented.

COMT inhibitors

To date, the entacapone is the only substance available in this therapeutic class and it is administered in association with levodopa as previously described. COMT inhibitors exert their therapeutic effects via inhibition of peripheral levodopa catabolism and therefore

increasing levodopa bioavailability. Thus, COMT inhibition is associated with an increased stability of levodopa plasma levels, suppressing peaks of levodopa concentrations, which are thought to be associated with motor complications (21).

MAO B inhibitors

The most diffused MAO B inhibitor in PD therapy is selegiline; it is a selective inhibitor of the oxidative catabolism of dopamine via irreversible inhibition of the monoamine-oxidase B. Therefore selegiline amplifies the effect of levodopa. In experimental studies selegiline was not only able to improve parkinsonian symptoms but also to exert some neuroprotective effects on dopaminergic neurons. However, clinical studies on the efficacy of this therapeutics have produced controversial results (21).

1.3.2 Surgical therapy

Recent advances in neurosurgery and imaging techniques have allowed the development of novel therapeutic approaches for PD. In general there is a main recently developed approach to the surgical therapy of PD: the deep brain stimulation (21) is a surgical treatment involving the implantation of a medical device called a brain pacemaker, which sends electrical impulses to specific parts of the brain.

1.4 ETIOLOGY

Parkinson Disease has a complex and multifactorial etiology, involving genetic and environmental factors. However the molecular details of the degenerative process are still barely known even though the discovery of PD related genes has shed new light on the cellular mechanisms that might be affected in the PD neurodegeneration.

1.4.1 Environmental Factors

The environmental etiology hypothesis posits that PD-related neurodegeneration results from exposure to some dopaminergic neurotoxins. Theoretically, the progressive neurodegeneration in PD could be produced by chronic neurotoxin exposure or by limited exposure initiating a self-perpetuating cascade of deleterious events (2). An example of how an exogenous toxin can mimic the clinical and pathological features of PD is the MPTP (1-methyl-4-phenyl-1, 2, 3, 6,-tetrahydropyridine or meperidine) intoxication (22). The discovery of MPTP as dopaminergic neurotoxin date in 1982 when young drug users developed a rapidly progressive parkinsonian syndrome due to intravenous use of a street preparation of 1-methyl-4-phenyl-4-propionoxypiperidine (MPPP), an analog of the narcotic Demerol (22) in which MPTP was present as contaminant. In humans and monkeys, MPTP produces an irreversible and severe parkinsonian syndrome characterized by all the PD features, including tremor, rigidity, slowness of movement, postural instability and freezing. In MPTP-intoxicated individuals the beneficial response to levodopa and development of long-term motor complications to medical therapy are virtually identical to those seen in PD patients. Similar to PD, MPTP susceptibility increases with age and is observed the same topologic pattern in the damages to the dopaminergic system (2) (23, 24) In PD, dopaminergic neurons seem to be more sensible to degeneration in respect to other neuronal populations in the brain, these neurons are also more susceptible to MPTP induced degeneration (2). All these clinical

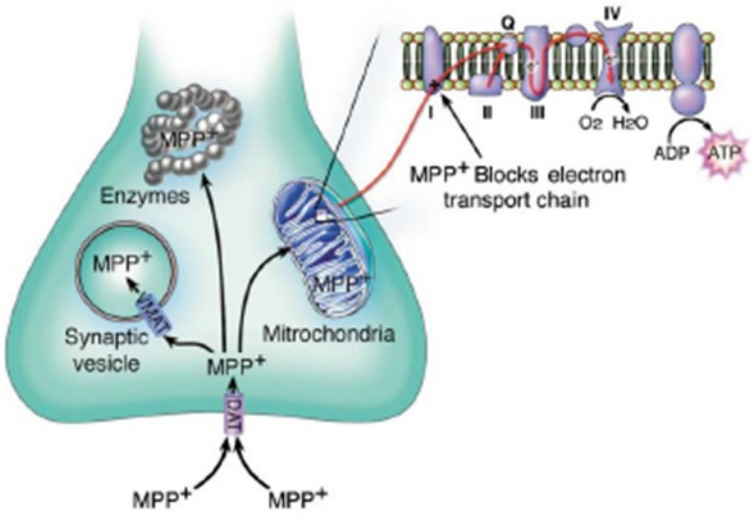

Figure 7: Schematic representation of MPP+ intracellular pathways.

manifestations on MPTP intoxication corroborates the environmental hypothesis of PD etiology and the MPTP-treated monkeys became a good model for PD studies. Some of these studies unraveled the MPTP mechanism of toxicity. After systemic administration, MPTP, which is highly lipophilic, cross the blood-brain barrier. Once in the brain the pro-toxin MPTP is oxidized to 1-methyl-4-phenyl-2, 3, -dihydropyridinium (MPDP+) by MAO-B in the glia, and probably by spontaneous oxidation it becomes MPP+, the active toxic molecule. Thereafter it is released in the extracellular space by an unknown mechanism. Finally is concentrated into dopaminergic neurons through its high affinity for the dopamine transporter (DAT). Inside neurons MPP+ can follow at least three routes: (i) it can bind to the vesicular monoamine transporter-2 (VMAT2) (25), which translocate MPP+ into synaptosomal vesicles; (ii) it can be concentrated within the mitochondria (26) and (iii) it can remain in the cytosol to interact with the cytosolic enzymes (27). The toxic mechanism of MPP+ is carried out in the mitochondria where damages electron transport chain (see figure 7). Here MPP+ blocks complex I, which interrupts the transfer of electrons to ubiquinone. This perturbation enhances the production of ROS species and decreases the synthesis of ATP with the final result of apoptosis in the neurons (2, 22). The MPTP toxicity mechanism supports the idea of an involvement of the mitochondria and oxidative stress in PD pathogenesis.

Many epidemiologic studies have been done to clarify if toxin exposure can cause PD. Subject of these studies have been pesticides and insecticides with structure similar to MPP+ as paraquat and rotenone but none of these studies reported unmistakable results. So far, there is no clear evidence that exposure to herbicides or insecticides can cause PD.

Other epidemiological studies reported that cigarette smoking and coffee drinking are inversely associated with the risk of PD development. Based on the apparent protective effect of smoking, the therapeutic effect of nicotine has been tested in a few clinical trials, but no improvement of motor symptoms with transdermal nicotine treatment has been documented (28).

Another possibility, which does not fit into a genetic or environmental category, is that an endogenous toxin may be responsible for PD neurodegeneration. Distortions of normal

metabolism might create toxic substances due to environmental exposures or inherited differences in metabolic pathways. One source of endogenous toxins may be the normal metabolism of DA, which generates harmful reactive oxygen species (ROS)(29). Consistent with this hypothesis is the report that patients harboring specific polymorphisms in the gene encoding xenobiotic detoxifying enzyme cytochrome P450 may be at higher risk of developing young onset PD (30). Further, toxic derivatives of isoquinoline have been recovered from PD brains (2, 31).

In addition to toxins, other environmental factors, which can be considered as risk factors rather than causative elements, are lifestyle and habits. For instance, repetitive or simply violent traumas can provoke a parkinson-like progressive syndrome as the one frequently observed among boxers from which the name "Pugilistic Parkinson Syndrome". Another two risk influencing factors are age and sex, males are indeed more affected in respect to women (in a 1,5:1 ratio). In humans, neuronal and SNpc neuromelanin loss increases around 60 years, coinciding with the average age of PD onset. Since neuromelanin has a protective effect in neurons against free radicals and toxins, the decrease in this pigment may predispose the brain of aged people to Parkinson (32).

Finally, it has been hypothesized an infective etiology: clinical manifestations similar to PD have been observed in patients affected, in the past, by a viral encephalitis propagated in pandemic in 1920 (33, 34).

1.4.2 Genetic Factors

For a long time Parkinson Disease has been considered a sporadic disease, until Leroux in 1880 tracked recurring PD cases in the same family. This observation led to the hypothesis that hereditary factors could increase susceptibility to the pathology.(28). In the last decade several genome wide association studies allowed the identification of numerous mutations in different genes in families with mendelian inheritance parkinsonisms. These findings have been made possible through the analysis of rare familial PD forms characterized by clinical and neuropathological features sometimes different from idiopathic forms. More

recently some susceptibility loci for PD have been identified, but further analysis are required to confirm their association with Parkinson Disease (35, 36).

Up to date, 16 mendelian transmission forms of Parkinson Disease are known. Some of them have an autosomal dominant (AD) inheritance pattern while others have an autosomal recessive (AR) one. Gene products have been associated to 10 out of these 16 forms whereas other causative (PARK 3) or predisponent (PARK 10, PARK 12, PARK 16) chromosomal loci are still waiting to be linked to a precise gene product (37) (See table 2).

Locus/ gene	Inheritance	Onset	Pathology	Map position	Gene	Tissue specificity	Cellular localization in neurons	Expression during development
PARK1	Dominant	40's	nigral degeneration with Lewy-bodies	4q21	α-synuclein	expressed everywhere except liver	presynaptic terminal, nucleus	embryonic expression, all tissues
PARK2	Recessive	20–40	nigral degeneration without Lewy-bodies,	6q25	Parkin	brain, heart, muscle, testis	ubiquitous	embryonic expression, all tissues
PARK3	Dominant	60's	nigral degeneration with Lewy-bodies, Plaques and tangles in some	2p13	?	?	?	?
PARK4	Dominant	30's	nigral degeneration with Lewy-bodies, vacuoles in neurons of the hippocampus	4q21	α-synuclein triplications and duplications	expressed everywhere except liver	presynaptic terminal, nucleus	embryonic expression, all tissues
PARK5	Dominant	~50	no pathology reported	4p14	ubiquitin C-terminal hydrolase L1	brain, neuroendocrine system, ovary	cell body and processes	embryonic expression, especially studied in NPCs
PARK6	Recessive	30–40	no pathology reported	1p35-37	PINK1	highly expressed in heart, skeletal muscle, testis, lower levels in brain, placenta, liver, kidney, pancreas, prostate, ovary and small intestine	mitochondrial, cytoplasmic	embryonic expression in testis, otherwise unknown
PARK7	Recessive	30–40	no pathology reported	1p38	DJ-1	pancreas, kidney, skeletal muscle, liver, testis, heart, lower levels in brain, placenta	cytoplasmic, nuclear, mitochdrial	unknown
PARK8	Dominant	~60	variable α-synuclein and tau pathology	12cen	LRRK2	ubiquitous	ubiquitous	embryonic expression in various tissues
PARK9	Recessive	20–40	no pathology reported	1p36	ATP13A2	ubiquitous	lysosome	unknown
PARK10	Dominant (?)	50–60	no pathology reported	1p32	?	?	?	?
PARK11	Dominant (?)	Late	no pathology reported	2q34	GIGYF2	heart, liver, kidney, brain and lung	?	?
PARK12	X-linked	Late	no pathology reported	Xq31	?	?	?	?
PARK13	?	Late	no pathology reported	2p12	OmiHtrA2	expressed everywhere	inner membrane space of mitochondria	embryonic expression in various tissues

Table 2: Summary of PARK1-PARK13 expression patterns (for references, please see text). From Biskup et al. (1)

Mendelian inheritance Parkinson forms and associated genes

Although genetic PD forms represent only a little percentage of the total cases, studies on cellular or animal models based on the expression familial Parkinson gene have importantly contributed to elucidate disease etiopathology. In this session, the main characteristics of PD associated genes are described, giving particular relevance to those ones that are widely accepted to be conclusively associated with mendelian forms of the disease (35) and have been more extensively studied (PARK1⁄4, PARK2, PARK5, PARK6, PARK7). For a more detailed presentation of PARK8 locus see paragraph 1.5.

- **Alpha-synuclein (SNCA or α-Syn) - PARK1/PARK4**

Although Lewy bodies (LB) represent one of the principal landmarks of PD, and their first observation date to 1912, only in 1997 Alpha Synuclein has been identified as the most important component of these protein inclusions (5). In the same year, 1997, the identification of SNCA as the first gene implicated in PD resulted from linkage analysis in the ''Contursi'' kindred, with the point mutation A53T being associated with the disease in this family. Since then, two other point mutations, A30P and E46K, as well as duplications and triplications of the SNCA gene, have been identified among PD patients. The point mutations and gene rearrangements result in rare autosomal dominant, middle to late onset PD. The loss of dopaminergic neurons and the presence of Lewy bodies, not only in the S*ubstantia Nigra*, but also in the L*ocus Coeruleus*, have been observed in the SNCA linked PD (35).

The SNCA gene has six exons, encoding an abundant 140 amino acid cytosolic protein, which is found at presynaptic terminals and thought to be involved in synaptic function (35). Despite intensive studies, the exact role of α-SYN at the synapse remains elusive. There is evidence that the protein plays a role in maintenance of synaptic vesicle pools and activity-dependent dopamine release (1), Larsen et al.(38) have provided evidence that α-SYN might modulate synaptic vesicle priming. Nevertheless α-SYN knockout mice have little or no obvious phenotype.

The α-synuclein protein is organized in three distinct domains: an N-terminal amphipathic region with conserved repeats (KTKEGV), a central hydrophobic NAC domain (non-amyloid component), and an acidic C-terminal region. All the three point mutations are located in the amphipathic region and are believed to exacerbate the toxic protofibril and fibril formation. Indeed, monomeric mutant a-synuclein has the propensity to form stable β-pleated sheets; the ensuing fibrillogenesis (formation of oligomers, protofibrils, and finally fibrils), results in the generation of pathological inclusions, known as Lewy bodies. Moreover, dopamine has been shown to modulate α-synuclein aggregation, perhaps explaining the selective vulnerability of *the Substantia Nigra* in PD.

Studies in drosophila indicate that Lewy bodies may be a way of detoxifying the cell of damaged α-synuclein. The enhanced toxicity of mutant α-synuclein may also be explained by the assembly of oligomeric α-synuclein into annular structures (39), that integrate into cellular membranes to form pores, thereby affecting membrane permeability. Of note, the overexpression of the wild-type protein is sufficient to cause PD, as duplications or triplications of the wild-type SNCA produce the disease in patients (35) although the precise relationship between aggregation, cellular dysfunction and cell death underlying PD is unknown (1).

- **Parkin - PARK2**

A year after the discovery of the SNCA gene, Parkin has been associated with PD (35). It is one of the largest genes in the human genome, mapping 1.38 Mb and comprising 12 exons (18). The Parkin gene encodes an ubiquitous 465 amino acid protein (35) organized in domains: an N-terminal ubiquitin like domain, a central linker region and C-terminal RING domain consisting of two RING finger motifs separated by an in between RING domain (19).

Parkin functions as an E3 ubiquitin protein ligase similar to other RING finger containing proteins by targeting misfolded proteins to the ubiquitin proteasome pathway for degradation, and the loss of its E3 ligase activity due to mutations lead to autosomal recessive early-onset PD. Parkin functions as a neuroprotective protein in a variety of toxic

insults crucial for dopamine neuron survival (19); it is therefore conceivable that the loss of parkin function may lead to the accumulation of a nonubiquitinated substrate, which is deleterious to the dopaminergic cell, but, due to its nonubiquitinated nature, does not form typical Lewy bodies (20).

Parkin interact with several presynaptic proteins (summarized by Moore (40). α-SYN and the α-SYN-binding synaptic protein (SNCAP) synphilin are two prominent examples. In addition parkin has been shown to modulate the function of a G-protein coupled receptor (GPR37) that interacts with the dopamine transporter DAT (1). The molecular events generated by mutated Parkin that lead to neuronal degeneration seem to be in this order: accumulation of substrates and other proteins, proteasome inhibition and cellular death. Actually, animal models allowed disclosing a possible additional role of Parkin in mitochondrial maintenance and oxidative stress prevention in cooperation with another PD-associated protein, PINK1 (see hereinafter). In particular, PINK1 would be involved in mitochondrial membrane integrity maintenance and could assist Parkin in the removal of damaged proteins.

Finally, oxidant molecules, among which dopamine itself, are able to alter Parkin solubility leading to its aggregation (41).

- **Ubiquitin carboxyl-terminal esterase L1, UCHL-1 - PARK5**

A mutation in Ubiquitin carboxyl-terminal esterase L1 gene was identified in affected members of one single family of German ancestry. To date, no other *bona fide* pathogenic mutations of this gene have been found. Whether UCHL1 really is a PD-responsible gene is not yet clear. Interestingly loss of UCHL1 function leads to neurodegeneration in mice (1). UCHL-1 is an abundant brain enzyme; its function might correlate with polymeric ubiquitin recycling and its conversion into monomeric units. Mutations in PARK 5 gene cause enzymatic activity reduction of UCHL-1 with consequent proteasome activity alteration (42).

- **PTEN-induced kinase 1, PINK-1 - PARK6**

This gene is particularly interesting within the context of the findings linking PD to mitochondrial dysfunction and oxidative stress, as PINK1 is a mitochondrial protein kinase.

The PINK1 gene encodes a 581 amino acid ubiquitous protein, consisting of an N-terminal 34 amino acid mitochondrial targeting motif, a conserved serine–threonine kinase domain and a C-terminal auto regulatory domain. The majority of the identified mutations are in the kinase domain, indicating the importance of PINK1 enzymatic activity in PD pathogenesis (35).

A substrate of PINK1 has been recently identified as TNF receptor-associated protein 1 (TRAP1). TRAP1 is a mitochondrial molecular chaperone, also known as heat shock protein 75. Wild-type PINK1 has been shown to phosphorylate TRAP1, moreover this phosphorylation is significantly increased in response to oxidative stress induced by H_2O_2. Interestingly, the PD-linked PINK1 mutants, G309D or L347P, abolish this kinase activity, although not affecting either the PINK1-TRAP1 interaction or their mitochondrial co-localization. Overexpression of wild-type PINK1 further revealed that cytochrome c release from mitochondria was reduced under oxidative stress conditions. TRAP1 is therefore proposed as being a downstream effector of PINK1: when phosphorylated by PINK1, TRAP1 may indirectly suppress cytochrome c release from mitochondria, protecting against oxidative stress-induced cell death (43). It is therefore plausible to assume that Parkin, PINK1, and TRAP1 are interacting in the same signaling pathway, the defects of which may lead to PD.

PINK1 seems to be involved in another important protection mechanism against oxidative stress, once again acting in concert with another protein, htrA2, which is a serine protease located in the mitochondria. PINK1 phosphorylates htrA2 thus tuning its proteolytic activity which in turn contributes to increased cell resistance to oxidative stress (44). More recently, Wang et al. described a new mechanism trough which PINK1, immobilizing damaged mitochondria, confines cellular damages produced by ROS species to a little region in the cell, putting damaged organelles to quarantine prior to their definitive

removal by autophagosome. Cells are able to maintain their energy balance preventing oxidative stress injuries by fine tuning of trafficking, distribution and clearance of mitochondria. PINK1 acts in the control of this balance intervening on mitochondrial motility. Specifically, it has been demonstrated that PINK1 phosphorylates the protein Miro, which is part of a complex anchoring the kinesin to the mitochondrial surface, thus controlling mitochondria transport alongside the axon (45). In fact phosphorylated Miro is targeted for degradation in a Parkin-dependent pathway. Removal of Miro from the mitochondrion also detaches kinesin from its surface arresting the damaged mitochondria until their complete degradation occurs, likely by autophagosome engulfment. This PINK1-Parkin activity is fundamental for ensuring the removal of damaged organelle preventing the injury diffusion in a larger area in the cell (46, 47). As a consequence, neurons defective for PINK1 and/or Parkin show an impairment in mitochondrial clearance which makes them susceptible to degeneration (42, 48).

- **DJ-1 - PARK7**

Parkinson Disease form 7 is one of the rare AR parkinsonisms with juvenile onset. Clinical features associated to PARK7 gene are very similar to those linked to PARK2 except for the presence of psychiatric symptoms. This gene, located in chromosome 1 encodes a 189 amino acids protein identified as DJ-1 by Bonifati et al. in 2003. It has ubiquitous expression in a variety of mammalian tissues including brain and it localized into mitochondria (49). The wild type form is present as homodimer located in the cytosol, nucleus and mitochondria, but upon oxidative stress conditions it is relocated in the matrix and in the intermembrane space of the mitochondrion where it exerts a protective activity against ROS. Many lines of evidences suggest that DJ-1 functions as an antioxidant protein. Oxidative stress leads to an acidic shift in the DJ-1 isoelectric point by oxidation of Cys106 which can be converted to cysteine sulfinic acid (Cys-SO_2H). Because of its inherent ability to undergo self-oxidation to eliminate H_2O_2 it may function as a scavenger of reactive oxygen species (ROS). In fact overexpression of wild-type DJ-1 both in cell culture and dopaminergic neurons in vivo protects against wide variety of toxic injury due to oxidative

stress. DJ-1 also functions like a redox-dependent chaperone to inhibit α-synuclein aggregation and subsequent cell death. Some familial DJ-1 mutants may have altered abilities to undergo key oxidative modifications, namely, a decreased propensity to undergo oxidation at position 106, and/or an increased susceptibility to undergo oxidative modifications with potentially deleterious effects on DJ-1(49) protective function.

1.5 LEUCINE RICH REPEAT KINASE 2 – (LRRK2)

1.5.1 Physio-pathological Role of LRRK2 (PARK8)

PARK8 locus have been associated for the first time to PD in 2002, by Funayama's group (50), in a Japanese family presenting a autosomal dominant form of parkinsonism without Lewy Bodies presence. Two years later two other groups independently have identified the gene LRRK2 in the PARK8 locus (51, 52); subsequently many pathological mutations have been identified.

LRRK2 mutations are usually associated to clinical parkinsonism – with typical movement problems of tremor, rigidity, bradykinesia and postural instability. Where autopsies have been performed, prominent loss of melanised dopaminergic neurons in the *Substantia Nigra pars compacta* has been noted. As might be expected, movement problems in these patients respond to L-DOPA treatment. PD cases due to LRRK2 mutation are therefore similar to sporadic PD and distinct from some other types of inherited parkinsonisms. Most, but not all, cases appear to have Lewy bodies, the characteristic pathology of α-synuclein deposition seen in PD and related conditions (53).

LRRK2 : general features and domains

The LRRK2 coding gene is located in chromosome 12 (12.q12), is composed of 51 exons giving rise to a 2527 amino acid protein consisting of 7 functional conserved domains (figure 10)(54, 55) :

- An "Armadillo Repeats" domain;
- An "Ankirin Repeats" domain;
- A "Leucine Rich Repeats" (LRR) domain, composed of a 22-28 amino acids motif repeated 13 times;
- A Roc domain with GTPase activity;
- A Carboxy Terminal of Roc (COR) domain
- A kinase domain, with homology with MAP-Kinase-Kinase-Kinase (MAPKKK)
- A C-terminal WD40 domain.

The "Armadillo Repeats" domain is composed by a repeated 42 amino acids motif organized in 3 α-helixes and was firstly identified in the "Armadillo" protein of Drosophila, which human homologous is β-catenin. The Armadillo domain forms a versatile molecular interaction platform available for different protein interactors (56).

The "Ankirin Domain" consists of seven ankyrin repeats, each forms two antiparallel helices followed by a β-hairpin or loop (Figure 8 - a from Mata et al 2006). The repeats stack together to form a gently curved structure in the ankyrin repeat domain. Ankyrin repeats are found in diverse bacterial and eukaryotic proteins, including cytoskeletal proteins, transcription factors, signaling proteins and cell cycle regulators (57).

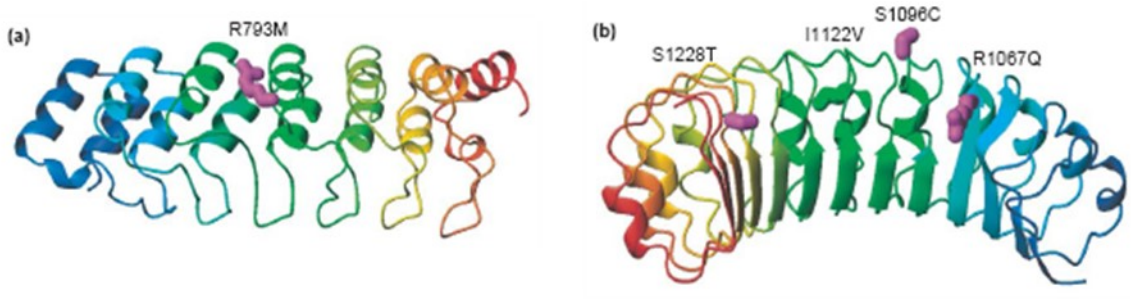

Figure 8: Schematic representation of tertiary structure of Ankirine (a) and LRR (b) domains. Amino acids of LRRK2 changed by putatively pathogenic LRRK2 mutations are highlighted in magenta, whereas residues whose substitutions are known to segregate with disease are shown in green. In all cases, the wild-type side-chain is depicted. In all models, the ribbon is colored from blue (corresponding to the N terminus) through the spectrum to red (corresponding to C terminus). From Mata et al. 2006

Each of the 13 identified LRRs in the leucine rich repeat domain is predicted to form a β-strand followed by an α-helix that line up side-by side to form an arch-like structure (Figure 8 - b from Mata et al. 2006). LRR domains participate in the interactions with different proteins through binding to their extended solvent-accessible surface (58).

The WD40 domain is composed by repeated motifs of 40 amino acids, mainly tryptophan-aspartate. Each repeat contains a four-stranded, antiparallel β-pleated sheet and together these repeats form a circular bladed propeller-like structure. The predicted WD40 domain of LRRK2 comprises seven WD40 repeats (Figure 9 - a modified from Mata et al. 2006). This seven-bladed propeller is thought to form a rigid platform for reversibly interacting with proteins, possibly including those that contain other WD40 domains. The WD40 domains are the most common repeats found in human proteins and normally they coordinate the assembling of multi proteic complexes. They have been identified in functionally diverse proteins including the Gβ subunit of heterotrimeric G proteins, transcriptional regulators, protein phosphatase subunits, RNA processing complexes, cytoskeletal assembly proteins, and proteins involved in vesicle formation and trafficking (58)

Catalytic domains of protein kinases are long 250-300 amino acid residues, containing a small N-terminal lobe and a larger C-terminal lobe connected by a hinge-like region to form a cleft in which Mg^{2+} -ATP and the protein substrate binds (Figure 9 - b - modified from

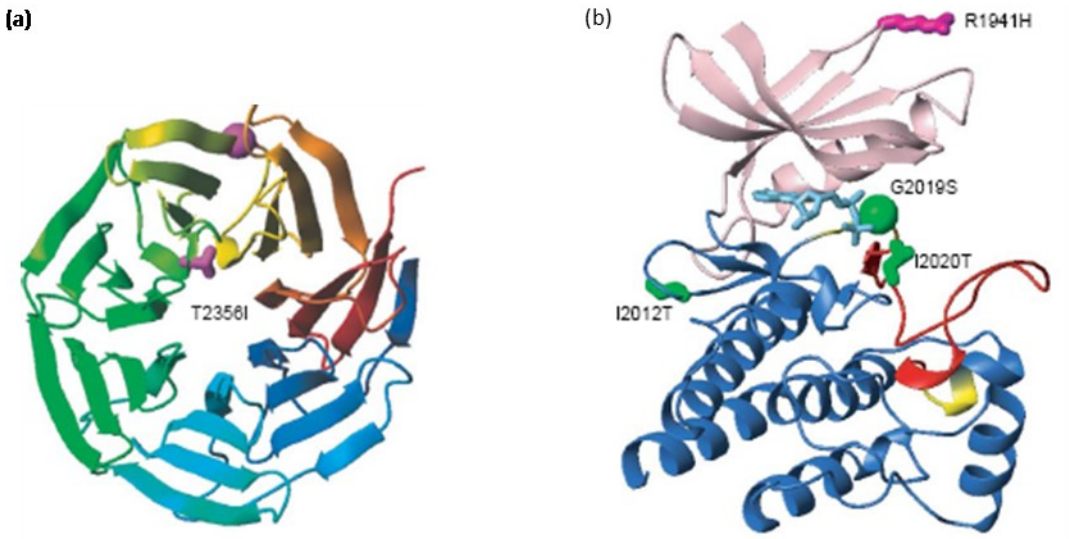

Figure 9: Schematic representation of tertiary structure of WD40 (a) and Kinase (b) domains. a) Amino acids of LRRK2 changed by putatively pathogenic LRRK2 mutations are highlighted in magenta, whereas residues whose substitutions are known to segregate with disease are shown in green. In all cases, the wild-type side-chain is depicted. In all models, the ribbon is colored from blue (corresponding to the N terminus) through the spectrum to red (corresponding to C terminus). b);N-terminal and C-terminal lobes are shown in pale pink and dark blue, respectively. The positions of the pathogenic mutations G2019S, I2020T in the activation segment, and I2012T in the Mg^{2+}binding region are indicated, along with the position of the R1941H mutation. The kinase activation loop is highlighted in red, the green sphere representing glycine residue 2019. From Mata et al. 2006

Mata et al. 2006). The activation segment is composed of 20–35-residues within the large C-terminal lobe. The majority of protein kinases require phosphorylation of the activation segment for full activity. Upon phosphorylation, the activation segment is believed to adopt an active conformation, enabling substrate access and catalysis to take place (58).

The putative GTPase domain of LRRK2 belongs to the ROCO family, in which the predicted GTPase (Roc) is always found in tandem with the COR domain, the function of which is still unknown. This Roc–COR module is conserved throughout evolution, suggesting the functional interdependence of the two domains. The Roc-GTPase domain of the LRRK2 resembles most closely the GTPases of Rab family, which have been implicated in vesicular

trafficking and transport (58) processes by acting as molecular/regulatory switches that cycle between GTP and GDP-bound conformations (59). A functional link is postulated to exist between the intrinsic GTPase activity and downstream kinase activity. Different studies have suggested that LRRK2 kinase activity is dependent on the existence of a functional GTPase domain, whereas GTPase activity can function independently of the kinase domain (59). An additional hypothesis proposes that GTPase activity would be able to regulate the kinase activity and/or the kinase activity would have the ability to regulate the GTPase activity by an auto-phosphorylation mechanism. In support of this latter hypothesis are the various studies that assess auto phosphorylation ability of LRRK2. The kinase domain is indeed not only able to phosphorylate some potential substrates but also, with highest efficacy, the protein itself in correspondence to the ROC domain (see figure 10 from Rideout et al. (55)).

Dimerization of the ROC or ROC-COR domains results in an intermolecular interaction between the kinase domains subsequently allowing an increased kinase activity, thereby structurally explaining the interplay between these enzymatic domains. Dimerization of LRRK2 has been demonstrated by yeast two-hybrid analysis, native gels, size exclusion chromatography and co-immunoprecipitation from mammalian cells (59, 60)

The presence of multiple protein interaction domains (armadillo, ankyrin, LRR and WD40) suggests that LRRK2, in addition to its predicted protein kinase and GTPase activities, might serve as a scaffold for assembly of a multiprotein signaling complex. However, because these domains bind diverse proteins ranging from transcription factors to signaling proteins (58), the physiological LRRK2 interactors and substrates and its function remain unknown.

Recent mRNA expression analysis studies demonstrate the LRRK2 transcript presence in the brain and in various peripheral districts. In rodents, high levels of LRRK2 mRNA have been detected in brain and lymph nodes. LRRK2 is particularly abundant in the dopamine-innervated areas as (53) *cortex, striatum, cerebellum, hippocampus and olfactory tubercle;* while lower levels are observed in the *substantia nigra* (55). The subcellular localization of LRRK2 is mainly cytosolic with an important component associated with the membranes,

vesicles and cellular organelles as Golgi, mitochondria, lysosomes and RE, as well as microtubules and cytoskeleton structures (61)

LRRK2 pathological mutations do not alter protein stability and/or localization but some of them increase the kinase activity; they are, in particular, clustered in the central part of the gene in the ROC GTPase domain and the kinase domain (36). An increase in the LRRK2 kinase activity appears to be sufficient to generate neuronal toxicity implicated in PD (54, 59, 62). Studies performed on cell lines demonstrate that LRRK2 has long half-life, and, especially if co-expressed with Parkin, tends to form aggregates which are prone to ubiquitination through a process involving Parkin (63)

More the 75 variants of LRRK2 are described, but not all of them are PD-causative mutations. On the other hand some mutations are associated to PD and they are localized in the enzymatic region of the protein (figure 10 from Rideout et al): The ROC domain is affected by multiple mutations: R1441G, R1441C, R1441H) (52). The effects of these mutations result in an alteration of GTPase activity, but the final effect of these alterations on the kinase activity are quite contrasting. In the ROC domain only a pathological mutation has been described (Y1699C) while in the kinase domain there are two adjacent mutations, G2019S and I2020T. G2019S is the most common pathogenic substitution in the familial forms of PD but is also associated to sporadic forms (36, 64, 65). Various studies performed on cellular models have consistently showed that this substitution leads to an increase in kinase activity up to threefold. The 2019 residue is indeed located in a loop which is closing like a string the catalytic site, the substitution of glycine with serine forces the catalytic site in a constitutively active state leading probably to the increased kinase activity (59, 66).

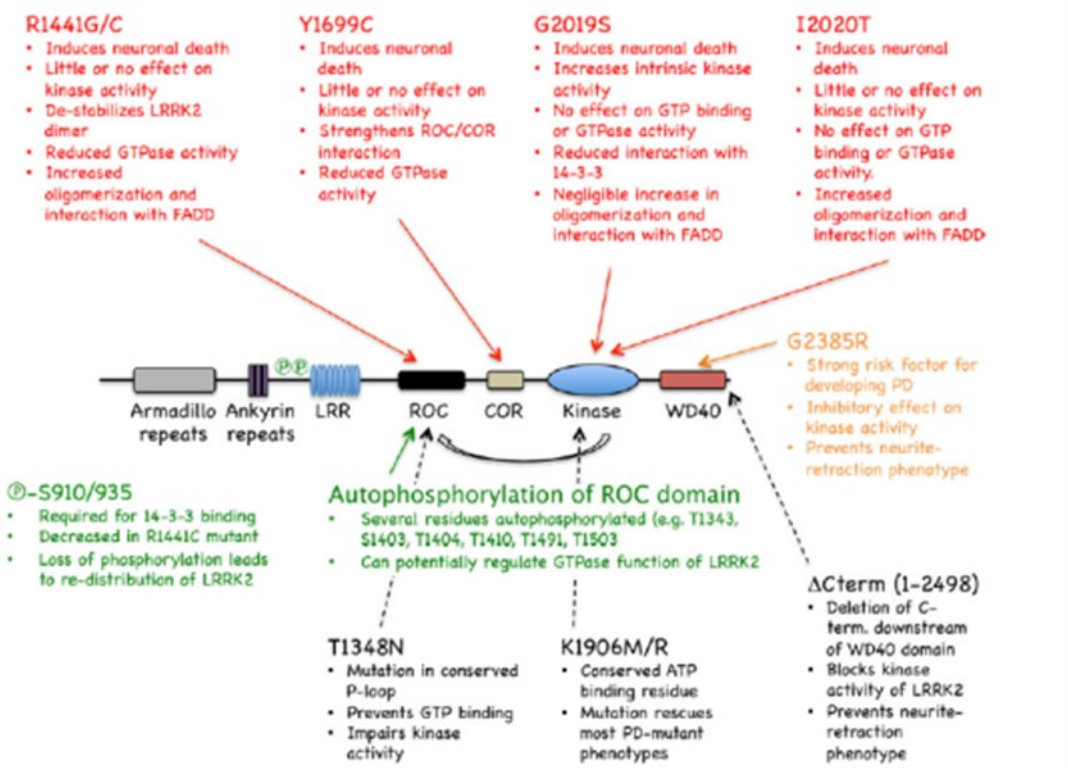

Figure 10: Schematic of LRRK2 domain organization. Pathogenic mutation clearly segregating with Parkinson's disease are indicated in red whereas risk factors are indicated in orange. Selected residues that are phosphorylated by other kinases, or autophosphorylated are indicated in green; and artificial mutations created to examine specific functional aspects of LRRK2 biology are indicated in black

From the first association between LRRK2 and PD in 2004, many epidemiologic studies have assessed that LRRK2 is responsible of roughly 10% of PD familial forms and importantly also the 4% of the sporadic ones. The glycine to serine substitution in 2019 position of LRRK2 represents the most frequent substitution in the Caucasian population; it is indeed responsible for 1-2% of idiopathic PD and 6% of familial PD; moreover, G2019S mutation is higher in some population of North Africa and in Ashkenazi Jews (13-41% sporadic cases and up to 40% of familial ones)(67).

Concerning Sardinia, a study published in 2006 by Cossu et al. shows that G2019S substitution is present in the highland with a lower frequency in respect to other mediterranean population, while R1441C is very uncommon in Sardinian population (68).

LRRK2 physiologic function and involvement in Parkinson Disease

Despite the extensive studies performed, up to date, the physiological role of LRRK2 remains elusive. Among these studies, very indicative of the possible function of LRRK2 are the identifications of potential protein interactors. Through different methodological approaches and various models, a plethora of interactors has been suggested; a summary of those is given in table 3, which link LRRK2 to a broad range of cellular functions. Inter alia, more than one group found that LRRK2 phosphorylates moesin, suggesting that LRRK2 can take part in neurite length maintenance (69, 70). Moesin is a member of ERM (Ezrin/Radixin/Moesin) protein family which main function is to anchor the actin cytoskeleton to the plasma membrane; moesin and radixin are indeed implicated in neurite elongation. In fact, LRRK2 pathological mutant expression causes neurite shortening and neurite branching inhibition (69, 71). In C. elegans, LRK-1, the worm homologue of LRRK2, plays a role in vesicle trafficking between axons and dendrites (72).

Other data support the hypothesis that LRRK2 is involved in cytoskeleton dynamics. Hyper-expressed LRRK2 co-immunoprecipitates with endogenous tubulin in HEK-293 cells. Furthermore, G2019S mutant is able to phosphorylate tubulin more than the WT protein leading to microtubules anomalies that interfere with the normal neuronal functionality (73). Studies using LRRK2 transgenic mice models describe an abnormal Golgi apparatus fragmentation, which integrity is maintained with the help of microtubules, with consequences on Golgi and endoplasmic reticulum balancing in vesicular trafficking control (70). Microtubule stability and integrity are fundamental both for cellular morphology maintenance and for molecules and organelles transport that in neurons must cover longer distances in respect to other cellular types.

Moreover Leucine Rich Repeat Kinase 2 might be involved in translation control, since it has been shown to interact with the 4E-BP1 translation initiation factor.

Furthermore LRRK2 seem to be implicated in apoptosis activation by interaction with FADD proteins and caspase (74, 75). Iaccarino et al. demonstrated that G2019S expression in SH-SY5Y cells causes neuronal death by mitochondrial dependent apoptosis mechanism. This

is carried out by caspase 3 activation depending on Apaf1 which together with pro-caspase 9 and cytochrome c participate in the apoptosome formation (75). In this study ETNA-/- cells had been used as control. These cells are deficient for Apaf1 and are a common cellular model for apoptosis studies in neurodegenerative diseases. When ETNA -/- are transfected with $LRRK2^{G2019S}$ the lacking of Apaf1 prevents caspase 3 activation and the nucleus condensation while cytochrome C is as usual released from the mitochondria. These results point at a pivotal role of the mitochondria in LRRK2 mutant induced cell death and indicate Apaf1 as a fundamental mediator in this pathway. In the same study Iaccarino et al. have analyzed the differential role of LRR and WD40 LRRK2 domains in LRRK2 mutants toxicity showing that the presence of these two domains ($LRRK^{\Delta LRR}$ or $LRRK2^{\Delta WD40}$) are essential for caspase 3 activation and cellular apoptosis.

An interesting study of Greggio et al. demonstrates that PD causing mutants of LRRK2 increase LRRK2 tendency to form cytoplasmic inclusions in cellular models (76) and this property seems to be linked with the kinase activity of the protein (64). Cellular proteic inclusions in neurons of PD patients bearing LRRK2 mutations suggest that one effect of PARK8 locus alterations can be the protein aggregation.

According to different studies there might be a common pathologic mechanism involving LRRK2 and α-Synuclein. The α-Synuclein deposited in Lewy bodies is indeed abundantly phosphorylated on Serine 129. Up to date, LRRK2 is not able to directly phosphorylate α-synuclein although Qing at al. were able to co-immuniprecipitate LRRK2 and α-synuclein from Lewy bodies positive tissues and oxidative stressed HEK-293 cells (77). Furthermore recombinant α-synuclein is phosphorylated by some kinases present in the protein lysates from HEK-293 expressing LRRK2 (77, 78). Finally, SH-SY5Y co-transfected with LRRK2 (WT or G2019S) and α-Synuclein show an increase in aggregation level, phosphorylation and release of α-synuclein (79). Taken together these data corroborate a current hypothesis of an important functional connection between LRRK2 and α-Synuclein in triggering neurodegeneration causing PD (80).

Very useful tools to gather clues on the physiopathology of LRRK2 are animal models. In *D. melanogaster*, overexpression of mutant LRRK2 causes loss of dopaminergic neurons, retinal degeneration, motor impairment and shorter life, whereas wild-type protein produces less severe phenotypes (53). In *C. elegans* models, overexpression of LRRK2 also causes phenotypic changes, including axonal damages in neurons, which seem to involve altered mitochondrial functions (53). Knockout of the nearest homologous gene in Drosophila produces variable effects, with loss of dopamine cells reported in one study, but this was not replicated in an independent laboratory. Knockout of the *C. elegans* homologue causes changes in axonal polarity and in neurite outgrowth in response to stress (53). Three independent mouse knockouts have been reported (80-82). In all three published studies, the brains of the animals were reported to be grossly normal and there was no loss of dopaminergic neurons in the *substantia nigra*. Therefore, LRRK2 appears to be dispensable for the survival of neurons under both basal and stressed conditions. Different LRRK2 transgenic rodents have been generated by independent groups. In a few cases the authors describe dopaminergic degeneration in animals expressing pathological mutants (83, 84) while sometimes a reduction in dopamine extracellular content was observed (83, 85, 86). More recently, two groups have reported that transient overexpression of mutant LRRK2 using viral vectors will result in loss of dopaminergic neurons in the *substantia nigra* of mice (87) or rats (88). Importantly, wild-type protein or kinase-dead versions of LRRK2 had no effect, suggesting that simple overexpression of any similar large protein would not be sufficient to cause neurodegeneration (53). Therefore, this approach has the potential to provide a model that more fully replicates the phenotypes seen in human LRRK2 patients than are not seen in conventional transgenic models. A feature shared by various murine models of PD is an abnormal level of phosphorylated protein Tau induced by G2019S and R1441G LRRK2 mutants. The Tau protein binds tubulin and promotes its assembly in microtubules; when phosphorylated, Tau induces on the contrary, microtubule fragmentation that damages the entire cytoskeleton network (85) (89). Finally, the blockage of *Zebrafish* LRRK2 protein by morpholinos caused embryonic lethality and severe development defects such as growth retardation and loss of neurons. In addition, the deletion of WD40 domain of *zebrafish*

LRRK2 revealed Parkinsonism-like phenotypes, including loss of dopaminergic neurons in the diencephalon and locomotion defects. Remarkably, another group failed to reproduce the phenotypic loss of dopaminergic neurons in *zebrafish* (90)

LRRK2 and vesicle trafficking

Different experimental approaches have demonstrated that LRRK2 is localized throughout the cytoplasm of neuronal perikarya and dendritic processes, where it is associated with vesicular and membranous structures, the microtubule network, mitochondria and other membrane-bound organelles (61, 91). Moreover it has been demonstrated its association with lipid rafts. Although the pathological mutations do not affect the LRRK2 membrane association, this localization is of particular interest since the lipid rafts play important roles in cellular functions such as signal transduction, membrane trafficking and cytoskeletal organization (92). Furthermore, lipid rafts associate with SNARE (soluble N-ethylmaleimide-sensitive fusion protein-attachment protein receptor) proteins and regulate endocytosis and exocytosis (93, 94). Lastly, an extensive analysis of LRRK2 subcellular localization performed by Biskup et al in 2006 either in primary cortical neurons or rodent brains showed that LRRK2 co-localizes consistently to Golgi apparatus and Golgi-associated vesicles, endoplasmic reticulum (ER), lysosomes and mitochondria, and, to a significantly lesser degree, to vesicle markers such as synaptotagmin.

Table 3: Molecular interactors of LRRK2 and co-localizing organelle markers. Abbreviations: MS: Mass Spectrometry; Y2H: Yeast Two Hybrid; SV: Synaptic Vesicle; OE: Over Expression; KD: Knock Down; RP recycling Pool; GNEF: Guanine Nucleotide Exchange Factor; P: Phosphorylation/Phosphate; WB: Western Blot; Co-IP: CoImmunoPrecipitation; ICC: ImmunoCitoChemistry; Mut: mutant/mutation.

Protein	Potential role	Technique	Analysis/Expression System	REF.	Notes
Tubulin-β § (Tubβ)	Kinase Substrate	In vitro assay	(hLRRK2 from insect cells + βTubuline from Bovine Brain)	(73)	- G2019S 3xP Tubβ. - In vitro co incubation bovine brain tubulins + LRRK2 ↑stability microtubules. - LRRK1 does not P βTub.
Tubulin-β §	Interactor	CoIP+MS	Mouse brain WT and LRRK2 expressing HEK-293 cells	(73)	
Moesin § (Thr 558)	Kinase Substrate of G2019S mutant.	KESTREL (kinase substrate tracking and elucidation screen) (an in vitro assay) P assay and MS	Rat brain extracts	(95)	- LRRK2 WT does not P Moesin. - The minimum catalytically active fragment ofLRRK2 requires an intact GTPase, COR and kinase domain, WD40 motif and a C-terminal tail. -P enable to bind F-Actine
Ezrin § (Thr 558)	Kinase Substrate of G2019S mutant.	KESTREL (kinase substrate tracking and elucidation) screen	Rat brain extracts	(95)	LRRK2 WT does not P Erzin
Radixin § (Thr 558)	Kinase Substrate of G2019S mutant.	KESTREL (kinase substrate tracking and elucidation) screen	Rat brain extracts	(95)	LRRK2 WT does not P Radixin
Rab5b (but not with Rab4a)	Interactor	Y2H GST pull down Co-IP	Yeast Mouse Brain and HEK cells	(96)	- a fraction of both proteins co-localize in SV - Interaction increased by GTPgS - Alteration of LRRK2 expression impairs SV endocytosis
NSF	Interactor	Co-IP	With endogenous LRRK2 in Mouse Brain	(97)	-All these interact with WD-40 Domain; -LRRK2 silencing alters storage and mobilization SV in the RP -LRRK2 KD increase recycling Syn number (Electrophysiology SiRNA cortical neurons)
NSF	Interactor	GST pull-down + LC MS/MS	GST-LRRK2 Domains on mouse brain	(97)	
		Sub cell fractionation	Cortical neurons lysates		
Syntaxin 1A	Interactor	Co-IP	With endogenous LRRK2 Mouse brain	(97)	
AP-2 complex subunits	Interactor	GST pull down	GST-LRRK2 Domains on mouse brain	(97)	
Synapsin 1	Interactor	GST pull down	GST-LRRK2 Domains on mouse brain	(103)	

Synaptic Vesicles glycoprotein 2A	Interactor	GST pull down	GST-LRRK2 Domains on mouse brain	(97)	
Actin	Interactor	GST pull-down	GST-LRRK2 Domains on mouse brain	(103)	
F-Actin and actin regulatory proteins	Interactor	QUICK (quantitative immunoprecipitation combined with knockdown) Validated: F-actin co-sedimentation assay + WB	All proteins Endogenous in NIH3T3 (fibroblast) cells.	(98)	
Myosin 1d	Interactor	QUICK (quantitative immunoprecipitation combined with knockdown)(assay in normal environment at proteic endogenous levels) Validated: WB IP	All proteins Endogenous in NIH3T3 cells.	(98)	LRRK2 binds F-Actin and effect its polymerization in vitro KD LRRK2 determines neurite shortening.
Tropomyosin	interactor	QUICK (quantitative immunoprecipitation combined with knockdown) Validated: WB IP	Endogenous LRRK2 in NIH3T3 cells.	(98)	
Arp3	Interactor	QUICK (quantitative immunoprecipitation combined with knockdown) Validated: WB IP	All proteins Endogenous in NIH3T3 cells.	(98)	
EndoA	Kinase substrate	purified human LRRK2 in a 33P-ATP in vitro assay	Drosophila	(99)	
EndoA	Genetic interaction		Drosophila	(99)	Lrrk2 negatively controls EndoA membrane association
ArfGAP1	Regulator – GAP/KIN substrate	Co-IP	In vitro: LRRK2 transfected HEK-293; in vivo: brain lysates wt and LRRK2 KO mice and in Drosophila	(106)	

ArfGAP1	Regulator – GAP/KIN substrate In vitro In vivo	Colorimetric assay for Pi release in vitro	In vitro	(100)	WD-40 + KIN. - ArfGAP1 binds LRRK2 and ↑ LRRK2 GTPase activity ↓toxicity ArfGAP ↑GTP Hydrolysis.
		In vivo	Mouse brain WT and lrrk2 KO		
		Co-IP	Mouse Brain endogenous LRRK2		P ArfGAP1 ↓GAP activity
ARHGEF7 (Beta-PIX) Indirect effect on cytoskeleton regulation CDC 42	-KIN substrate -Regulator: GEF	Co-IP	HEK293	(101)	
			In vitro		-ARHGEF7 enhances R1441C's GTP affinity
					ARHGEF7 enhances WT's GTP hydrolysis
FADD	Interactor	Co-IP	293T cells	(74)	-Interaction enhanced by LRRK2 pathological mutations
			WT mice brain		
TRADD	Interctor	Co-IP	293T cells	(74)	No effect of pathological LRRK2 mutants
GMI;CD55; (Lipid Rafts)	Co-localization	ICC	COSI cells	(91)	
'Y adaptin (TGN)	Co-localization	ICC	COSI cells	(91)	No mutant effect on
EAA1 (Early Endosomes)	Co-locazation	ICC	COSI cells	(91)	No mutant effect on
Lysotracker (Lisosomes)	Co-localization	ICC	COSI cells	(91)	No mutant effect on
MytoTracker (Mitochondria)	Co-localization	ICC	COSI cells	(91)	No mutant effect on
Synaptotagmin I (Secretory Vesicles)	Co-localization	ICC	-mouse primary cultured neurons -COSI cells	(91)	No mutant effect on
Nr1a	Interactor	WB	Mouse Brain	(91)	No mutant effect on
Synaptophysin	Interctor	WB	Mouse Brain	(91)	No mutant effect on
Thy-1.2,GM1, phosphatidylinositol (Lipid Rafts)	Co-localization	ICC	Mouse cortical Neurons	(91)	No mutant effect on

Rab5b		Subcell fractionation+WB ICC -	Rat cortex Lysates 293T cells, Rat hippocampal Neurons	(96)	-No mutant effect on -Rab5 rescues LRRK2 OE/KD endocytosis defect
SNCA	Co-localization	Immunostraining	Human post mortem brain	(77)	
SNCA	Interactor	Co-IP	Co-transfected HEK-293 under oxidative stress conditions	(77)	- Co-IP is not validated in brain extracts
SNCA	Kinase Substrate	WB with anti phospho antibodies	In vitro	(78)	-LRRK2 P SNCA at Ser-129 -G2019S LRRK2 has grater P capacity on SNCA
14-3-3	Interactor	quantitative SILAC-based MS Co-IP with endogenous LRRK2 from Swiss 3T3 cells	Hek-293	(102)	- 14-3-3 binds P-Ser 910 and P-Ser 935 - Mut abolish binding but not G2019S - Binding disruption cause cytoplasmic aggregation.

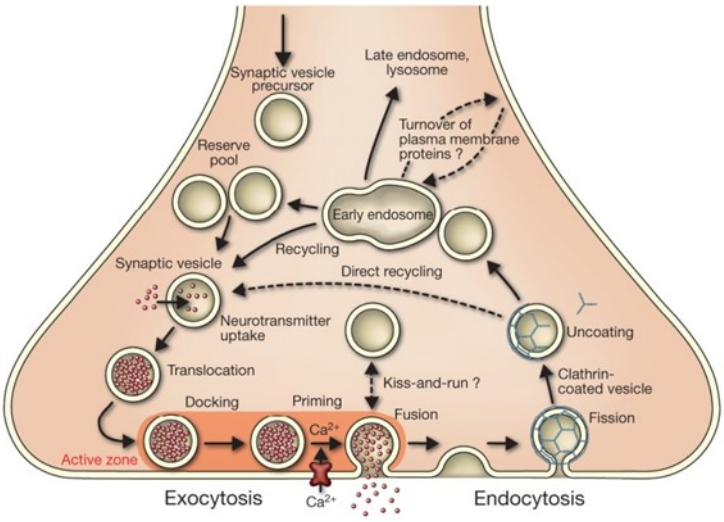

Figure 11: Synaptic vesicles are filled with neurotransmitter and stored in the cytoplasm. Active vesicles are translocated to release sites in the active zone where they dock. Priming involves all steps required to acquire release readiness of the exocytotic complex. Although usually assumed to occur after docking, priming and even triggering may precede docking during sustained activity, resulting in immediate fusion of an arriving vesicle. After exocytosis, the vesicle proteins probably remain clustered and are then retrieved by endocytosis. Despite some lingering controversies, consensus is emerging that retrieval is generally mediated by clathrin-mediated endocytosis. After clathrin uncoating, synaptic vesicles are regenerated within the nerve terminal, probably involving passage through an endosomal intermediate. Actively recycling vesicles are in slow exchange with the reserve pool.

To elucidate the physiological role of LRRK2, Piccoli et al. (97) analyzed the presynaptic and postsynaptic properties of cortical neurons in which LRRK2 had been silenced by short hairpin-mediated RNA interference. Electrophysiological analysis of these neurons revealed that LRRK2 silencing alters synaptic transmission. In the same study, a structural analysis of this system revealed LRRK2 silencing perturbs vesicle dynamics and distribution within the recycling pool, determining a significant decrease in docked vesicles, but an increase in the amount of vesicle recycling, (an overview of vesicle dynamics at the nerve terminal is represented in figure 11 from (103)). At the molecular level, LRRK2 interacts, mainly through the WD40 domain, with a number of proteins involved both in endo- and exo-cytosis of synaptic vesicles (see table X). Unfortunately, under the same experimental conditions, the overexpression of LRRK2 is toxic, therefore not allowing a comparative analysis between protein absence and overexpression. Besides many of those proteins are presynaptic proteins: NSF that catalyzes the release of the SNARE complex and allows the first step of the endocytic cycle; the AP-2 subunit of the clathrin complex which

is one of the major pathways for synaptic vesicles (SV) recycling from the membrane to the resting pool; the glycoprotein SV2A, that together with SV2B, controls the storage and mobilization of SV in the readily releasable pool; and the synapsin that are thought to immobilize SV in the reserve pool by crosslinking vesicles to the actin cytoskeleton (97). Among LRRK2 identified interactors, Rab5 is interesting because involved in SV endocytosis regulation. In general Rab proteins are GTPases localized in vesicular cellular compartments with regulatory role in the membrane trafficking. Rab5 has a key role in carrying endocytic vesicles from plasma membrane to early endosomes (104). Shin et al. have characterized in depth the Rab5-LRRK2 interaction (96) measuring endocytosis and exocytosis speed in hippocampal neuronal cells transfected with LRRK2 WT or mutants revealing a decrease in endocytosis but no effect on exocytosis of synaptic vesicles. This effect on endocytosis is recovered co-transfecting Rab5, but it is not if co-transfected the Q79L mutant form of Rab5, which is not able to hydrolyze GTP (96).

Two independent groups have recently identified ArfGAP1 (ADP-ribosylation factor GTPase-activating protein 1) as a specific LRRK2 interactor both in vivo and in vitro (100, 105). Interestingly, ArfGAP1 promotes the GTP hydrolysis of Arf1 (ADP-ribosylation factor 1), a small GTPase that is critical for maintaining normal Golgi morphology, and Arf1 GTP hydrolysis is also required for the dissociation of coat proteins from Golgi-derived membranes and vesicles (106).

An alternative explanation for the dysregulation of vesicle trafficking could arise from the described role of LRRK2 in the modulation of cytoskeleton dynamics. Both the microtubule and actin cytoskeletons make essential contributions to intracellular vesicle and organelle motility (107). There are two mechanisms for actin-based motility (92). First, actin polymerization itself can propel vesicles, and, secondly, actin serves as a track for the motor protein myosin belonging to ERM (ezrin/radixin/moesin) family. In fact, LRRK2 modulates both ERM protein phosphorylation and actin polymerization mainly in filopodia structures (108).

Cytoskeletal dynamics, motor protein function and vesicle trafficking are all regulated through the Rab, Arf and Rho families of GTP-binding proteins. Notably, LRRK2 contains a

GTP-binding domain and interacts with ArfGAP1, a protein regulating the GTP hydrolysis of Arf1 (106), leading to the interesting possibility that LRRK2 may affect, directly or indirectly, the secretory and endocytic pathways modulating cytoskeleton dynamics and vesicle motility.

Moreover LRRK2 appears to be localized in different intracellular districts that play a critical role in the control of vesicular trafficking: ER, Golgi apparatus and associated vesicles, cytoskeleton, lipid raft and finally lysosomes (Figure 12 from (109)).

Figure 12 : Schematic representation of LRRK2 localization in different cellular districts affecting membrane trafficking LRRK2 (indicated by asterisks) largely co-localizes with the ER, Golgi apparatus and Golgi-associated vesicles, cytoskeleton, synaptic vesicles and lipid rafts. All of these structures are involved to a different extent in both anterograde and retrograde transport regulating vesicle generation, motility, secretion and endocytosis. Moreover, LRRK2 also co-localizes with lysosomes that are generated by the addition of hydrolytic enzymes to early endosomes from the Golgi apparatus. Thus membrane trafficking regulates different aspects of neuronal physiology ranging from neurotransmitter or neurotrophic factor release, insertion of cell membrane components (including both membrane proteins and lipids) and, not least, organelle biogenesis.

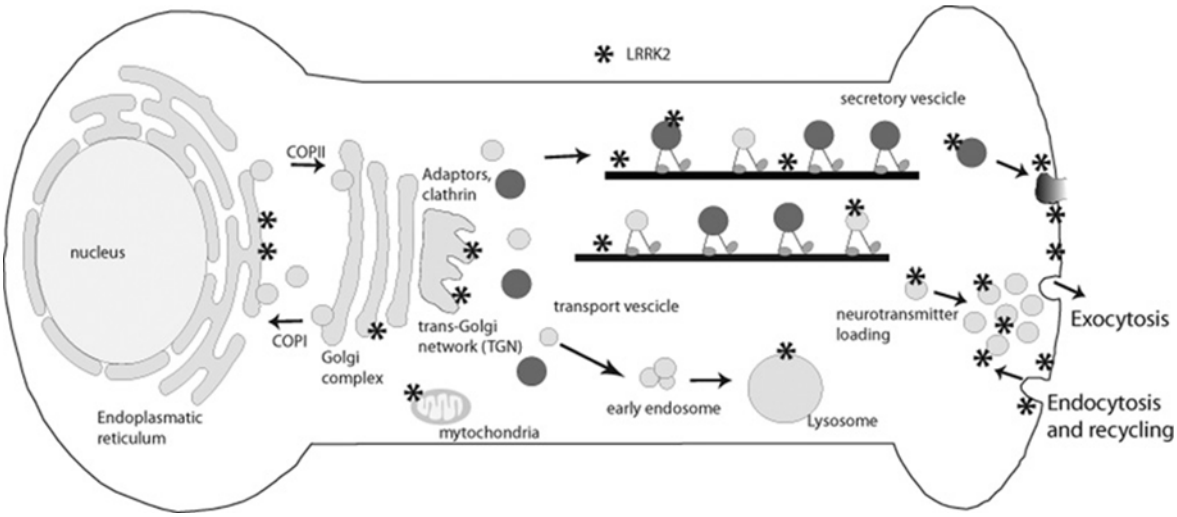

Although some results are somewhat contradictory or difficult to interpret, it is evident that LRRK2 participates in a protein network regulating synaptic vesicle trafficking. Vesicle trafficking is a complex process regulating multiple different cellular functions, in addition to neurotransmitter release, such as neurotrophic factor release, localization of membrane receptors, changes in plasma membrane composition at the cell surface and, not least, organelle biogenesis. The molecular mechanisms regulating the exo/endo-cytosis for

proteins or membranes are different from those regulating neurotransmitter release. The LRRK2 cellular localization mainly with the ER and the Golgi apparatus and Golgi-associated vesicles, but to a significantly lesser degree with vesicle markers (61), could suggest an involvement of LRRK2 in anterograde or retrograde vesicle trafficking between the ER and Golgi apparatus or Golgi and cell membrane or Golgi and lysosomes, rather than a simple control of neurotransmitter release at synapse.

1.6 LEUCINE RICH REPEAT KINASE 2 AND LEUCINE RICH REPEAT KINASE 1

In vertebrates, the LRRK2 gene has one paralogue: LRRK1 (leucine-rich repeat kinase 1). The two proteins display a conserved domain architecture and are both members of the ROCO family. ROCO proteins were formally described and named by Bosgraaf and Van Haastert in 2003 (110). Both proteins are expressed in the brain and are highly phosphorylated. However, despite their close homology and their similar expression profile, no mutations in LRRK1 have been genetically associated with PD. This group of proteins contains two conserved domains named ROC (Ras of complex proteins), a GTPase domain with high sequence similarity to Ras and other related small GTPases, and COR (C-terminal of ROC), a domain of unknown function, that represents a fingerprint of all ROCO proteins (111).

LRRK1 and LRRK2 share a similar domain organization, which includes a serine-threonine kinase domain, C-terminal of ROC (COR) domain together with a ROC domain, and leucine-rich and ankyrin-like repeats at the N-terminus. The major differences between LRRK1 and LRRK2 are at the N-terminal region, where LRRK2 has a large number of unique repeats and unique phosphorylated consensus binding sites for 14-3-3. There are important differences also in the C-terminal regions that show the lowest degree of homology compared to other domains (Fig. 13 from (112)). This divergence may be relevant with respect to a recently proposed pre-synaptic function of LRRK2, which was shown to interact with a number of presynaptic proteins via its C-terminal WD40 domain (112). Previous studies have shown that both LRRK1 and LRRK2 bind GTP, are basally p

hosphorylated in cells and share a similar cytoplasmic distribution. Overall, the absence of a complex and extended N-terminal region from LRRK1, the minimal similarity of the C-terminal tail and the lack of homologous residues for 14-3-3 binding may represent important differences that affect protein function (111). On the other hand, the ROC–COR–kinase domain architecture is clearly preserved in both proteins, thus biochemical data obtained for LRRK1 may help to elucidate the molecular mechanism leading to LRRK2-

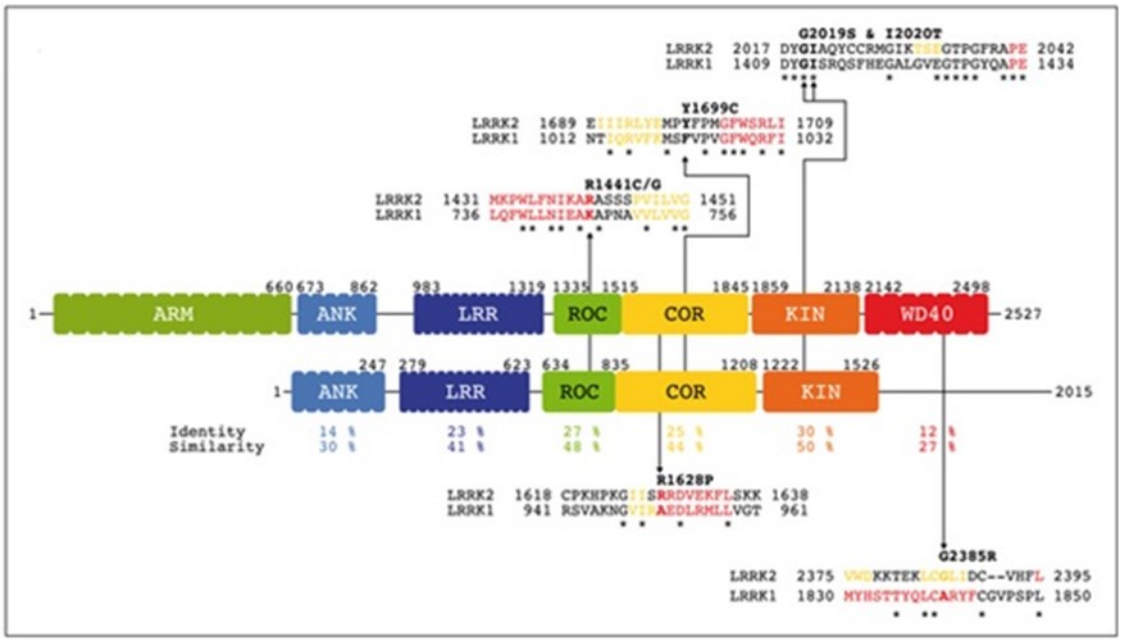

Figure 13: Schematic alignment of LRRK1 and LRRK2. Predicted functional domains are drawn to scale at the relative location within the full protein sequence. For domains containing repeat sequences, predicted individual repeat units are depicted. The sequence identity and similarity for the LRR, ROC, COR and Kinase domains are given below the schematic. Also given are detailed alignments of LRRK1 and LRRK2 at the level of common LRRK2 clinical mutations. Abbreviations for the domains: ARM, armadillo repeat domain; ANK, ankyrin repeat domain; LRR, leucine rich repeat domain; ROC, Ras of comple proteins domain; COR, Cterminal of ROC domain; Kin, kinase domain; WD40, WD40 repeat domain. From: Civiero L, Vancraenenbroeck R, Belluzzi E, Beilina A, et al. (2012) Biochemical Characterization of Highly Purified Leucine-Rich Repeat Kinases 1 and 2 Demonstrates Formation of Homodimers. PLoS ONE 7(8): e43472. doi:10.1371/journal.pone.0043472

dependent PD (111). In a recent study, Civiero et al. suggest that the sequence similarity between LRRK1 and LRRK2 is reflected in functional similarity for some domains. From their biochemical characterization study emerged that GTP binding affinities of LRRK1 and LRRK2 were comparable using an isotopic displacement assay. While both LRRK proteins can bind to ATP as predicted for kinases, their kinase activity revealed striking differences.

In particular they could not observe LRRK1 kinase activity toward itself or against generic or LRRK2 specific substrate; concluding that LRRK1 phosphorylation properties are fundamentally different from those of LRRK2, substrate specificity differs and while autophosphorylation is robust in LRRK2, it is not likely to play a significant role for LRRK1. Therefore, although the kinase domains are similar for LRRK1 and LRRK2, at the functional level the two proteins are likely to be very different (112). More than this, Civiero et al. show that highly purified LRRK1 and LRRK2 can associate in dimeric structures in absence of their molecular partners confirming other similar previous results, inter alia those of Dachsel et al. (113) which also suggested that the LRRK2 dimer is the functional unit.

However, results on LRRK1 and LRRK2 localization in tissues are slightly discordant. Until the last months the results of several studies analyzing LRRK mRNA and protein levels in different tissues and organs indicate that the expression of the two proteins generally overlaps and, in some tissues, levels are comparable (113, 114). However, in organs such as the brain and the kidneys, LRRK2 mRNA expression is higher than that of LRRK1 (115). If LRRK1 and LRRK2 possess partially overlapping functions, then LRRK1 may compensate for the effects of LRRK2 deficiency only in those tissues where their expression is similar, but not in the brain or kidneys where LRRK1 expression is low. Giesert et al. examined the distribution of Lrrk2 and Lrrk1 mRNA the adult brain of Mus musculus, and also compared Lrrk1 and Lrrk2 expression in the same tissues drawing the anatomical localization of both proteins (116). The mesencephalic region of the substantia nigra, which contains the most vulnerable neuronal populations affected in PD, exhibited only moderate Lrrk2 expression in the adult brain while the target area of these dopaminergic neurons (i.e. caudate putamen in the striatum) shows the highest level of Lrrk2 mRNA. In contrast to Lrrk2, Lrrk1 was barely detectable in the adult mouse brain. From these and other observations it is well established now that, despite their high degree of homology and their comparable expression patterns during development, the adult brain almost exclusively expresses Lrrk2. Nevertheless, this finding suggests that LRRK1 does not compensate for LRRK2 function in the adult. Furthermore it may also explain why, up to now, no PD-associated mutation has been identified in LRRK1 (116).

At present, little is known about LRRK1 biochemical properties. The cellular function of LRRK1 has been much less investigated because LRRK1 is not clearly linked to a human disease. In 2011, Hanafusa et al. (117) published an elegant paper demonstrating that LRRK1 plays a role in endocytosis of epidermal growth factor receptor (EGFR). In this study, it was shown that LRRK1 forms a complex with activated EGFR through an interaction with Grb2 (growth-factor-receptor-bound protein 2). In addition, LRRK1 regulates EGFR transport from early to late endosomes. Of note, LRRK1 was found to interact with proteins involved in the dynein-mediated endocytosis process.

Taken together, these observations imply that LRRK1 and LRRK2 may share convergent functions, possibly acting as scaffolds but in different steps of the vesicle trafficking (111)(120) or in different tissues.

CHAPTER 2

MATERIALS AND METHODS

2.1 Materials

Antibodies: anti-TH (1:4000 Sigma), anti-Myc (1:5000 Sigma), anti-DRD1 (1:2000 Sigma), anti-NR1 (1:2000 Sigma), anti-Sec8 (1:4000 BD-Biosciences), anti-clathrin (1:5000 BD-Biosciences).

Sheep anti-LRRK1 was obtained from Prof. Dario Alessi (University of Dundee, Dundee, UK) and used at 1:200. Anti-LRRK2 antibodies used were the rabbit monoclonal antibodies C41-2 and UDD3 (antibody produced by Epitomics with the support of the Michael J. Fox Foundation) and used 1:1000) (118)

Reagents: Tween 20 (Polyethylene glycol sorbitan monolaurate), Phenylmethanesulfonyl fluoride (PMSF), protease inhibitor cocktail and (2)-Nicotine hydrogen tartrate salt were obtained from Sigma-Aldrich. LRRK2 inhibitor GSK2578215A was from Tocris. The phosphate-buffered saline (PBS) solution was made using NaCl (137 mM), KCl (2.7 mM), Na2HPO4 (8.1 mM), KH2PO4 (1.47 mM), CaCl2 (1.19 mM), MgCl2 (0.54 mM), and glucose (7.5 mM) from Sigma and then adjusted to pH 7.4. Dulbecco's modified Eagle's medium (DMEM)–F12, Streptomycin/ Penicillin, Hygromycine B, Geneticin-G418 were purchased from Invitrogen and doxycycline from BD Biosciences. The tetracycline-free Fetal Bovine Serum (FBS) was from Lonza Sales Ltd (Switzerland). The blasticidin 10 µg/ml (Invivogen, San Diego, CA, USA), and Gentamicin from Sigma.

Cell lines and stable clones

HEK293 human embryonic kidney cells were cultured in Dulbecco's modified Eagle's medium (DMEM) supplemented with 10% fetal bovine serum at 37°C and 5% CO2 .

Human neuroblastoma SH-SY5Y cells (ATCC number CRL- 2266) were grown in DMEM-F12 (Invitrogen), 10% fetal calf serum (FCS, Invitrogen) at 37°C and 5% CO2.

For the microdialysis experiments a PC12-TET-ON cell line (Clontech Laboratories Inc) or PC12-TET-ON cell lines expressing the plasmid pTRE2 containing cDNAs coding for LRRK2 variants (WT or R1441C or G2019S) were used. The plasmid pTRE2 vectors containing

cDNAs coding for LRRK2 variants (WT or R1441C or G2019S) were cotransfected with p-TK-Hyg in a 8:1 molar ratio into PC12- TET-ON cells, using Lipofectamine LTX Reagent (Life Technologies) according to the manufacturer's protocol. The different PC12-TET-ON clones were maintained under selection by 400 μg/mL of G418 and 200 μg/mL of hygromicin-B. Individual clones expressing both antibiotic resistances were picked after 14 days of selection, moved in a 96 well plate, and maintained in selective medium till confluence growth. Different individual clones were analyzed for LRRK2 expression upon induction by doxycycline (0.2 μg/mL). All the PC12-TET-ON and PC12-TET-ON derived cell lines (Clontech Laboratories Inc) were cultivated in DMEM-F12 supplemented with 10% Tetracycline-free FCS (Lonza) and maintained under selection by 200 μg/mL of G418 and 100 μg/mL of hygromicin-B at 37°C and 5% CO2.

For the LRRK1-LRRK2 functional redundancy study a combination of four different cell lines derived from SH-SY5Y cells was used. Namely stably SH-SY5Y cells previously generated in the lab by co-transduction of lentiviral (LV) knockdown (KD) constructs (blasticidin selected) and a lentiviral construct for eGFP-LRRK1 or eGFP-LRRK2 expression following the scheme below.

CONTROL SH-SY5Y+ e-GFP LRRK1 (LV_miR_Fluc_ctrl)	SH-SY5Y KD LRRK2 + e-GFP LRRK1 (LV_miR_LRRK2_6251)
CONTROL SH-SY5Y + e-GFP LRRK2 (LV_miR_Fluc_ctrl)	SH-SY5Y KD LRRK1 + e-GFP LRRK2 (LV_miR_LRRK1_6734)

Further information on the LV construct used for KD are reported in table 4 (note that the number immediately following the gene name refers to the position on the cDNA sequence of the first base of the short hairpin sequence).

Name of oligonucleotide	Oligonucleotide sequence	Start position of the short hairpin sequence in target's reference sequence
sh1 miR30 LRRK1 S	GAGCG G**CCCAGGTCTCAGATGGAATTA** *TAGTGAAGCCACAGATGTA* **TAATTCCATCTGAGACCTGGG**G T	6734
sh3 miR30 LRRK2 S	GAGCG A**GCCAGAGGAAATGTCATTTAT** *TAGTGAAGCCACAGATGTA* **ATAAATGACATTTCCTCTGGC**A T	6251

Table 4: List of primers used to generate lentiviral vectors expressing short hairpin RNA (microRNA based). Forward and reverse primers are given, sequences depicted in bold correspond to the hairpin stem sequence containing the LRRK1 or LRRK2 target sequence, sequences given in italics are the loop sequence.

Stably transduced SH-SY5Y human neuroblastoma cells used in the functional redundancy study were cultured in Dulbecco's modified Eagle's medium (DMEM) supplemented with 15% fetal bovine serum and 1x non-essential amino acids (Life Technologies) at 37°C and 5% CO2. These cell lines co-express a blasticidin selection marker, thus growth medium was supplemented by blasticidin 10 μg/ml (Invivogen, San Diego, CA, USA).

Animals

LRRK2 G2019S transgenic mice were provided by prof. Ted M. Dawson Department of Neurology, Johns Hopkins University School of Medicine, Baltimore, Maryland, USA.

Mice were housed and treated in strict accordance with the NIH Guide for the Care and Use of Laboratory Animals. All animal procedures were approved by the Institutional Animal Care and Use Committees of the Johns Hopkins Medical Institutions (Animal Welfare Assurance No. A3272-01). Mice were maintained in a pathogen-free facility and exposed to a 12 h light/dark cycle with food and water provided ad libitum

2.2 Methods

Plasmid constructions

The plasmids for inducible expression of LRRK2 were obtained by digestions of cDNAs corresponding to human LRRK2 (WT or R1441C or G2019S) in fusion with 5X myc repeats [26] with BamHI and XhoI and subcloned in BamHI/EcoRV cloning sites in pTRE2 vector (Clontech).

cDNA coding for mouse growth hormone (GH, NM_008117.2) was RT–PCR amplified from mouse pituitary gland mRNA (oligo forward: ATCAGGATCCTTGGCAATGGCTACAGACTC, reverse: ATCAGGATCCGAAGGCACAGCTGCTTTCC), digested with BamHI restriction enzyme and cloned in BamHI cloning site of pCS2-5X-myc-tag containing the tag in C-terminal position. Plasmid pTL2-DRD1 (kindly provided by E. Borrelli, University of California, Irvine) was used as template for DRD1 cDNA, the PCR fragment oligo forward: ATCCTCGAGAAGATGGCTCCTAACACTTCTACCA, oligo reverse: CTCCTCGAGGGTTGAATGCTGTCCGCTGTG) was digested with XhoI and subcloned into pcDNA3.1-3X-flag-tag containing the tag in the C-terminal position.

p-TK-Hyg (Clontech Laboratories Inc) was used to provide hygromycin resistance to PC12 ON cells.

Use of restriction and modification enzymes

The digestion reactions are usually assembled with 3 units enzyme/µg DNA and the specific reaction buffer. The incubation is performed for one hour at 37°C. After the digestion with appropriate enzymes, vectors are treated, at 37 °C for one hour, by CIP (Calf Intestinal Phosphatase, Promega), to remove phosphate groups at 5' ends of the linearized plasmid.

Agarose gel electrophoresis

The agarose is melted in 1X in TAE (40 mM Tris-HCl, pH [8.5], 1 mM EDTA, 20 mM acetic acid) and ethidium bromide (EtBr) is added at a final concentration of 0.04 µg/ml. DNA samples are loaded using loading buffer (0.04% bromophenol blue, 0.04% xylene cianol,

30% glycerol) and run at 120V. Nucleic acid bands are visualized under UV light. The size of the fragments is estimated in the presence of a ladder of known molecular weight.

DNA purification from agarose gel

Kit Wizard ® SV Gel and PCR Clean-Up System (Promega) are used to isolate a DNA fragment as folloes: excide the DNA bands from the agarose gel and place in a 1.5 ml microcentrifuge tube. Add Membrane Binding Solution (10µl/10mg of gel slice). Vortex and incubate at 50-65°C until gel slice is completely dissolved. Insert SV Minicolumn into Collection Tube. Transfer dissolved gel mixture to the Minicolumn assembly. Incubate at room temperature for 1. Centrifuge at 16,000 ×g for 1'. Discard flow through and reinsert Minicolumn into Collection Tube. Add 700µl Membrane Wash Solution (ethanol added). Centrifuge at 16,000 ×g for 1'. Discard flow through and reinsert Minicolumn into Collection Tube. Repeat Step 4 with 500µl Membrane Wash Solution. Centrifuge at 16,000 ×g for 1'. Empty the Collection Tube and centrifuge again the column assembly for 1' with the microcentrifuge lid open (or off) to allow evaporation of any residual ethanol. Carefully transfer Minicolumn to a clean 1.5 ml microcentrifuge tube. Add 50 µl of Nuclease-Free Water to the Minicolumn. Incubate at room temperature for 1'. Centrifuge at 16,000 ×g for 1'. Discard Minicolumn and store DNA at 4°C or -20°C.

Ligation reaction

Ligase reaction is set up as follows: in a final volume of 15 µl, incubate 20-80 ng of linearized plasmid and a variable quantity of insert in the presence of 1 unit of T4 DNA ligase (Promega) in an appropriate buffer (Ligase buffer 10X, Promega). Evaluate, for each cloning, the optimal ratio vector/insert for the reaction. After an incubation O/N at 16°C, transform E. coli DH5 α cells with 5 µl of the reaction.

Bacterial transformation

The DH5apha strain cells were used. The reaction has been performed as follows: add 5 µl of a ligation reaction to 80 µl of competent cells. After incubation on ice for 30', shock the cells at 37 °C for 3', then incubate at room temperature for 10'. Add 500 µl of LB and

incubate at 37 °C for 50', centrifuge for few seconds to obtain a pellet and, eliminated 500 ml of LB, dissolve the pellet. Plate cells on a selective solid medium (LB agar and appropriate antibiotic) and incubate O/N at 37 °C.

Plasmid DNA purification (Miniprep)

Wizard®Plus SV Minipreps DNA Purification System (Promega) is used to purify plasmidic DNA. Pellet 5 ml of overnight culture. Thoroughly resuspend pellet with 250 µl of Cell Resuspension Solution. Add 250 µl of Cell Lysis Solution to each sample; invert 4 times to mix. Add 10 µl of Alkaline Protease Solution; invert 4 times to mix. Incubate 5 minutes at room temperature. Add 350 µl of Neutralization Solution; invert 4 times to mix. Centrifuge at top speed for 10' at room temperature. Insert Spin Column into Collection Tube. Decant cleared lysate into Spin Column. Centrifuge at top speed for 1' at room temperature. Discard flowthrough, and reinsert Column into Collection Tube. Add 750 µl of Wash Solution (ethanol added). Centrifuge at top speed for 1'. Discard flowthrough and reinsert column into Collection Tube. Repeat washing step with 250 µl of Wash Solution. Centrifuge at top speed for 2' at room temperature. Transfer Spin Column to a sterile 1.5 ml microcentrifuge tube, being careful not to transfer any of the Column Wash Solution with the Spin Column. If the Spin Column has Column Wash Solution associated with it, centrifuge again for 1' at top speed, then transfer the Spin Column to a new, sterile 1.5 ml microcentrifuge tube. Add 100 µl of Nuclease-Free Water to the Spin Column. Centrifuge at top speed for 1' at room temperature. Discard column, and store DNA at -20°C.

DNA quantification by UV spectrophotometry

Dilute 5 µl of sample in 1 ml of H_2O into a quartz cuvette. Measure the absorbance at a wavelength of 260 nm and 280 nm by spectrophotometry. Absorbance (OD) of the sample at 260 nm provides a measure of the amount of nucleic acids present in the sample considering 1 OD=50µg/ml for DNA and 1 OD=40 µg/ml for the RNA, the absorbance at 280 nm estimates the amount of protein contaminants.

PCR reaction

DNA/cDNA 2.5 ng/µl	2µl
Pfu (Promega)	1 µl
dNTP 2mM	2µl
Oligo forward + reverse mix 10µM	2µl
Pfu Buffer 10x (Promega)	2µl
H_2O	11µl
Final volume	20µl

Amplification conditions are:

1. 3' 94°C

2. 30'' 94°C denaturation,

3. 30'' at the specific annealing temperature of the primer

4. 1' at 72 °C per kb of DNA for the extension

5. 10' at 72°C

Steps 2-3-4 are repeated for 30 cycles.

Analysis of Intracellular and Extracellular Dopamine and Metabolites

Intracellular and extracellular dopamine (DA), 3-methoxytyramine (3-MT), 3,4-Dihydroxyphenylacetic acid (DOPAC), and homovanillic acid (HVA) were determined by HPLC with electrochemical detection as previously described (119). In brief, cells were lysed in 250 µL 1% metaphosphoric acid containing 1 µM EDTA. After centrifugation

(17,500 g for 10 min at 4°C), the supernatant was filtered, and a 15- µL aliquot was immediately injected into the HPLC system. In each experiment, 100 X 10^3 cells/cm2 were plated and treated 24 h later (time 0) with doxycycline 0.2 µg/mL. After 48 h, the medium was aspirated from each well and stored, and the cells were collected in metaphosphoric acid. Samples were subsequently analyzed for levels of total DA (DA+3-MT) and its metabolites DOPAC and HVA in cell lysates and incubation medium. Values in cell lysate were expressed as nanomoles per milligram of protein. Total cell extract protein concentration was determined using the method of Lowry et al. (1951).

Capillary Tube Construction for in vitro Microdialysis

The capillary tube for microdialysis of PC12 cell lines is an adaptation of an in vitro device described previously (120, 121). The microdialysis probe was constructed using two sections of plastic coated silica tubing (150 µm o.d., 75 µm i.d., Scientific Glass Engineering, Milton Keynes, UK), each placed in the centre of a semipermeable polyacrylonitrile dialysis fiber (AN-69, Hospal Industrie, Meyzieu, France). Each semipermeable membrane had an active length of 40 mm. Then each section of plastic-coated silica tubing was positioned in the centre of polyethylene tubing (0.58 mm i.d., 35 mm long, Portex). This section of silica tubing served as the inlet. Dialysates from polyacrylonitrile dialysis fiber were collected from polyethylene tubing, which served as the outlet. All parts were coated with quick-drying epoxy glue. Afterwards the microdialysis probe (the semipermeable polyacrylonitrile dialysis fiber plus sealed plastic-coated silica tubing) was placed in non heparinized microhematocrit capillary tubes (7.5 mm long, 1.1 mm i.d., Chase Scientific Glass, Rockwood, IL, USA). The final volume of microdialysis chamber was approximately 50 µL.

Microdialysis Procedures

Microdialysis experiments were performed during the exponential phase of cell growth. 5 X 10^4 cells/cm^2 were plated and treated 24 h later (time 0) with different Doxycycline concentrations. After 48 h cells were washed twice using 5 ml of modified PBS and 10% DMEM (perfusion medium), harvested and centrifuged (94 g for 5 min). Cells were

resuspended in PBS/ DMEM and the number of cells/ml was assessed in a Burker chamber. The initial volume of the cell suspension was eventually adjusted to reach a final concentration of $1X10^6$ cells/50 µL. Nicotine (5 mM) effect on DA secretion from PC12 lines was evaluated by means of microdialysis in vitro as previously described (121). The cellular microdialysis probe was perfused with PBS/DMEM by means of a peristaltic microinfusion double-channel pump (P720 peristaltic pump (Instech, Plymouth Meeting, PA, USA), which pumped PBS/DMEM at a flow rate of 3.0 µL/min. The pump channels were connected to the inlet by a length of polythene tubing. The perfusion apparatus was then filled with 50 µL of the PC12 cell suspension by aspiration, which was performed manually by means of a 1.0 mL syringe connected to the plastic coated silica tubing sealed outside the polythene tubing. Thereafter, the perfusion apparatus was kept at 37°C. After 1 h of stabilization, 3 microdialysis samples (60 µL each) were recovered at 20 min intervals. Nicotine was added to the perfusion medium and removed after 60 min. In case of LRRK2 inhibitor treatments, GSK2578215A (1 µM) was added at the beginning of stabilization. Samples were recovered during the next two hours. Subsequently, a 35 µL aliquot of each collected dialysate was analysed by HPLC. The concentration of neurochemicals detected after the first 20 min of perfusion was taken as time 0 concentration. Cell viability was assessed before the start and at the end of each experiment by trypan blue exclusion. The viability rate was given as the difference between final and initial percentage of non-viable cells (120, 121).

Chromatographic Analysis of Dialysates from PC12 Cell Suspension

DA was quantified in dialysates of selected experiments (1.0 X 10^6 cells) by HPLC–EC, as described previously (120) using an Alltech 426 HPLC pump (Alltech, Sedriano, Italy) equipped with a Rheodyne injector (model 7725, Rohnert Park, CA, USA), a column (15 cm, 4.6 mm i.d., ODS80TM C18, Toso Haas, Stuttgart, Germany), an electrochemical detector ANTEC– Leyden EC controller (ANTEC, Zoeterwoude, The Netherlands), and a PC-based ADC system (Varian Star Chromatographic Workstation, Varian, Walnut Creek, CA, USA). The mobile phase was citric acid (0.1 M), ethylenediaminetetraacetic acid (EDTA, 1.0 mM), methanol (8.7%) and sodium octylsulfate (48 mg/L), with a flow rate of 1.2 mL/min and pH 2.9

Transient Transfections and Analysis of GH Secretion

Transient transfection were performed with Lipofectamine LTX Reagent (Life Technologies) according to the manufacturer's instructions. After an incubation of 4–6 h with transfection reagents, the cells were cultured in normal growth medium for 24 or 48 h. For GH secretion analysis, SH-SY5Y cells (1.0 X 10^5 cells) were seeded in 24 mm plates and co-transfected the following day either with GH-5Xmyc and pCS2-MTK empty vector or with GH-5Xmyc and the different pCS2-5Xmyc-LRRK2 isoforms in a ratio of 1:10. 24 hours after transfection, the cells were washed twice with fresh medium and normal growth medium was added for another 16 h. In case of LRRK2 inhibitor treatments, GSK2578215A was added 1 h before medium change and then after medium change. The extracellular medium was then collected and centrifuged at 10000xg for 10 min to eliminate cell debris, while the cells were washed twice with PBS and immediately lysed by Laemmli buffer 1X.

For DRD1 membrane localization experiments, the cells were co-transfected in 6 cm plates as described above (in a ratio of 1:5 respectively for DRD1-3Xflag and 5Xmyc-LRRK2 or empty vector) for 48 hours. The quantification of either GH-5Xmyc or DRD1-3Xflag in the different fractions was performed by western blot analysis and densitometric evaluation of the obtained bands (Quantity-One Biorad).

Subcellular Fractionation of Cells or Mouse Tissues

Tissues from 2 months old LRRK2 WT or LRRK2 G2019S transgenic mice [16] were quickly dissected and frozen. Subcellular fractionation was conducted as described in (100). Briefly, SHSY5Y or HEK293 cells or striatum were homogenized in ice-cold homogenization-buffer (320 mM sucrose, 4 mM HEPES, pH 7.4, protease inhibitor cocktail from Sigma). The homogenates were centrifuged at 1000 X g for 10 min to produce the pellet containing nuclei and large debris fraction (P1). The supernatant (S1) was further fractionated into pellet (P2 containing the membrane fraction) and supernatant (S2) by centrifugation at 10,000 X g for 20 min. The S2 was ultracentrifuged at 100,000 X g to obtain the pellet (P3 containing the vesicle fraction). Protein content was determined using the Bradford protein assay. Equal amount of protein extracts were loaded into the SDS-PAGE.

SDS PAGE and Western immunoblotting

Protein content was determined using the Bradford protein assay. Equal amount of protein extracts were resolved by standard SDS/PAGE. Samples were electroblotted onto Protan nitrocellulose (Schleicher & Schuell GmbH). Membranes were incubated with 3% low-fat milk in 1 X PBS-Tween 0.05% solution with the indicated antibody for 16 h at 4°C. Anti-Rabbit IgG (whole molecule)- and Anti-Mouse IgG (whole molecule)-Peroxidase antibody were used to reveal immunocomplexes by enhanced chemioluminescence (Pierce).

EGF-R internalization assay

SH-SY5Y cell lines were cultured in Dulbecco's modified Eagle's medium containing 15% Foetal bovine serum, 1% MEM NEAA, gentamicin. For cell lines co-expressing a blasticidin selection marker, growth medium was supplemented by blasticidin 10 µg/ml (Invivogen, San Diego, CA, USA). The cells are cultured for 16 hours in serum free medium and then incubated with medium containing 100 ng/ml fluorescently labelled Rhodamine-conjugated EGF (EGF-Rh) at 37°C. Cells are then washed two times with PBS 1X to remove excess labelled EGF and fixed in formaldehyde 4% w/w in PBS for the time points indicated in the result section (0-30 minutes). Cells were imaged by confocal microscopy with an Olympus FV1000 microscope. Imaged cells were scored for co-localization of LRRK1 or LRRK2 with EGF-Rh positive endosomes. Cells with at least 5 double positive endosomes are scored as positive. For each condition tested, at least 3 wells with 20-100 cells per well were scored.

Statistical analysis

All quantitative data are expressed as means ± SEM, all experiments were performed in triplicate or better.

Concentrations of neurochemicals in dialysates from PC12 cell suspension were expressed in µM and given as mean ± SEM. Drug effects on neurochemicals were statistically evaluated in terms of changes in absolute dialysate concentrations. Differences within or

between groups were determined by paired or unpaired t-tests (ANOVA followed by Student–Newman–Keuls post-hoc analysis). The null hypothesis was rejected when $p < 0.05$.

CHAPTER 3

RESULTS

3.1 Characterization of PC12 Cells Stably Expressing Doxycycline-inducible LRRK2 WT or Pathological Mutants (*in collaboration with the Department of Clinical and Experimental Medicine – University of Sassari)*

For the microdialysis experiments described below a PC12-TET-ON cell line (Clontech Laboratories Inc) or PC12-TET-ON cell lines expressing the plasmid pTRE2 containing the cDNAs coding for LRRK2 variants (WT or R1441C or G2019S) were used.

The TET-ON System allows the inducible expression of LRRK2 variants coded in the pTRE2 plasmid and is shown in figure 14. The TET-ON system utilizes doxycycline, a tetracycline analogue, to induce transcription. When Doxycycline is added into the cell medium, the transactivator, (already stably expressed in TET-ON cells), is engaged in a conformational change allowing it to bind the tetracycline response elements (TRE) which in turn leads to transcriptional activation.

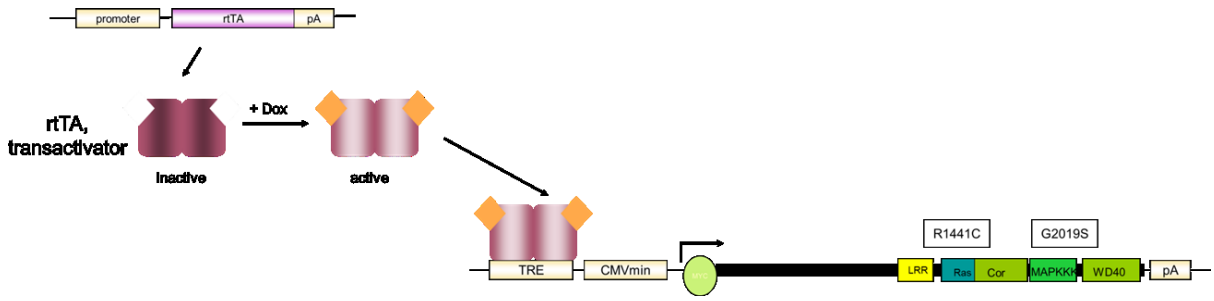

Figure 14: The TET-ON expression system.

In particular in the PC12 cell lines used in this work express the "tet reversed activator system" in which a tetracycline repressor mutant is fused with the Herpes Simplex VP16 activation domain thus acting as a transactivator.

To generate the PC12-ON stable line, plasmid constructs for wild type LRRK2 or for pathological mutants LRRK2 G2019S and LRRK2 R1441C were transfected in PC12-ON cell lines. After several weeks of selection by hygromicin, single stable clones were isolated. Different clones were characterized and finally three clones expressing comparable level of

LRRK2 protein after 48 h of induction by 0.2 μg/ml doxycycline treatment were chosen (Figure 15 A upper panel). All cell lines expressed comparable levels of Tyrosine Hydroxylase (TH) after the same treatments (Figure 15 A, middle panel). A higher dose of doxycycline (1 μg/mL) does not further increase the LRRK2 expression level (Figure 15 B). The doxycycline concentration of 0.2 μg/ml was used in all the following experiments.

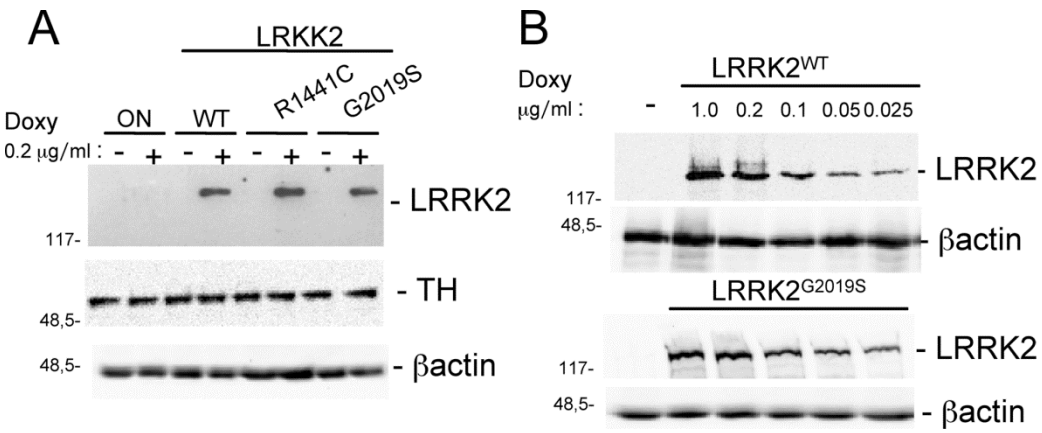

Figure 15. Characterization of PC12 cell expressing WT or mutant LRRK2. (A) PC12-derived cells expressing myc-tagged human WT or mutant-LRRK2 were left untreated (-) or treated (+) for 48 h with 0.2 μg/mL doxycycline to induce expression of transgenic LRRK2. Cell lysates were subjected to reducing SDS/PAGE. The anti-myc antibody was used to visualize LRRK2 and anti-TH for tyrosine hydroxylase. β-actin serves as controls for equal loading of samples. (B) Dose dependent expression of doxycyline-inducible LRRK2 G2019S. Cells were treated for 48 h with the indicated concentration of doxycycline and equal amounts of protein were tested in Western blot analysis with anti-myc or anti-β-actin antibodies

Once established the expression homogeneity of the different LRRK2, the dopamine and dopamine metabolites levels in the different clones were assessed in basal growth conditions. 48 hours after 0.2 μg/ml doxycycline treatment, the intracellular and extracellular dopamine (DA) level and its metabolism products were analyzed in the different cell lines (Figure 16). All the stable clones show comparable intracellular and extracellular levels of DA content as well as the intracellular and extracellular level of DOPAC+HVA, allowing the comparative analysis between the different stable clones performed in the following experiments.

	Intracellular content (nmol/mg protein)		Medium Contentration (μM)	
	DA	DOPAC+HVA	DA Total (DA+3-MT)	DOPAC+HVA
PC12-LRRK2^{WT}	6.14 ± 0.55	0.24 ± 0.05	0.76 ± 0.12	15.23 ± 5.85
PC12-LRRK2^{R1441C}	6.15 ± 0.50	0.21 ± 0.008	0.58 ± 0.05	18.24 ± 6.61
PC12-LRRK2^{G2019S}	6.80 ± 1.31	0.17 ± 0.002	0.60 ± 0.11	14.41 ± 5.98

Figure 16. Characterization of PC12 cell expressing WT or mutant LRRK2. Effect of doxycycline on DA and DOPAC+HVA concentration in PC12 cells lysates and extracellular medium after 48 h expression. At the beginning of each experiment, 105 PC12 cells/cm^2 were plated and after the desired incubation period, the medium was aspirated from each well and stored, and the cells were collected in metaphosphoric acid. Samples were subsequently analyzed for levels of DA and its metabolites DOPAC and HVA in cell lysates and incubation medium. Results are the means ± SEM of three experiments performed in triplicate.

3.2 LRRK2 Influences the Basal and Nicotine-induced secretion of DA in PC12 Cells *(In collaboration with the Department of Clinical and Experimental Medicine – University of Sassari)*

In order to evaluate the effect of the expression of LRRK2 on basal and nicotine-induced secretion of DA, a microdialysis study was performed on the PC12 cell model [33] treated with 0.2 μg/mL doxycycline for 48 h compared with untreated (2) cells. This doxycycline dose was chosen because, in preliminary experiments, it did not show any significant effect on DA secretion on PC12-ON cells in contrast to 1 μg/mL of doxycycline that had a negative effect on DA secretion. Microdialysates were collected at 20 minute intervals after 1 h of stabilization (Figure 17 A–B–C–D). The time course analysis of basal and nicotine induced dopamine release in the absence (Figure 17 A) or presence (Figure 17 C) of doxycycline is shown. In Figure 17 B–D, the Area Under Curve (AUC) of the different samples is shown; in particular, the baseline of DA+3-MT is represented from the AUC of points 20–60 minutes before nicotine treatment in absence. (Figure 17 B bars) or presence of doxycycline (Figure 17 B barred bars), while the DA+3-MT nicotine-induced release is represented by the AUC related to points 80–220 minutes in absence (Figure 17 D black bars) or presence of doxycycline (Figure 17 D dotted bars). The expression of LRRK2 G2019S induces an 85%

increase ($p<0.05$) vs corresponding control in the basal level of total extracellular DA (DA+3-MT), as shown in figure 17 C (20–40–60 minutes) compared to 17 A (20–40–60 minutes) and quantified by the AUC in Figure 17 B. In contrast, under the same experimental conditions expression of either LRRK2 WT or LRRK2 R1441C does not induce a significant increase in total DA extracellular levels (Figure 17 A–C and quantified in 17 B). Interestingly, the presence of mutant LRRK2 determines an increase in nicotine-induced DA compared to PC12-ON or LRRK2 WT cells (Figure 17 C 60–220 minutes vs 17 A 60–220 minutes). Quantification by AUC of secreted DA indicates an increase of 22% (although not statistical significant) and 61% ($p<0.05$), respectively for LRRK2 R1441C and LRRK2 G2019 (Figure 17 D). Under the same experimental conditions, were measured extracellular levels of DOPAC+HVA. A significant change both in the basal condition and after nicotine infusion is observed following doxycycline treatment in PC12 cells expressing LRRK2 WT or LRRK2 R1441C (Figure 18 A–B–C–D). In particular the values are 261.4% for WT and 251.7% for LRRK2 R1441C in doxycycline treated samples and 264.9% for WT and 245.3% for R1441C mutant by doxycycline and nicotine treatment. No significant differences were observed in PC12-ON cells or expressing the LRRK2 G2019S mutant. To evaluate the importance of LRRK2 kinase activity on increased DA extracellular level, we used the LRRK2 inhibitor GSK2578215A on PC12-ON or PC12-ON expressing the LRRK2 G2019S. The presence of LRRK2 inhibitor does not influence the DA extracellular level in basal conditions (20–40–60 minutes in figure 19 A vs B or the relative AUC in Figure 19 C) in both cellular types. In presence of nicotine, the inhibitor does not affect the expected increase in DA extracellular level in PC12-ON cells while it determines a reduction in PC12-ON expressing the LRRK2 G2019S mutant although this DA extracellular level decrease does not rich statistical significance in three independent experiments (Figure 19 A from 60 to 220 minutes vs 19 B from 60 to 220 minutes and the relative AUC in Figure 19 D). Under the same experimental conditions, the GSK2578215A inhibitor does not affect the concentration of DOPAC+HVA.

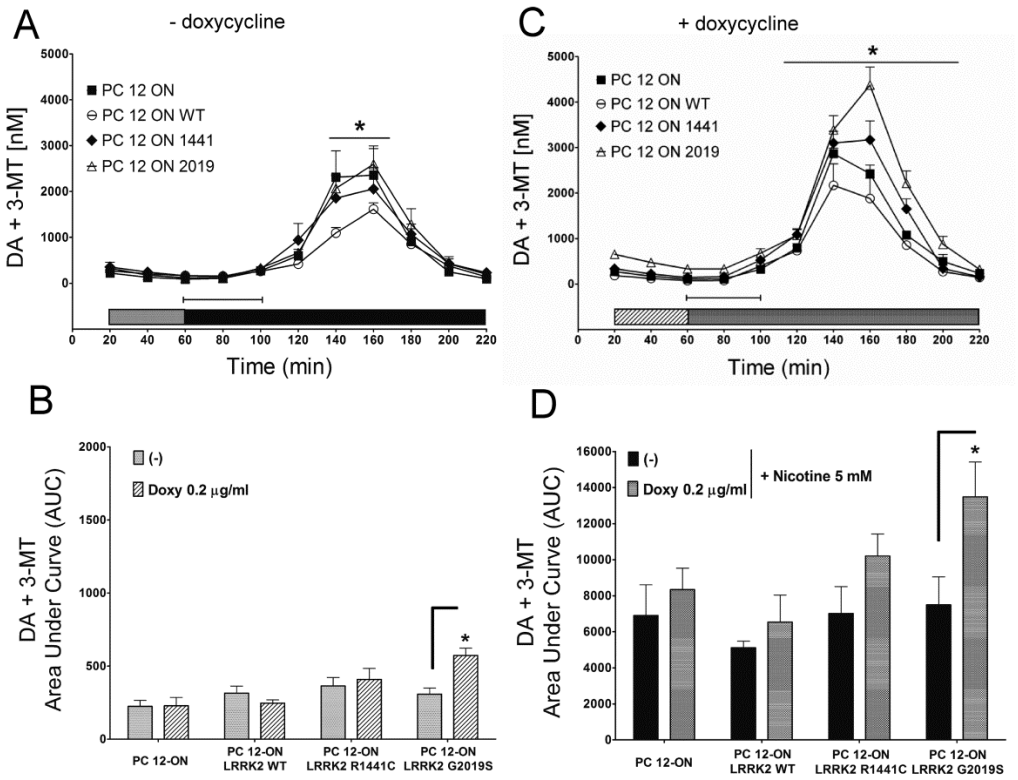

Figure 17. Effect of LRRK2 expression on dopamine (DA+3-MT) extracellular level. PC12-derived cell lines were left untreated (A) or treated (C) for 48 h with 0.2 µg/mL doxycycline. After 60 minutes of stabilization, three baseline dialysates were collected at 20-minute intervals [gray bars in panel (A), and gray bars with stripes in panel (C)]. Starting from 60 minutes, nicotine was infused for 60 minutes (capped lines). Microdialysates wer continuously recovered during drug infusion and after nicotine discontinuation [black bars in panel (A), and dotted bars in panel (C)]. Values are mean ± SEM and refer to dopamine concentrations in dialysates. Statistical significance was assessed using analysis of variance (ANOVA) for differences over time determined by Newman-Keules t test and unpaired t-tests. *$p < 0.05$ compared with pertinent baseline values of all groups. Graphs in panel (B) and (D) represent the area under curve (AUC) values. (B) Basal dopamine concentration in dialysates of PC12 cell lines untreated (gray bars corresponding to the same color in panel A) or treated with 0.2 µg/mL doxycycline [gray bars with stripes corresponding to same color in panel (C)]. (D) Dopamine concentrations in dialysates integrated after nicotine administration in PC12 cell lines untreated [black bars corresponding to same color in panel (A)] or treated with 0.2 µg/mL of doxycycline [dotted bars corresponding to same color in panel (C)]. AUC values are mean ± SEM. *$p < 0.05$ vs corresponding control.

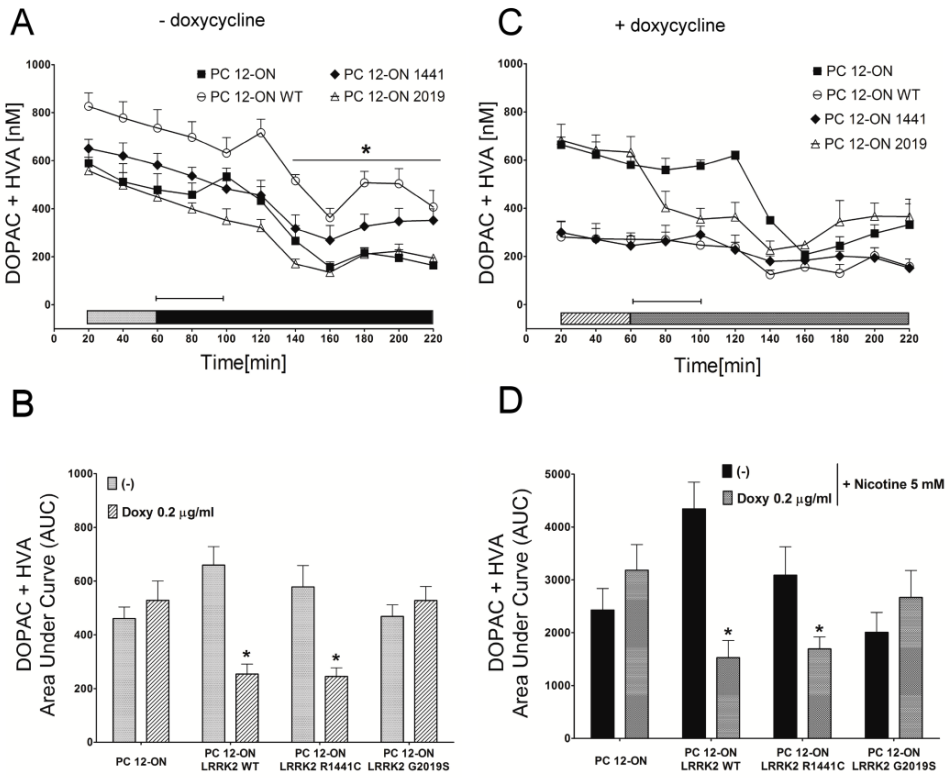

Figure 18. Effect LRRK2 expression on DOPAC+HVA concentrations. PC12-derived cell lines were left untreated (A) or treated (C) for 48 h with 0.2 μg/ml doxycycline. After 60 minutes of stabilization, three baseline dialysates were collected at 20-minute intervals [bars in panel (A), and grey bars with stripes in panel (C)]. Starting from 60 minutes, nicotine was infused for 60 minutes (capped lines). Microdialysates were continuously recovered during drug infusion and after nicotine discontinuation [black bars in panel (A), and dotted bars in panel (C)]. Values are mean ± SEM and refer to DOPAC+HVA concentrations in dialysates. Statistical significance was assessed using analysis of variance (ANOVA) for differences over time determined by Newman-Keules t test and unpaired t-tests. *p < 0.05 compared with pertinent baseline values of all groups. Graphs in panel (B) and (D) represent the area under curve (AUC) values. (B) Basal DOPAC+HVA concentration in dialysates of PC12 cell lines untreated [bars corresponding to the same colour in panel (A)] or treated with 0.2 μg/mL doxycycline [bars with stripes corresponding to the same colour in panel (C)]. (D) DOPAC+HVA concentrations in dialysates integrated after nicotine administration in PC12 cell lines untreated [black bars corresponding to the same colour in panel (A)] or treated with 0.2 μg/ml doxycycline [dotted bars corresponding to the same color in panel (C)]. AUC values are mean ± SEM. *p < 0.05 vs corresponding control.

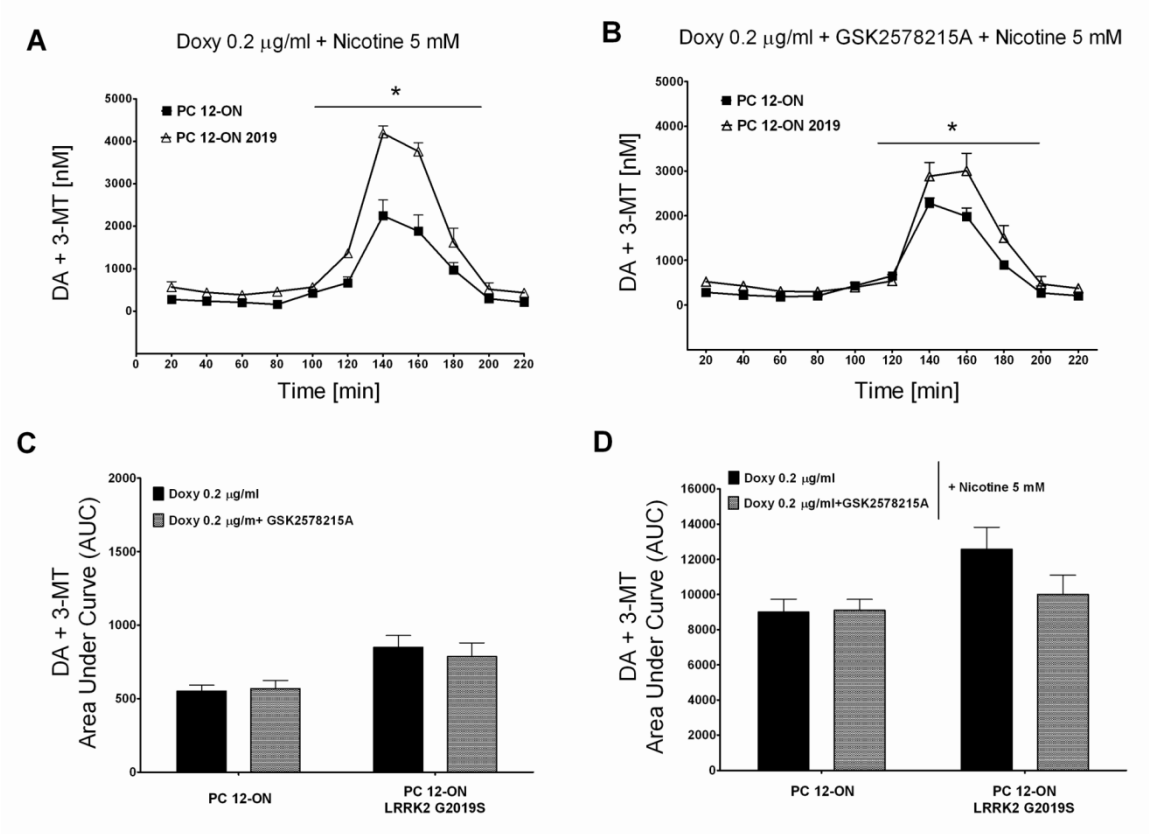

Figure 19: Effect of LRRK2 inhibitor GSK2578215A on dopamine (DA+3-MT) extracellular level. PC12-derived cell lines were left untreated (A) or treated (B) by 1 μM of GSK2578215A. After 60 minutes of stabilization, three baseline dialysates were collected at 20-minute intervals as previously described. Starting from 60 minutes, nicotine was infused for 60 minutes. Values are mean ± SEM and refer to dopamine concentrations in dialysates. Statistical significance was assessed using analysis of variance (ANOVA) for differences over time determined by Newman-Keules t test and unpaired t-tests. *$p < 0.05$ compared with pertinent baseline values of all groups before nicotine treatment. Graphs in panel (C) and (D) represent the area under curve (AUC) values. (C) Basal dopamine concentration in dialysates of PC12 cell lines untreated or treated with 1 μM of GSK2578215A (minutes 20–40–60 before nicotine treatment of Figure 19 A vs B). (D) Dopamine concentrations in dialysates integrated after nicotine administration in PC12 cell lines untreated or treated with 1 μM of GSK2578215A (from minutes 80 to 220 after nicotine treatment of Figure 19 A vs B). AUC values are mean ± SEM.

3.3 Vesicle Distribution in PC12 Cells Expressing LRRK2 G2019S Pathological Mutant

Results obtained on dopamine extracellular levels changes associated with LRRK2 expression prompted to understand whether LRRK2 might be involved in synaptic vesicle (SV) movement/distribution.

The vesicles distribution in PC12-ON or PC12-ON-LRRK2 G2019S cell lines was studied using an electron microscopy approach. Expression was induced for 24 hours with 0.2 μg/mL doxycycline and cells were quickly fixed for electron microscopy. Non-induced cells served as a control. Analysis of SV dimensions or relative abundance did not show significant differences between the different groups. Conversely LRRK2 expression seemed to influence synaptic vesicle distribution in terms of shorter distance to the plasma membrane. Namely it is displayed a clear increase in the relative abundance of vesicles located in close proximity to the membrane in presence of LRRK2 G2019S mutant compared to the same cells not expressing the mutant or to PC12 ON cells either treated or untreated with doxycycline (Figure 20 A–B). The level of LRRK2 expression in the different cell lines was analyzed by Western blot using an aliquot of cells before fixation and it is shown in Figure 20 C.

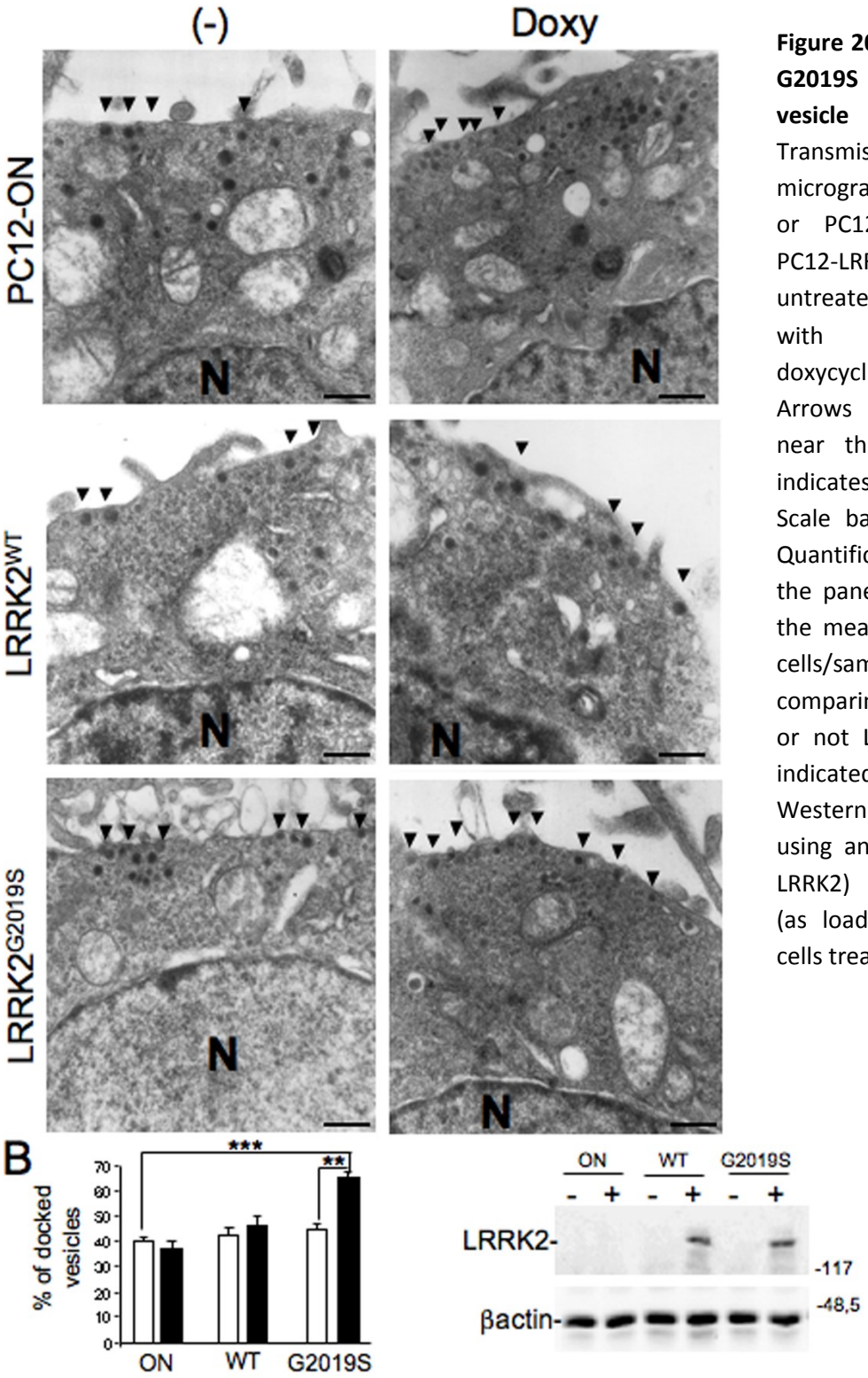

Figure 20: Effect of LRRK2 G2019S expression on vesicle distribution. Transmission electron micrographs of PC12-ON or PC12-LRRK2 WT or PC12-LRRK2 G2019S cells untreated (-) or treated with 0.2 μg/ml doxycycline for 48 h (+). Arrows point at vesicles near the membrane. N indicates the nucleus. Scale bars = 0,5 μm (B) Quantification of data in the panel. Bars represent the mean ± SEM (n = 30 cells/sample). **p < 0.01 comparing cells expressing or not LRRK2 G2019S as indicated. (C) Control Western blot analysis using anti-myc (to detect LRRK2) and anti-β-actin (as loading standard) on cells treated as in (A).

3.4 LRRK2 Increases Growth Hormone Extracellular Level in Neuronal Cells

To further evaluate the involvement of LRRK2 in the mechanisms of vesicle trafficking a plasmid construct to follow secreted proteins was used. This construct consists of mouse growth hormone (mGH), containing a myc-tag at the C-terminal position. GH secretion has been largely used to follow neuronal secretion, since GH is localized predominantly in vesicles in regulated secretory pathways [34,35]. mGH was co-transfected alone or together with different LRRK2 constructs in both neuronal in SH-SY5–or non-neuronal (HEK293) cells. 24 h after co-transfections the cell medium was changed and the level of GH secretion was evaluated collecting the extracellular medium 16 h later. As shown in figure 21 A, the presence of LRRK2 WT in SH-SY5Y determines a slight increase in extracellular GH level. This level is further increased in the presence of mutant LRRK2, with LRRK2 G2019S inducing the maximum effect (Figure 21 A–E). Total cell lysates were used to analyze the intracellular level of mGH, LRRK2 and β-actin as control for homogeneity of transfection efficiency and protein amount loading (Figure 21 A). Interestingly, the effect of LRRK2 on GH secretion was not visible performing similar experiments in kidney HEK-293 cells (Figure 21 B–E) suggesting a possible neuronal-specific mechanism of action for LRRK2. In order to understand the role of LRRK2 kinase activity in the control of GH extracellular level two different approaches were used. First, we analyse the effect of two LRRK2 dead kinase mutants carrying a deletion (delta-kinase) or point mutation (D1994A). Surprisingly, the absence of kinase domain completely abolishes the LRRK2 effect on GH extracellular level, while LRRK2 D1994A has an effect roughly comparable to LRRK2 WT (Figure 21 C). And secondly, to further evaluate the importance of LRRK2 kinase activity we used the LRRK2 inhibitor GSK2578215A. The presence of LRRK2 inhibitor significantly reduces the increase in GH extracellular level due to LRRK2 G2019S expression (Figure 21 D–F).

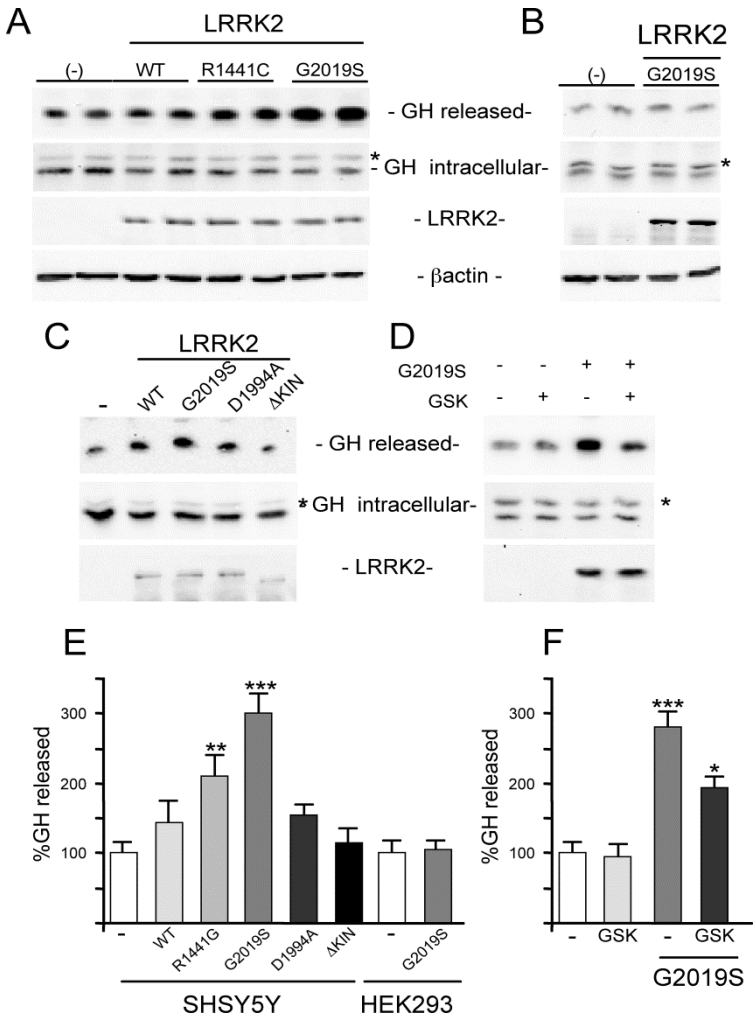

Figure 21. Effect of LRRK2 expression on released GH from neuronal and non-neuronal cells. (A) SH-SY5Y were transfected with plasmids coding for GH alone (-) or with the indicated mutant LRRK2s. Western blot on the extracellular medium (released GH) or cell protein extracts were performed using anti-myc antibodies for GH or LRRK2 and anti-β-actin as controls for equal loading of samples. The asterisk (*) indicates a nonspecific band. (B) HEK293 cells were transfected with GH alone (-) or with LRRK2 G2019S. Western blot on the extracellular medium (released GH) or cell protein extracts were performed using Anti-myc antibody for GH or LRRK2 and anti-β-actin as controls for equal loading of samples. The asterisk (*) indicates a non-specific band. (C) Analysis of LRRK2 D1994A or LRRK2 Δ kinase on GH extracellular level in the same experimental conditions. (D) Effect of LRRK2 inhibitor on GH extracellular level in the same experimental conditions (E) Quantification by Student's t test of data obtained in (A–B–C). **p < 0,01 and ***p < 0,001 versus (-). (F) Quantification by Student's t test of data obtained in (D). *p < 0,05 and ***p,0,001 versus (-).

3.5 LRRK2 Affects the Localization of Dopamine Receptor D1 both in Neuronal Cells and Transgenic Mouse Tissues

Vesicle trafficking is a complex process regulating multiple different cellular functions, including neurotransmitter or protein release and localization of membrane receptors. The previous results prompted the analysis of the possible effect of LRRK2 on membrane receptor localization using the membrane levels of dopamine receptor D1 (DRD1) as a read-out. DRD1 is highly expressed in the *prefrontal cortex, striatum* and *nucleus accumbens*, although it is absent in dopaminergic cells where Dopamine D2 receptors (DRD2) are expressed(122). SH-SY5Y cells were co-transfected with plasmid coding for DRD1 in absence or in presence of one among LRKK2 WT, LRKK2 G2019S, LRKK2 R1441G, LRKK2 D1994A or LRKK2 Δ kinase. 48 hours after transfection, the sub-cellular distribution of DRD1 receptors was analysed by cell fractionation. As shown in figure 22, the presence of LRRK2 G2019S and LRKK2 R1441G, and, to a lesser extent, of LRRK2 WT or LRRK2 D1994A determines a significant increase in the level of membrane-associated DRD1 compared to controls with DRD1 alone, while the effect is completely abolished in presence of LRKK2 delta-kinase. In agreement with previous findings on GH secretion, this effect is not observed in HEK293 cells (Figure 22 B). To extend the analysis to in vivo models the distribution of two neurotransmitter receptors was analyzed in the striatum of transgenic LRRK2 G2019S mice compared to non-transgenic mice. In particular, was compared the distribution of NMDA-NR1 receptor (NR1) and DRD1 in total, membrane or vesicle fractions obtained from the striatum of 5 different animals of the two genotypes. The samples were independently prepared, quantified and pooled together before SDS-PAGE loading using the same amount of protein. As shown in Figure 23 A the expression of LRRK2 G2019S leads to a significant increase of DRD1 in membrane fraction paralleling a significant decrease in vesicle fraction, with no significant differences in total protein extracts between the two genotypes (Figure 23 B). No significant differences in the different fractions were observed for NR1, clathrin or sec8, a member of the exocyst complex.

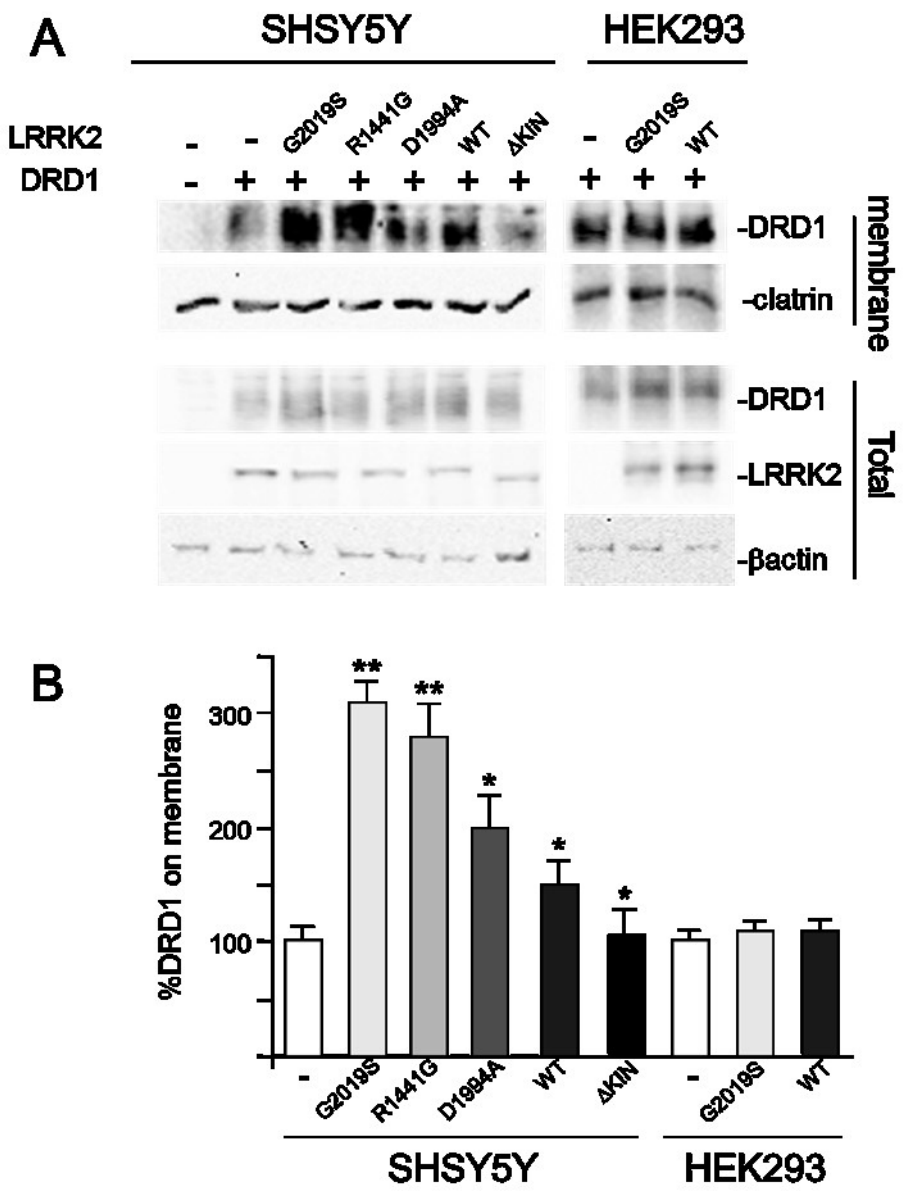

Figure 22. Effect of LRRK2 on Dopamine D1 receptor (DRD1) distribution on neuronal and non-neuronal cells). A) SH-SY5Y or HEK293 were transfected with DRD1 alone (-) or with the indicated mutant LRRK2. Western blot on the total and membrane fraction proteins were performed using anti-flag antibody for DRD1 or anti-myc for LRRK2 and anti-β-actin or clathrin as controls for equal loading of samples. Note that for SDS-PAGE analysis the protein samples were not boiled as suggested in anti-DRD1 data sheet. (B) Quantification by Student's t test of data obtained in (A). *p < 0,05 **p < 0,01 and ***p < 0,001.

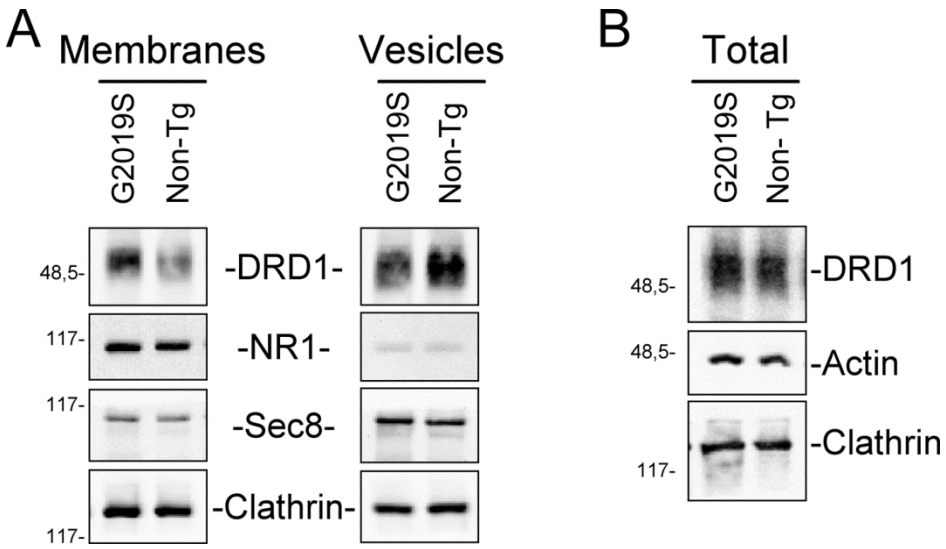

Figure 23. Effect of LRRK2 on Dopamine D1 receptor (DRD1) distribution on the striatum of G2019S LRRK2 or non-transgenic mice. The total, membrane or vesicle fractions were purified from 5 different LRRK2 G2019S transgenic mice or relative control (Non-Tg). Each of the five fractions were quantified and pooled together. A) Analysis of DRD1 level on protein extracts from membrane or vesicle fraction obtained from striatum of Non-Tg or LRRK2 G2019S transgenic mice. The western blot was performed using anti-DRD1, anti-NR1, anti-Sec8, or anti-clathrin antibodies. Note that for DRD1 analysis the samples were not boiled for the SDS-PAGE analysis as recommended in the antibody data sheet. B) Analysis of DRD1 level on total protein extracts obtained from striatum of Non-Tg or LRRK2 G2019S transgenic mice. The western blot was performed using anti-DRD1, anti-actin or anti-clathrin antibodies. Note that for DRD1 analysis the samples were not boiled for the SDS-PAGE analysis.

3.6 LRRK1 and LRRK2 functional redundancy in receptors trafficking

Epidermal growth factor treatment induces translocation of LRRK1, but not LRRK2, to endosomes.

To assess a potential cross-talk between LRRK1 and LRRK2 in respect to EGF receptor (EGFR) trafficking pathway a combination of four different cell lines derived from SH-SY5Y cells was used. Namely stably SH-SY5Y cells generated by co-transduction of a LRRK1 knockdown (KD) or KD control construct and a full-length eGFP-LRRK2 construct, or alternatively, a LRRK2 KD or KD control construct and full-length eGFP-LRRK1 construct. A western blot displaying LRRK1 and LRRK2 expression levels in control and knockdown cell lines is showed in figure 24. The combination of cell lines used for the experiments here described is represented in the scheme below, the lentiviral (LV) construct names in brackets refer to the western blot lanes in figure 24.

CONTROL SH-SY5Y+ e-GFP LRRK1 (LV_miR_Fluc_ctrl)	SH-SY5Y KD LRRK2 + e-GFP LRRK1 (LV_miR_LRRK2_6251)
CONTROL SH-SY5Y + e-GFP LRRK2 (LV_miR_Fluc_ctrl)	SH-SY5Y KD LRRK1 + e-GFP LRRK2 (LV_miR_LRRK1_6734)

The four different SH-SY5Y used in the following experiments

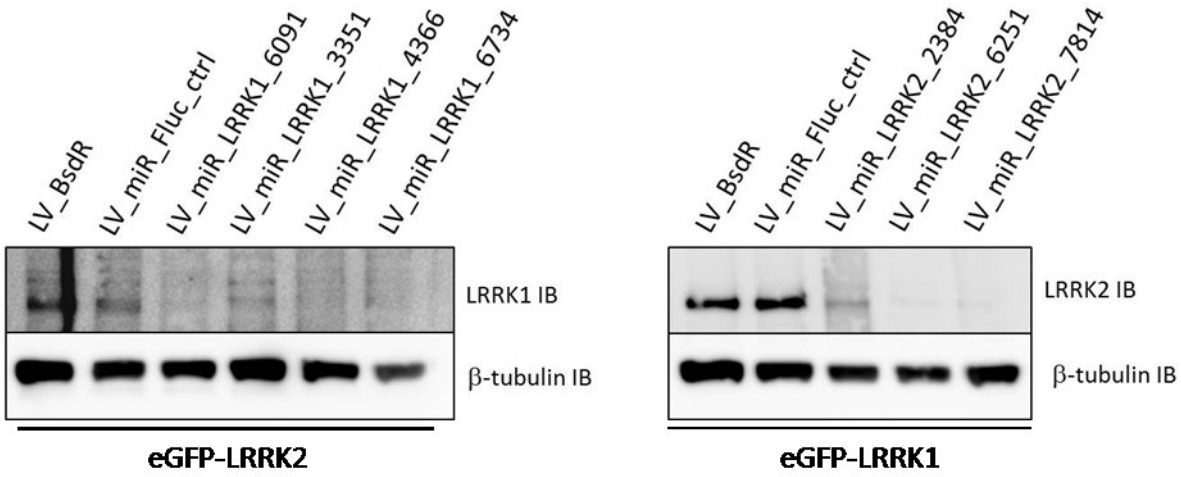

Figure 24: Western blot showing LRRK1 and LRRK2 expression levels in control and knockdown cell lines. The cell lines were obtained co-transducing SH-SY5Y cells with lentiviral vectors expressing eGFP-LRRK2 or eGFP-LRRK1 and the short hairpin RNA (microRNA based) vectors respectively for LRRK1 or LRRK2 knockdown or knockdown control vectors targeting the fire luciferase (Fluc) sequence. (The number immediately following the gene name refers to the position on the cDNA sequence of the first base of the short hairpin sequence).

LRRK1 has previously been shown to translocate to endosomes upon treatment of HeLa cells with EGF (117). This occurs through activation of the endogenous EGF receptor (EGFR), which is also expressed endogenously in SH-SY5Y cells (123). To confirm the LRRK1 EGF-induced translocation in neuronal cells, SH-SY5Y cells stably expressing eGFP-LRRK1 and a knock-down control construct (knockdown construct targeting the firefly luciferase gene) were treated with Rhodamine-conjugated EGF (EGF-Rh) at 100 ng/ml for 5, 15 or 30 minutes in order to mark EGFR positive endosomes. LRRK1 is recruited to EGFR positive endosomes assuming a punctate pattern (see figure 25) while upon the same EGF-Rh stimulation SH-SY5Y-eGFP-LRRK2 stable lines do not show any change in LRRK2 localization (figure 26 and 30-a). Statistical significance of these observations was confirmed by a two way ANOVA analysis: all the experiments have been performed in triplicate and imaged cells were scored for co-localization of LRRK1 or LRRK2 with EGF-Rh positive endosomes. Cells with at least 5 double positive endosomes were scored as positive. For each condition tested, at least 3 wells with an average of 84 cells per well were scored. Two way ANOVA

results for the experiments described above are reported in table 5.

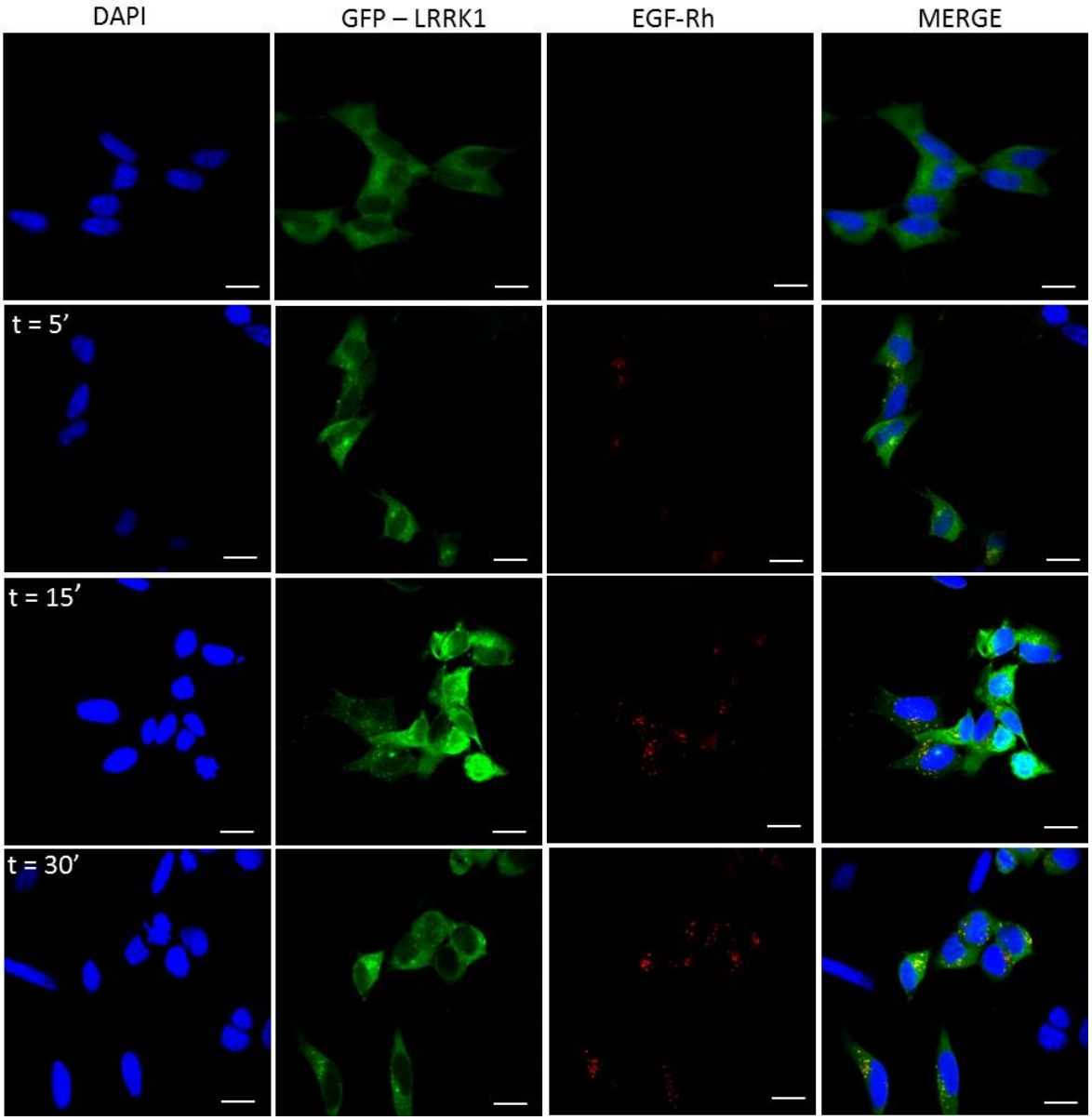

Figure 25: EGF induced translocation of LRRK1. Confocal laser scanning micrographs of SH-SY5Y stably expressing eGFP-LRRK1: untreated (t=0') or treated with 100 ng/mL EGF-Rhodamine conjugate for 5, 15 and 30 minutes. EGF-Rh internalized by the cells is visible as red punctate pattern corresponding to endosomal structures. EGF treatment induces GFP-LRRK1 translocation in punctate structures in the cytoplasm which co-localizes with EGF-Rh positive endosomes. Scale bar, 10 µM applies to all photomicrographs.

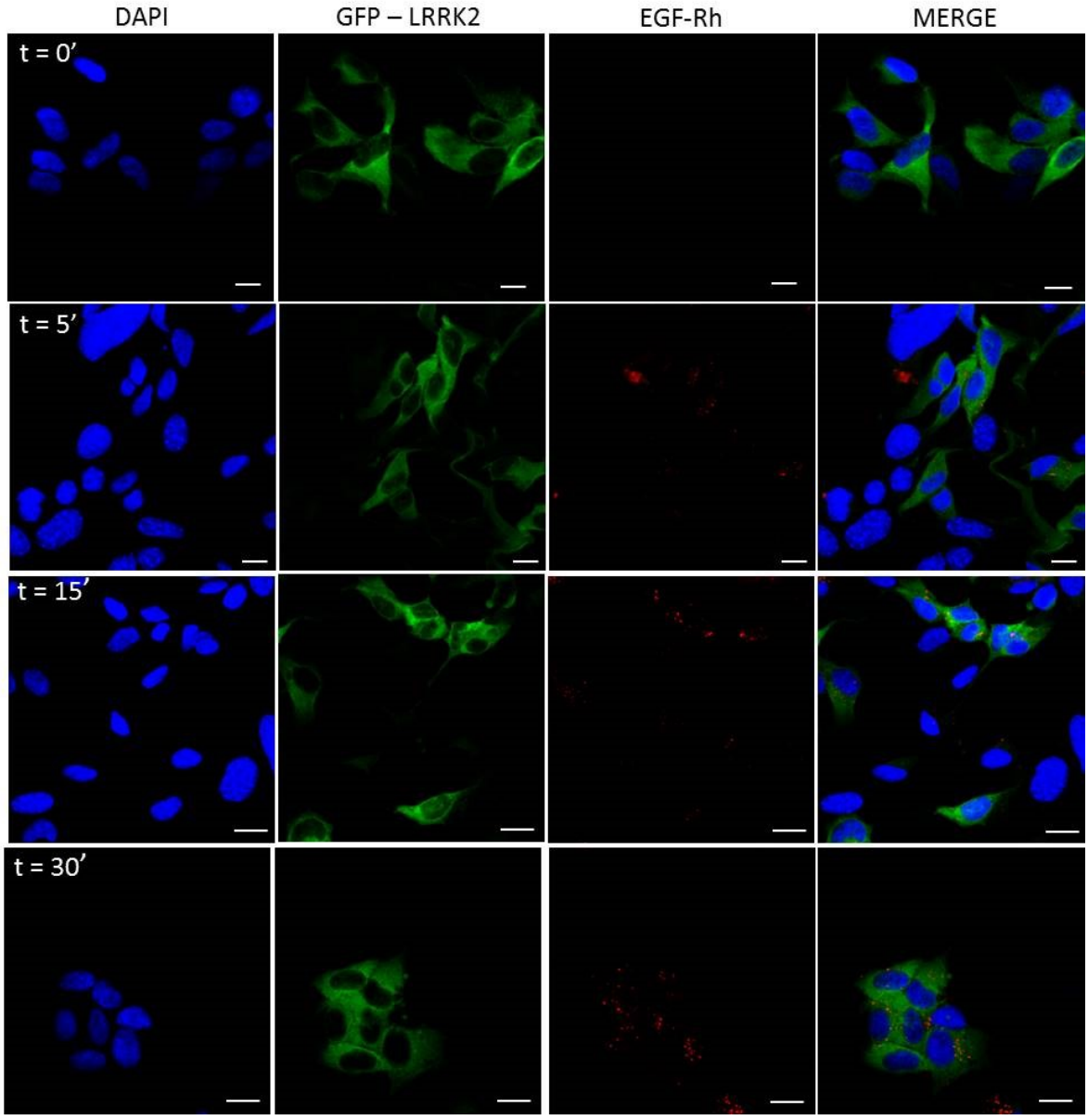

Figure 26: EGF does not induce translocation of LRRK2. Confocal laser scanning micrographs of SH-SY5Y stably expressing eGFP-LRRK2 untreated (t=0') or treated with 100 µg/mL EGF-rhodamine conjugate for 5, 15 and 30 minutes. EGF-Rh is internalized by the cells showing a red punctate pattern but any translocation of GFP-LRRK2 is observed at any EGF-Rh treatment time-point. Scale bar, 10 µM applies to all photomicrographs**.**

GFP-LRRK1 (CTRL) vs GFP-LRRK2 (CTRL)				
Time point EGF-Rh	Difference	t	P value	Significance
0 min	0	0	P > 0.05	ns
5 min	-5,133	0,4689	P > 0.05	ns
15 min	-49,76	4,545	P<0.001	***
30 min	-44,71	4,084	P<0.01	**

Table 5: Two way ANOVA results. Comparison between GFP-LRRK1 control and GFP-LRRK2 control cell lines treated with EGF-Rh 100 ng/ml for 5, 10, 15 or 30 minutes or untreated (0 min). Significance is indicated with *.

As LRRK1 has been reported to interact with LRRK2 (113, 124), I tested whether LRRK2 was required for the recruitment of LRRK1 to endosomes. For this, cells stably expressing eGFP-LRRK1 and LRRK2 KD (LV_miR_LRRK2_6251) were treated with EGF-Rh 100 ng/ml. The EGF induced LRRK1 recruitment to endosomes was comparable in the presence of LRRK2 knockdown compared to control cell lines (Figure 28 and Figure 30 panel b).

Lastly, to assess whether LRRK2 was able to supply LRRK1 function in EGFR trafficking I used stable expressing eGFP-LRRK2 and LRRK1 KD (LV_miR_LRRK1_6734) treating them as previously described with EGF-Rh. As shown in figure 29 figure 30 (panel b) LRRK2 is neither recruited to EGF-Rh positive endosomes or changing distribution pattern in a LRRK1 knock-down background.

To assess whether differences between the various conditions analyzed had statistical significance a two way ANOVA analysis was performed. All the experiments have been performed in triplicate and imaged cells were scored for co-localization of LRRK1 or LRRK2 with EGF-Rh positive endosomes. Cells with at least 5 double positive endosomes were scored as positive. For each condition tested, at least 3 wells with an average of 84 cells per well were scored. As summarized in figure 27, differences between GFP-LRRK1 + KD control and GFP-LRRK1 + LRRK2 KD group, or GFP-LRRK2 + KD control and GFP-LRRK2 + LRRK1 KD

group have no statistical significance, thus KD of LRRK2 does not influence LRRK1 recruitment to EGF-Rh positive endosomes and vice versa KD of LRRK1 does not influence LRRK2 behavior in the same conditions. (for the two ways ANOVA results see table 6) .

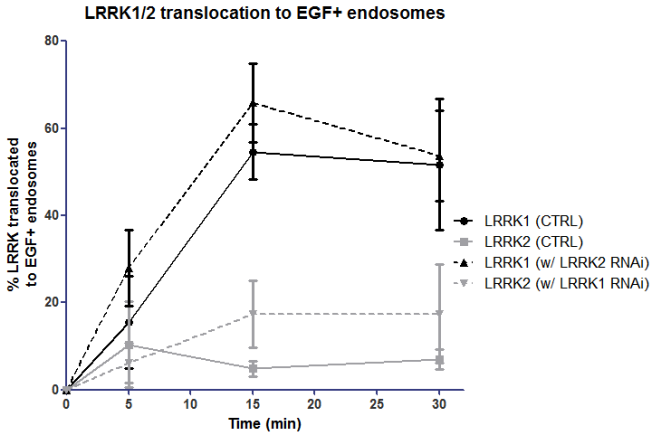

GFP-LRRK1 (CTRL) vs LRRK2 KD + GFP-LRRK1			
Time point EGF-Rh	Difference	P value	Significance
0 min	0	P > 0.05	ns
5 min	12,43	P > 0.05	ns
15 min	11,22	P > 0.05	ns
30 min	2,05	P > 0.05	ns

LRRK2 (CTRL) vs LRRK1 KD + GFP-LRRK2			
Time point EGF-Rh	Difference	P value	Significance
0 min	0	P > 0.05	ns
5 min	-4,3	P > 0.05	ns
15 min	12,51	P > 0.05	ns
30 min	10,4	P > 0.05	ns

Figure 27: Two away ANOVA analysis of confocal images: KD of LRRK2 does not influence LRRK1 recruitment to EGF-Rh positive endosomes and vice versa KD of LRRK1 does not influence LRRK2 behavior in the same conditions. Differences between GFP-LRRK1 (KD control) and GFP-LRRK1/LRRK2 KD (refer to upper table) or GFP-LRRK2 (KD control) and GFP LRRK2/LRRK1 KD (refer to lower table) are not statistical significant.

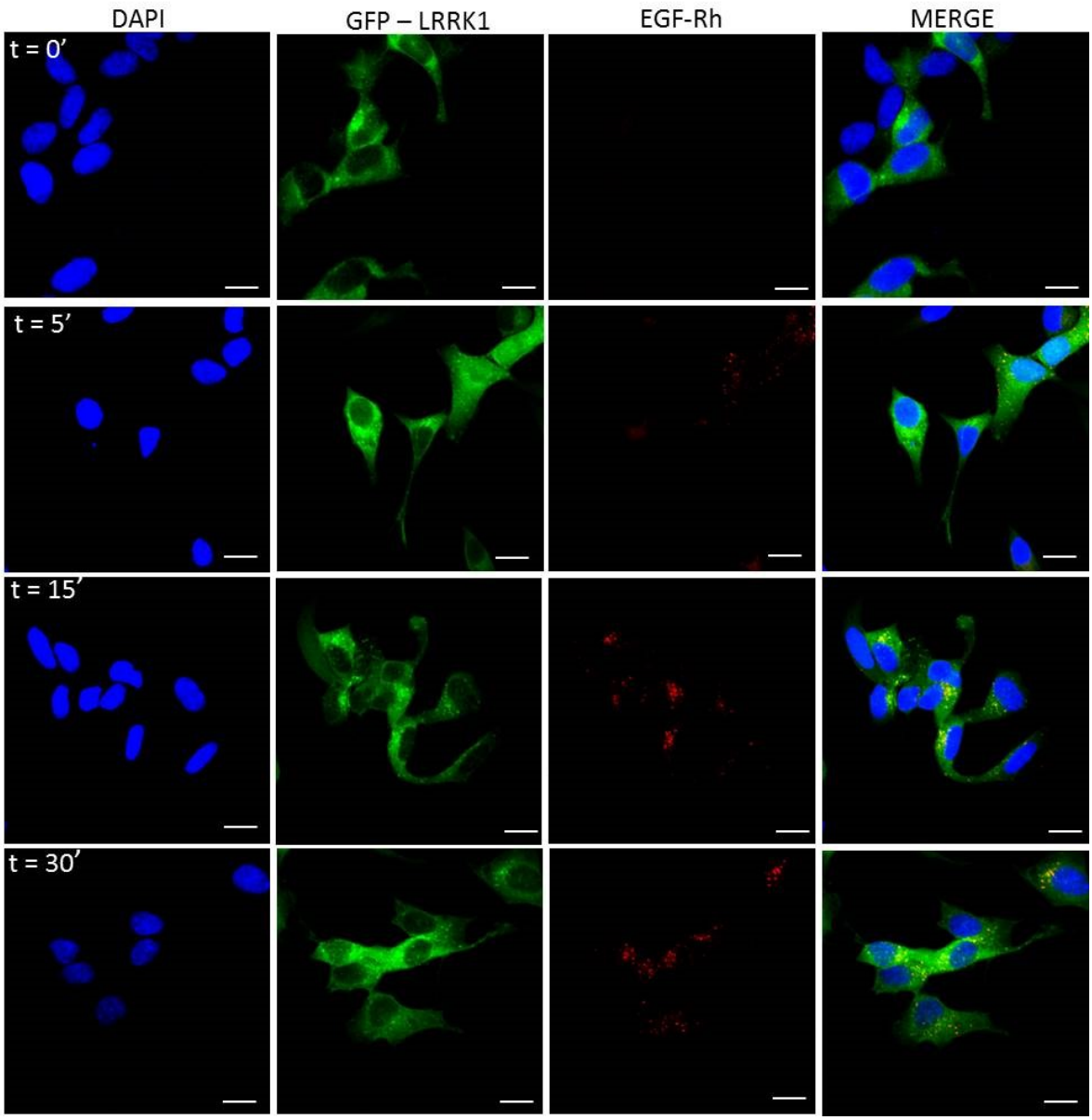

Figure 28: EGF does induce LRRK1 translocation in a LRRK2-KD background. Confocal laser scanning micrographs of SH-SY5Y stably expressing eGFP-LRRK1 + KD LRRK2 untreated (t=0') or treated with 100 µg/mL EGF-rhodamine conjugate for 5, 15 and 30 minutes. EGF-Rh is internalized by the cells showing a red punctate pattern co-localizing with GFP-LRRK1 puncta. Scale bar, 10 µM applies to all photomicrographs**.**

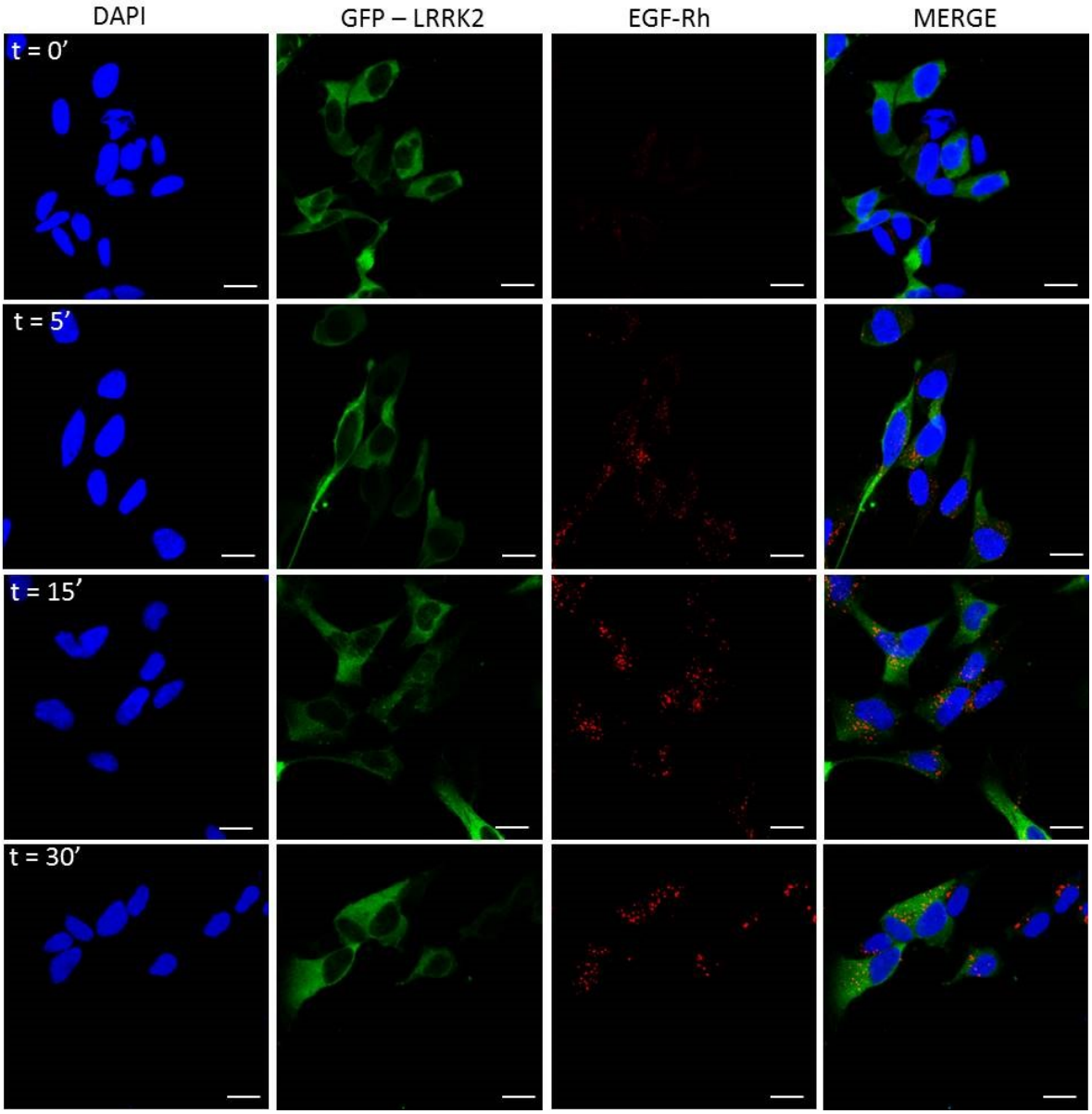

Figure 29: EGF does not induce translocation of LRRK2 in a LRRK1-KD background. Confocal laser scanning micrographs of SH-SY5Y stably expressing eGFP-LRRK2 + KD LRRK1 untreated (t=0') or treated with 100 µg/mL EGF-rhodamine conjugate for 5, 15 and 30 minutes. EGF-Rh is internalized by the cells showing a red punctate pattern but any translocation of GFP-LRRK2 is observed at any EGF-Rh treatment time-point. Scale bar, 10 µM applies to all photomicrographs**.**

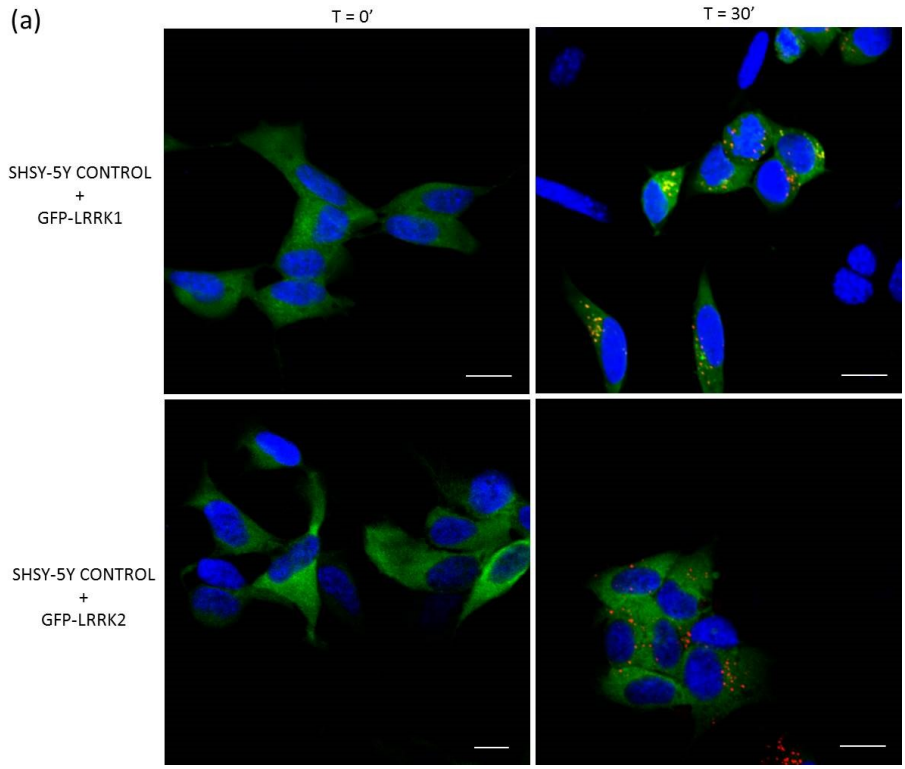

Figure 30--a: EGF induces LRRK1 but not LRRK2 translocation.. Confocal laser scanning micrographs of SHSY-5Y stably expressing eGFP-LRRK1 and eGFP-LRRK2 are compared. Untreated condition is indicated as t=0' and compared with 30 minutes treatment with EGF-rhodamine 100 ng/ml. Scale bar, 10 µM.

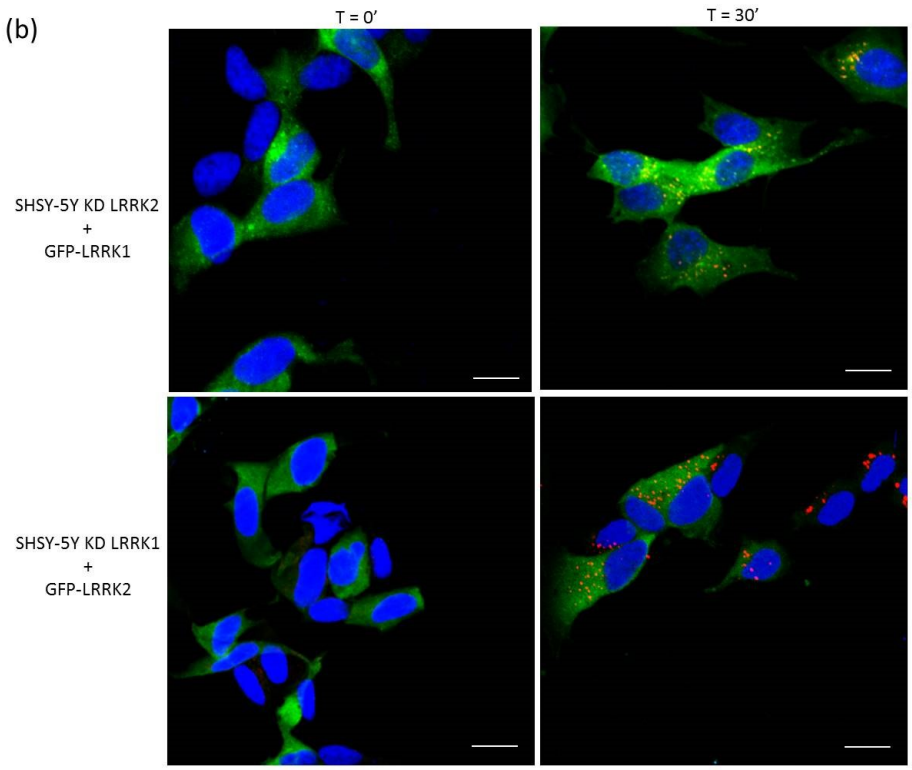

Figure 30—b: LRRK2 is not required for EGF-Rh induced LRRK1 translocation. Scale bar, 10 µM.

GFP-LRRK1 (CTRL) vs GFP-LRRK2 (CTRL)				
Time point EGF-Rh	Difference	t	P value	Significance
0 min	0	0	P > 0.05	ns
5 min	-5,133	0,4689	P > 0.05	ns
15 min	-49,76	4,545	P<0.001	***
30 min	-44,71	4,084	P<0.01	**

GFP-LRRK1 (CTRL) vs LRRK1 KD + GFP-LRRK2				
Time point EGF-Rh	Difference	t	P value	Significance
0 min	0	0	P > 0.05	ns
5 min	-9,433	0,8617	P > 0.05	ns
15 min	-37,25	3,403	P<0.01	**
30 min	-34,3	3,133	P < 0.05	*

GFP-LRRK1 (CTRL) vs LRRK2 KD + GFP-LRRK1				
Time point EGF-Rh	Difference	t	P value	Significance
0 min	0	0	P > 0.05	Ns
5 min	12,43	1,136	P > 0.05	ns
15 min	11,22	1,025	P > 0.05	ns
30 min	2,05	0,1873	P > 0.05	ns

GFP-LRRK2 (CTRL) vs LRRK2 KD + GFP LRRK1				
Time point EGF-Rh	Difference	t	P value	Significance
0 min	0	0	P > 0.05	ns
5 min	17,57	1,605	P > 0.05	ns
15 min	60,98	5,57	P<0.001	***
30 min	46,76	4,271	P<0.001	***

LRRK2 (CTRL) vs LRRK1 KD + GFP-LRRK2				
Time point EGF-Rh	Difference	t	P value	Significance
0 min	0	0	P > 0.05	ns
5 min	-4,3	0,3928	P > 0.05	ns
15 min	12,51	1,143	P > 0.05	ns
30 min	10,4	0,9503	P > 0.05	ns

LRRK2 KD + GFP-LRRK1 VS LRRK1 KD + GFP-LRRK2				
Time point EGF-Rh	Difference	T	P value	Significance
0 min	0	0	P > 0.05	ns
5 min	-21,87	1,997	P > 0.05	ns
15 min	-48,47	4,427	P<0.001	***
30 min	-36,35	3,321	P<0.01	**

Table 6. Two way ANOVA result tables

CHAPTER 4

DISCUSSION

In neurons, vesicle trafficking mediates neurotransmitter or protein release and uptake, localization of membrane receptors, changes in plasma membrane composition at the cell surface and, not least, organelle biogenesis, thus underlying virtually all functions of the nervous system. The transport, binding and fusion of secretory vesicles with the cell surface are tightly regulated and their dysregulation has been implicated in PD and other neurological disorders(125).

There are two exocytosis pathways, constitutive and regulated, by which secretory proteins are released from cells. Regulated exocytosis is triggered by signals originating outside the cell, usually through a rise in Ca^{2+} concentration at release sites; however, the regulated pathway also exhibits basal or unstimulated secretion, which is distinct from constitutive secretion (126).

Moreover, there is now a general consensus that synaptic vesicles formation relies predominantly on the endocytic pathway (127) strongly suggesting a prominent role of endocytosis in the control of neurotransmitter extracellular level or membrane receptor level.

Neurons and neuroendocrine cells (for example, PC12 cells) have both constitutive and regulated exocytosis, while most non-neuronal cells have only constitutive secretion. Chromaffin PC12 cells have been extensively used as cellular model of dopaminergic neurons to study vesicle trafficking under basal or stimulated conditions (128). In fact, PC12 cells mimic many features of central DA neurons; they are characterized by the presence of catecholamine synthesizing enzymes (i.e. tyrosine hydroxylase) (129), catecholamine storage granules of about 0.2–0.5 mm (129, 130) and DA receptors, as well as by DA uptake mechanisms. Like dopaminergic neurons, PC12 cells also contain the type A isoform of monoamine oxidase (MAO) (131). Finally, the microdyalisis results presented in this work and previous results from other groups have demonstrated that PC12 cells release catecholamines in response to different stimulations (121, 132). Moreover, PC12 cells together with SH-SY5Y neuronal cells have been largely used to analyze the LRRK2 physio-pathological functions (75, 76, 133, 134).

This research highlights an important cellular function of LRRK2 in the regulation of vesicle trafficking. Using different experimental approaches is demonstrated that the presence of PD-linked mutant LRRK2 determines an increase in DA extracellular level in short-time dynamic experiments in PC12 cells, an increase in GH release in SH-SY5Y cells and an increase of DRD1 on cell membrane of both SH-SY5Y cells and striatum of LRRK2 G2019S transgenic mice. Moreover a functional redundancy study performed by an *ad hoc* designed immunocytochemistry assay demonstrates that LRRK2 is not involved in the control of EGF receptor trafficking whereas its homologue LRRK1 does, providing clues to define which pathway or pathways could involve LRRK2 and be linked with neurodegeneration in PD.

The content of intracellular DA, DOPAC and HVA and DA, 3-MT, DOPAC and HVA in culture medium is similar in all the LRRK2-containing clones, whether or not expression of the protein has been induced (Figure 16). This result suggests that LRRK2 expression does not interfere with basal dopamine metabolism. An alternative explanation is that long time sampling of extracellular content (48 h) may mask small/significant differences in DA secretion and metabolism among different PC12 clones since catecholamine medium content is the result of several biological phenomena including secretion, reuptake and enzymatic oxidative metabolism, but as well as the outcome of chemical events such as autoxidation of hydroxyl groups (121). However, short-time dynamic experiments performed using in vitro microdialysis demonstrate a basal increase of DA secretion in cells expressing LRRK2 G2019S and a nicotine induced increase of extracellular DA in those expressing both mutated LRRK2 genes (Figure 17 A–B). Interestingly, these results on PC12 cells match that of LRRK2 G2019S transgenic rat model (135), in which temporally induced, but not constitutive, overexpression of LRRK2 G2019S determines an increased DA extracellular level and an increased motor activity, probably due to an impairment in dopamine reuptake by dopamine transporter (135).

In our PC12 cells, LRRK2 expression negatively affects the DA enzymatic metabolism, resulting in a decrease of DOPAC+HVA in basal microdialysate samples with the exception of the LRRK2 G2019S cells and the same trend is emphasized by nicotine treatment. This

difference may be explained by the increased DA secretion in LRRK2 G2019S expressing cells with the consequent reuptake and rise of the substrate available for intracellular MAO-A enzymes.

The expression of LRRK2 G2019S also affects the vesicle distribution in PC12 cells in terms of shortest distance from cell membranes. Although the ultrastructural analysis does not discriminate univocally the three different SV classes (136), it has generally been assumed that the vesicles closest to release sites (in a range of 100 nm) and the docked vesicles represent the readily releasable pool (RRP) and thus are recruited first during synapse activity (137). Moreover it has been shown that the electrophysiological properties as well as the proper vesicular trafficking and spatial distribution in the presynaptic pool depend on the presence of LRRK2 as an integral part of presynaptic protein complex (97). Thus, electron microscopy results may suggest that the increase in extracellular DA level either in basal conditions or after nicotine stimulation may be due to alteration in vesicle distribution inside the cells**.** Strikingly, an increased DA turnover has been noticed in presymptomatic LRRK2 mutation carriers (138). It has been suggested that increased DA turnover might by itself contribute to disease progression secondary to DA associated toxicity (139, 140). A role for LRRK2 as presynaptic scaffold protein regulating vesicle trafficking and indirectly DA turnover, as suggested by our results, fits perfectly in this picture. The increase in DA level in the extracellular medium of PC12 expressing LRRK2 G2019S is comparable to the biological effect detectable in SH-SY5Y cells using GH or DRD1 as read-out in the presence of LRRK2 pathological mutants (Figure 21–22).

To date, the role of kinase activity in LRRK2 physio-pathological function is still controversial because different pathological or risk factor mutants exist with unchanged or reduced kinase activity (for review see Greggio et al. 2009, (141)) and because in different experimental models the kinase dead LRRK2 mutants behave as the pathological mutants (99). Under our experimental conditions, the LRRK2 D1994A mutant protein shows smaller but consistent effect on both DRD1 membrane level and secreted GH compared to pathological mutants despite the fact that LRRK2 D1994A has a robust reduction in kinase activity (75, 133). In agreement with this result, the LRRK2 inhibitor GSK2578215A reduces

but does not fully eliminate the LRRK2 G2019S effect either on DA or GH extracellular level. Taken together, these results seem to suggest that LRRK2 may primarily act as a regulatory scaffolding protein, where the LRRK2 kinase activity may further support this function. The absence of biological effect of LRRK2 lacking the kinase domain ($LRRK2^{\Delta KIN}$) on both GH and DRD1 readouts may be in part explained by a destabilization of the protein due to the large amino acid deletion.

Interestingly, the LRRK2 biological effects, in all the tested experimental conditions, seem to be neuronal specific, since no increase in GH extracellular level or DRD1 membrane level was observed in HEK293 cell when mutant LRRK2 is present. Neuronal-specific mechanisms of vesicle trafficking are well described (126) and this aspect could explain at least partially the neuron specific toxicity of mutant LRRK2. This view is supported by experiments in vivo, showing that the LRRK2 effects on DRD1 localization in neuronal cells is observed in the striatum of G2019S transgenic mice. The transgene expression determines an increase of DRD1 in the plasma membrane fraction that correlates with a decrease in the vesicle fraction. This effect is possibly specific for this receptor since it is not detectable for NMDA-NR1 or EGF receptor (EGF-R). It is generally accepted that membrane receptors show different turnover rate and different endocytic pathways. For instance, NMDARs are considered to be relatively stable once delivered to the cell surface of mature neurons, especially when compared with AMPARs that, even under basal conditions, cycle much more rapidly to and from the surface (142) whereas DRD1s internalize rapidly following agonist-induced activation (143). EGF-R is a member of tyrosine kinase receptors family, whereas DRD1 is a G protein coupled receptor. The confocal microscopy results suggest that LRRK2 is not involved in EGF-R trafficking after EGF stimulation, corroborating the hypothesis of a specific influence of LRRK2 in DRD1 trafficking.

Taken together all these observations indicate that the LRRK2 protein does not seem to exert a general control in secretion but rather accurately modulates the vesicle turnover. The amount of secreted neurotransmitter or plasma membrane protein at steady state level is the sum of the transport reaching the cell surface from biosynthetic pathways, the leaving of the surface via the endocytic pathway, and the returning to plasma membrane

from the intracellular endosomal pools; consequently, a change in any of these parameters could be responsible for the differences that we observe in DA or GH release and DRD1 membrane localization.

For instance, LRRK2 has been implicated to different extents in vesicle trafficking either directly throughout endocytosis regulation (96, 97, 99) or indirectly throughout interaction with actin or tubulin (108, 144) that in turn may affect vesicle movement among the cytoskeleton. The dysregulation on vesicle trafficking may have important consequences on neuronal toxicity. It is believed that inter-related processes like oxidative stress, excitotoxicity, inflammation, mitochondrial dysfunction and altered proteolysis are involved in the cascade of events that will lead to DA neuron death (145).

In this respect, the increase in neurotransmitter levels in the inter-synaptic space or the increase in membrane receptors in neuronal plasma membrane due to the expression of mutant LRRK2 could alter the normal neuronal physiology that in turn may lead to neuronal toxicity. For instance, a dysregulation in DA level has been extensively studied as prominent PD etiological factor for the neurotoxic properties of DA metabolites (146, 147).

LRRK1 and LRRK2 have similar domain arrangements and are each other closest homologs. Leucine rich repeat kinase 1 and 2 are members of the ROCO family of multidomain proteins (148), characterized by the presence of a Ras of complex (ROC) proteins domain and a C-terminal of ROC domain (COR) which is unique to the ROCO proteins. Although, LRRK1 has been shown to interact with LRRK2 (113, 124), and it has been suggested that LRRK1 may therefore be involved in the same cellular processes as LRRK2, little is known about this. However, LRRK1 is not linked to PD, thus clues for the specificity of LRRK2 function can be obtained from comparative studies with LRRK1.

LRRK1 has previously been shown to translocate to EGF-R transporting endosomes upon treatment of HeLa cells with EGF (117), while nothing is known about possible role of LRRK2 in endosomal EGF-R trafficking. As consequence, EGFR trafficking is a good terms of comparison for a functional redundancy study between the two LRRK proteins. After demonstrating that EGF treatment induces the translocation to both EGF-R and LRRK1 to

endosomes in neuronal cells, I assessed that LRRK2 is not showing the same behavior. Moreover LRRK2 is not required for recruitment of LRRK1 to EGF-R transporting endosomes, since LRRK1 recruitment to endosomes was comparable in LRRK2 knockdown conditions compared to control. Farther LRRK2 seems to be not essential for EGF-R trafficking to endosomes in general, given that EGF-R internalization appeared normal in LRRK2 knockdown cell lines. Furthermore LRRK2 is not able to supply LRRK1 function in EGF-R trafficking in neuronal cells as LRRK2 is neither recruited to EGF-R positive endosomes or changing the distribution pattern in a LRRK1 knock-down background.

Actually, EGF-R trafficking does not show any perturbation when LRRK1 is knocked down in the SH-SY5Y model used for this study. This result, contrasting with those obtained on Hela cells by Hanafusa et al (117), can be explained with the complexity of the receptors trafficking machinery involving many different proteins. Among those proteins, probably in neuronal cells, some may have functional redundancy with LRRK1. Taken together this observations display no possibilities for cross-talk between LRRK1 and LRRK2 in the EGF-R trafficking process in neuronal cells. Considering that EGF-R is a broadly expressed receptor outside the SNC, while DRD1 is specifically expressed in the PD degeneration interested areas, these results provide a clue on the possible mechanisms underlying the specific degeneration of the dopaminergic system of PD, despite LRRK2 is expressed not only through the brain but also in some peripheral districts.

Recent literature supports the notion that LRRK1 and LRRK2 may play distinct biological functions. For instance, LRRK1 and LRRK1 containing mutations equivalent to those seen in LRRK2 PD do not exhibit the same level of toxicity as LRRK2, suggesting that there is a divergence in the function of these proteins (114). This is supported by genetic analyses that have excluded LRRK1 as being involved in PD (149, 150). Moreover is reported that LRRK2 overexpression in cells and in vivo impairs the activity of the ubiquitin-proteasome pathway, and that this accounts for the accumulation of diverse substrates with LRRK2 overexpression but in the same study such abnormalities are not seen with overexpression of LRRK1 (151).

Therefore, despite the similarity of domain arrangement and catalytic activity, and the possibility of a dimerization, LRRK1 and LRRK2 seem to possess distinctive properties that may account for LRRK2 specific association with PD and this functional redundancy study supports this hypothesis too. Moreover the absence of functional redundancy between LRRK1 and LRRK2 in respect to EGF-R trafficking point to a specific LRRK2 function for the DRD1 trafficking.

OPEN ACCESS Freely available online

PLOS ONE

LRRK2 Affects Vesicle Trafficking, Neurotransmitter Extracellular Level and Membrane Receptor Localization

Rossana Migheli[1,9], Maria Grazia Del Giudice[2,9], Ylenia Spissu[1], Giovanna Sanna[2], Yulan Xiong[3], Ted M. Dawson[3,4,6], Valina L. Dawson[3,4,5,6], Manuela Galioto[2], Gaia Rocchitta[1], Alice Biosa[1], Pier Andrea Serra[1], Maria Teresa Carri[7,8], Claudia Crosio[2,7], Ciro Iaccarino[2,7]*

1 Department of Clinical and Experimental Medicine, University of Sassari, Sassari, Italy, **2** Department of Biomedical Sciences, University of Sassari, Sassari, Italy, **3** Neuroregeneration and Stem Cell Programs, Institute for Cell Engineering, Johns Hopkins University School of Medicine, Baltimore, Maryland, United States of America, **4** Department of Neurology, Johns Hopkins University School of Medicine, Baltimore, Maryland, United States of America, **5** Department of Physiology, Johns Hopkins University School of Medicine, Baltimore, Maryland, United States of America, **6** Solomon H. Snyder Department of Neuroscience, Johns Hopkins University School of Medicine, Baltimore, Maryland, United States of America, **7** Fondazione Santa Lucia, IRCCS, Rome, Italy, **8** Department of Biology, University of Rome "Tor Vergata", Rome, Italy

Abstract

The leucine-rich repeat kinase 2 (*LRRK2*) gene was found to play a role in the pathogenesis of both familial and sporadic Parkinson's disease (PD). LRRK2 encodes a large multi-domain protein that is expressed in different tissues. To date, the physiological and pathological functions of LRRK2 are not clearly defined. In this study we have explored the role of LRRK2 in controlling vesicle trafficking in different cellular or animal models and using various readouts. In neuronal cells, the presence of LRRK2^{G2019S} pathological mutant determines increased extracellular dopamine levels either under basal conditions or upon nicotine stimulation. Moreover, mutant LRRK2 affects the levels of dopamine receptor D1 on the membrane surface in neuronal cells or animal models. Ultrastructural analysis of PC12-derived cells expressing mutant LRRK2^{G2019S} shows an altered intracellular vesicle distribution. Taken together, our results point to the key role of LRRK2 to control vesicle trafficking in neuronal cells.

Citation: Migheli R, Del Giudice MG, Spissu Y, Sanna G, Xiong Y, et al. (2013) LRRK2 Affects Vesicle Trafficking, Neurotransmitter Extracellular Level and Membrane Receptor Localization. PLoS ONE 8(10): e77198. doi:10.1371/journal.pone.0077198

Editor: Patrick Lewis, UCL Institute of Neurology, United Kingdom

Received November 29, 2012; **Accepted** September 7, 2013; **Published** October 22, 2013

Funding: This work was supported by Fondazione Banco di Sardegna, PRIN 2008 (grant n° 20083R593R_002 and 20083R593R_001) and Regione Sardegna (grant n°CRP-17171). Maria Grazia Dal Giudice is supported by a fellowship of Regione Sardegna. This work was supported in part by National Institutes of Health/National Institute of Neurological Disorders and Stroke (NIH/NINDS) P50NS038377. Ted M. Dawson is the Leonard and Madlyn Abramson Professor in Neurodegenerative Diseases. The funders had no role in study design, data collection and analysis, decision to publish, or preparation of the manuscript.

Competing Interests: Ted M. Dawson is a PLOS ONE editorial board member. This does not alter the authors' adherence to all the PLOS ONE policies on sharing data and materials.

* E-mail: ciaccarino@uniss.it

These authors contributed equally to this work.

Introduction

Most Parkinson's disease (PD) cases occur sporadically and several genes associated with monogenetic forms of the disease have been identified in patients [1]. Mutations in the leucine-rich repeat kinase 2 gene (LRRK2, PARK8) cause late-onset, autosomal dominant PD that is clinically and neurochemically indistinguishable from idiopathic forms [2,3]. The LRRK2 gene encodes a large protein of 2527 amino acids belonging to the ROCO protein family [4]. Similar to other ROCO proteins, LRRK2 contains a Ras-of-complex (Roc) GTPase domain and a C-terminal of Roc (COR) domain in conjunction with a protein kinase domain with close homology to members of the mixed-lineage and receptor-interacting protein kinase families. LRRK2 also contains a number of repeat domains (armadillo, ankyrin, leucine-rich repeats and C-terminal WD40 repeats that surround the central Roc-COR-kinase catalytic region) of uncertain function. Interestingly, multiple amino acid substitutions of the same residue R1441 (R1441C, R1441G, and R1441H) in the highly conserved GTPase domain and multiple mutations (I2012T, G2019S, and I2020T) in the kinase domain have been identified in patients [5]. The most common pathological mutation G2019S increases the kinase activity of LRRK2 by 2–3 fold [6,7], however some other mutations show an unchanged or reduced kinase activity [8]. Studies from several independent groups have evaluated the frequency of LRRK2 mutations in many different populations, and such mutations have been found not only in 3–5% of familial PD but also in approximately 1–3% of idiopathic PD cases [9]. Despite extensive studies based on both animal and cellular models, the pathological role of LRRK2 in PD onset and progression is still largely unclear, and LRRK2 substrate(s) remain fairly elusive. To date, LRRK2 has been involved in different physiological functions ranging from miRNA processing [10] to translation regulation [11], cytoskeleton organization [12,13,14], autophagy-lysosomal pathways [15,16] and immunoregulation [17]. Different experimental approaches seem to suggest a potential role of LRRK2 in vesicle trafficking [18]. Firstly, LRRK2 appears to be localized in different intracellular compartments that play a critical role in the control of vesicular trafficking: endoplasmic reticulum, Golgi apparatus and associated vesicles,

cytoskeleton, lipid rafts and synaptic vesicles [19,20]. Secondly, alteration in dopamine (DA) release has been described in different LRRK2 transgenic rodents, ranging from a reduction in DA extracellular content without [14,21] or with pharmacological manipulation [21,22] to an increased DA extracellular content in transgenic WT LRRK2 mice [22] or in transgenic rats expressing mutant LRRK2^{G2019S} [23]. In primary neuronal cells, LRRK2 silencing perturbs vesicle dynamics and distribution within the recycling pool, leading to a significant decrease in docked vesicles but an increase in the amount of vesicle recycling [24]. Moreover, alteration of LRRK2 expression by knockdown of endogenous LRRK2 in primary neuronal cells significantly impairs synaptic vesicle endocytosis [24,25], but a similar effect was observed following LRRK2 overexpression [25] thus leaving unclear which is the exact role of this protein.

In this work we have analysed the role of LRRK2 in controlling neurotransmitter extracellular levels as well as the neurotransmitter receptor membrane levels through different experimental approaches. Taken together, our results point to a key role of LRRK2 in controlling vesicle trallicking and distribution.

Materials and Methods

Animals

Mice were housed and treated in strict accordance with the NIH Guide for the Care and Use of Laboratory Animals. All animal procedures were approved by the Institutional Animal Care and Use Committees of the Johns Hopkins Medical Institutions (Animal Welfare Assurance No. A3272-01). Mice were maintained in a pathogen-free facility and exposed to a 12 h light/dark cycle with food and water provided *ad libitum*.

Reagents and Solutions

Antibodies: anti-TH (1:4000 Sigma), anti-Myc (1:5000 Sigma), anti-DRD1 (1:2000 Sigma), anti-NR1 (1:2000 Sigma), anti-Sec8 (1:4000 BD-Biosciences), anti-clathrin (1:5000 BD-Biosciences). Reagents: Tween® 20 (Polyethylene glycol sorbitan monolaurate), Phenylmethanesulfonyl fluoride (PMSF), protease inhibitor cocktail and (−)-Nicotine hydrogen tartrate salt were obtained from Sigma-Aldrich (Milano, Italy). LRRK2 inhibitor GSK2578215A was from Tocris. The phosphate-buffered saline (PBS) solution was made using NaCl (137 mM), KCl (2.7 mM), Na2HPO4 (8.1 mM), KH_2PO_4 (1.47 mM), $CaCl_2$ (1.19 mM), $MgCl_2$ (0.54 mM), and glucose (7.5 mM) from Sigma and then adjusted to pH 7.4. Dulbecco's modified Eagle's medium (DMEM)–F12, Streptomycin/Penicillin, Hygromycine B, Geneticin-G418 were purchased from Invitrogen and doxycycline from BD Biosciences. The tetracycline-free Fetal Bovine Serum (FBS) was from Lonza Sales Ltd (Switzerland).

Plasmid Constructions

The plasmids for inducible expression or LRRK2 were obtained by digestions of cDNAs corresponding to human LRRK2 (WT or R1441C or G2019S) in fusion with 5X myc repeats [26] with *Bam*HI and *Xho*I and subcloned in *Bam*HI/*Eco*RV cloning sites in pTRE2 vector (Clontech).

cDNA coding for mouse growth hormone (GH, NM_008117.2) was RT–PCR amplified from mouse pituitary gland mRNA (oligo forward: ATCAGGATCCTTGGCAATGGCTACAGACTC, reverse: ATCAGGATCCGAAGGCACAGCTGCTTTCC), digested with *Bam*HI restriction enzyme and cloned in *Bam*HI cloning site of pCS2-5X-myc-tag containing the tag in C-terminal position. Plasmid pTL2-DRD1 (kindly provided by E. Borrelli, University of California, Irvine) was used as template for DRD1 cDNA, the PCR fragment (oligo forward: ATCCTCGAGAAGATGGCTCCTAACACTTCTACCA, reverse: CTCCTCGAGGGTTGAATGCTGTCCGCTGTG) was digested with *Xho*I and subcloned into pcDNA3.1-3X-flag-tag containing the tag in the C-terminal position. p-TK-Hyg (Clontech Laboratories Inc) was used to impart hygromycin resistance to PC12 ON cells.

Cell Lines and PC12 Stable Clones

Human neuroblastoma SH-SY5Y cells (ATCC number CRL-2266) were grown in DMEM-F12 (Invitrogen), 10% fetal calf serum (FCS, Invitrogen) at 37°C. The PC12-TET-ON cell line (Clontech Laboratories Inc) was cultivated in DMEM-F12 supplemented with 10% Tetracycline-free FCS (Lonza) at 37°C.

The plasmid pTRE2 vectors containing cDNAs coding for LRRK2 variants (WT or R1441C or G2019S) were co-transfected with p-TK-Hyg in a 8:1 molar ratio into PC12-TET-ON cells, using Lipofectamine® LTX Reagent (Life Technologies) according to the manufacturer's protocol. The different PC12-TET-ON clones were maintained under selection by 400 µg/mL of G418 and 200 µg/mL of hygromicin-B. Individual clones expressing both antibiotic resistances were picked after 14 days of selection, moved in a 96 well plate, and maintained in selective medium till confluence growth. Different individual clones were analyzed for LRRK2 expression upon induction by doxycycline (0.2 µg/mL).

Analysis of Intracellular and Extracellular Dopamine and Metabolites

Intracellular and extracellular dopamine (DA), 3-methoxytyramine (3-MT), 3,4-Dihydroxyphenylacetic acid (DOPAC), and homovanillic acid (HVA) were determined by HPLC with electrochemical detection as previously described [27]. In brief, cells were lysed in 250 µL 1% metaphosphoric acid containing 1 mM EDTA. After centrifugation (17,500 g for 10 min at 4°C), the supernatant was filtered, and a 15- µL aliquot was immediately injected into the HPLC system.

In each experiment, 100×10^3 cells/cm^2 were plated and treated 24 h later (time 0) with doxycycline 0.2 µg/mL. After 48 h, the medium was aspirated from each well and stored, and the cells were collected in metaphosphoric acid. Samples were subsequently analyzed for levels of total DA (DA+3-MT) and its metabolites DOPAC and HVA in cell lysates and incubation medium. Values in cell lysate were expressed as nanomoles per milligram of protein. Total cell extract protein concentration was determined using the method of Lowry et al. (1951).

Capillary Tube Construction for *in vitro* Microdialysis

The capillary tube for microdialysis of PC12 cell lines is an adaptation of an *in vitro* device described previously [28,29]. The microdialysis probe was constructed using two sections of plastic-coated silica tubing (150 µm o.d., 75 µm i.d., Scientific Glass Engineering, Milton Keynes, UK), each placed in the centre of a semipermeable polyacrylonitrile dialysis fiber (AN-69, Hospal Industrie, Meyzieu, France). Each semipermeable membrane had an active length of 40 mm. Then each section of plastic-coated silica tubing was positioned in the centre of polyethylene tubing (0.58 mm i.d., 35 mm long, Portex). This section of silica tubing served as the inlet. Dialysates from polyacrylonitrile dialysis fiber were collected from polyethylene tubing, which served as the outlet. All parts were coated with quick-drying epoxy glue. Afterwards the microdialysis probe (the semipermeable polyacrylonitrile dialysis fiber plus sealed plastic-coated silica tubing) was

placed in non heparinized microhematocrit capillary tubes (7.5 mm long, 1.1 mm i.d., Chase Scientific Glass, Rockwood, IL, USA). The final volume of microdialysis chamber was approximately 50 µL.

Microdialysis Procedures

Microdialysis experiments were performed during the exponential phase of cell growth. 5×10^4 cells/cm^2 were plated and treated 24 h later (time 0) with different Doxycycline concentrations. After 48 h cells were washed twice using 5 ml of modified PBS and 10% DMEM (perfusion medium), harvested and centrifuged (94 g for 5 min). Cells were resuspended in PBS/DMEM and the number of cells/ml was assessed in a Burker chamber. The initial volume of the cell suspension was eventually adjusted to reach a final concentration of 1×10^6 cells/50 µL. Nicotine (5 mM) effect on DA secretion from PC12 lines was evaluated by means of microdialysis *in vitro* as previously described [30].

The cellular microdialysis probe was perfused with PBS/DMEM by means of a peristaltic microinfusion double-channel pump (P720 peristaltic pump (Instech, Plymouth Meeting, PA, USA), which pumped PBS/DMEM at a flow rate of 3.0 µL/min. The pump channels were connected to the inlet by a length of polythene tubing. The perfusion apparatus was then filled with 50 µL of the PC12 cell suspension by aspiration, which was performed manually by means of a 1.0 mL syringe connected to the plastic coated silica tubing sealed outside the polythene tubing. Thereafter, the perfusion apparatus was kept at 37°C. After 1 h of stabilization, 3 microdialysis samples (60 µL each) were recovered at 20 min intervals. Nicotine was added to the perfusion medium and removed after 60 min. In case of LRRK2 inhibitor treatments, GSK2578215A (1 µM) was added at the beginning of stabilization. Samples were recovered during the next two hours. Subsequently, a 35 µL aliquot of each collected dialysate was analyzed by HPLC. The concentration of neurochemicals detected after the first 20 min of perfusion was taken as time 0 concentration. Cell viability was assessed before the start and at the end of each experiment by trypan blue exclusion. The viability rate was given as the difference between final and initial percentage of non-viable cells [29,30].

Chromatographic Analysis of Dialysates from PC12 Cell Suspension

DA was quantified in dialysates of selected experiments (1.0×10^6 cells) by HPLC–EC, as described previously [29] using an Alltech 426 HPLC pump (Alltech, Sedriano, Italy) equipped with a Rheodyne injector (model 7725, Rohnert Park, CA, USA), a column (15 cm, 4.6 mm i.d., ODS80TM C18, Toso Haas, Stuttgart, Germany), an electrochemical detector ANTEC–Leyden EC controller (ANTEC, Zoeterwoude, The Netherlands), and a PC-based ADC system (Varian Star Chromatographic Workstation, Varian, Walnut Creek, CA, USA). The mobile phase was citric acid (0.1 M), ethylenediaminetetraacetic acid (EDTA, 1.0 mM), methanol (8.7%) and sodium octylsulfate (48 mg/L), with a flow rate of 1.2 mL/min and pH 2.9.

Transient Transfections and Analysis of GH Secretion

Transient expression of each vector was performed with Lipofectamine LTX Reagent (Life Technologies) according to the manufacturer's instructions. After an incubation of 4–6 h with transfection reagents, the cells were cultured in normal growth medium for 24 or 48 h. For GH secretion analysis, SH-SY5Y cells (1.0×10^5 cells) were seeded in 24 mm plates and co-transfected the following day either with GH-5Xmyc and pCS2-MTK empty vector or with GH-5Xmyc and the different pCS2-5Xmyc-LRRK2 isoforms in a ratio of 1:10. 24 hours after transfection, the cells were washed twice with fresh medium and normal growth medium was added for another 16 h. In case of LRRK2 inhibitor treatments, GSK2578215A was added 1 h before medium change and then after medium change. The extracellular medium was then collected and centrifuged at 10000×g for 10 min to eliminate cell debris, while the cells were washed twice with PBS and immediately lysed by Laemmli buffer 1X. For DRD1 membrane localization experiments, the cells were co-transfected in 6 cm plates as described above (in a ratio of 1:5 respectively for DRD1-3Xflag and 5Xmyc-LRRK2 or empty vector) for 48 hours. The quantification of either GH-5Xmyc or DRD1-3Xflag in the different fractions was performed by western blot analysis and densitometric evaluation of the obtained bands (Quantity-One Biorad).

Subcellular Fractionation of Cells or Mouse Tissues

Tissues from 2 months old LRRK2^{WT} or LRRK2^{G2019S} transgenic mice [16] were quickly dissected and frozen. Subcellular fractionation was conducted as described in [31]. Briefly, SH-SY5Y or HEK293 cells or striatum were homogenized in ice-cold homogenization-buffer (320 mM sucrose, 4 mM HEPES, pH 7.4, protease inhibitor cocktail from Sigma). The homogenates were centrifuged at 1000×g for 10 min to produce the pellet containing nuclei and large debris fraction (P1). The supernatant (S1) was further fractionated into pellet (P2 containing the membrane fraction) and supernatant (S2) by centrifugation at 10,000×g for 20 min. The S2 was ultracentrifuged at 100,000×g to obtain the pellet (P3 containing the vesicle fraction). Protein content was determined using the Bradford protein assay. Equal amount of protein extracts were loaded into the SDS-PAGE.

Western Blot Analysis

Western blot analysis was performed as previously described [32]. Briefly, protein content was determined using the Bradford protein assay. Equal amount of protein extracts were resolved by standard SDS/PAGE. Samples were electroblotted onto Protan nitrocellulose (Schleicher & Schuell GmbH). Membranes were incubated with 3% low-fat milk in 1×PBS-Tween 0.05% solution with the indicated antibody for 16 h at 4°C. Anti-Rabbit IgG (whole molecule)- and Anti-Mouse IgG (whole molecule)-Peroxidase antibody were used to reveal immunocomplexes by enhanced chemioluminescence (Pierce).

Statistical Analysis

Concentrations of neurochemicals in dialysates from PC12 cell suspension were expressed in µM and given as mean ± SEM. Drug effects on neurochemicals were statistically evaluated in terms of changes in absolute dialysate concentrations. Differences within or between groups were determined by paired or unpaired t-tests (ANOVA followed by Student–Newman–Keuls post-hoc analysis). The null hypothesis was rejected when $p<0.05$.

Results

Generation and Characterization of PC12 Cells Stably Expressing Doxycycline-inducible WT or Pathological Mutant LRRK2s

Plasmid constructs for wild type LRRK2 (LRRK2^{WT}) or for pathological mutants LRRK2^{G2019S} and LRRK2^{R1441C} were transfected in PC12-ON cell lines. After several weeks of selection

by hygromicin, single stable clones were isolated. Different clones were characterized and finally three clones expressing comparable level of LRRK2 protein after 48 h of induction by 0.2 μg/mL doxycycline treatment were chosen (Figure 1A upper panel). All cell lines expressed comparable levels of Tyrosine Hydroxylase (TH) after the same treatments (Figure 1A, middle panel). A higher dose of doxycycline (1 μg/mL) does not further increase the LRRK2 expression level (Figure 1B). 48 hours after doxycycline treatment, we analysed the intracellular and extracellular dopamine (DA) level and its metabolism products in the different cell lines (Figure 1C). All the stable clones show comparable intracellular and extracellular levels of DA content as well as the intracellular and extracellular level of DOPAC+HVA, allowing the comparative analysis between the different stable clones performed in the following experiments.

LRRK2 Influences the Basal and Nicotine-induced Secretion of DA in PC12 Cells

In order to evaluate the effect of the expression of LRRK2 on basal and nicotine-induced secretion of DA, we performed a microdialysis study on cells [33] treated with 0.2 μg/mL doxycycline for 48 h compared with untreated (−) cells. This doxycycline dose was chosen because, in preliminary experiments, it did not show any significant effect on DA secretion on PC12-ON cells in contrast to 1 μg/mL of doxycycline that had a negative effect on DA secretion (data not shown). Microdialysates were collected at 20 minute intervals after 1 h of stabilization (Figure 2A–B–C–D). The time course analysis of basal and nicotine induced dopamine release in the absence (Figure 2A) or presence (Figure 2C) of doxycycline is shown. In Figure 2B–D, the Area Under Curve (AUC) of the different samples is shown; in particular, the baseline of DA+3-MT is represented from the AUC of points 20–60 minutes before nicotine treatment in absence

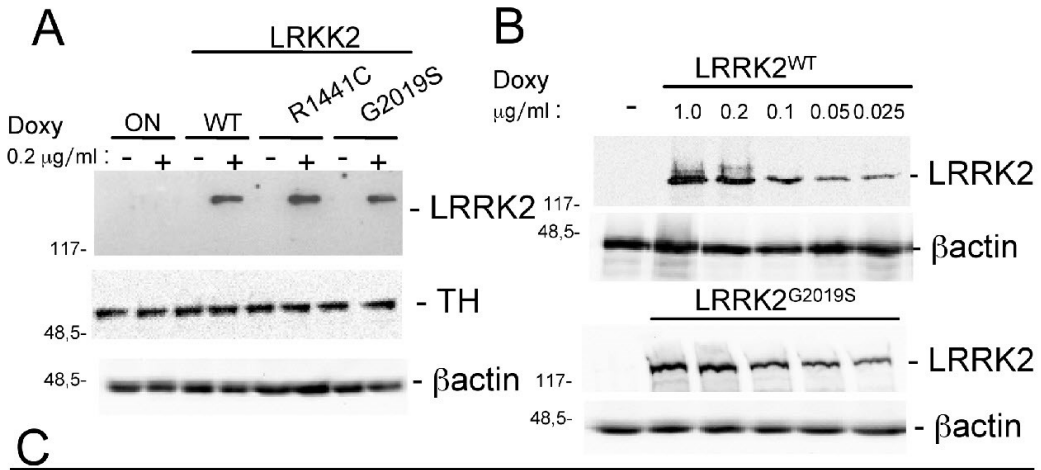

C

	Intracellular content (nmol/mg protein)		Medium Concentration (μM)	
	DA	DOPAC+HVA	DA Total (DA+3-MT)	DOPAC+HVA
PC12-LRRK2^{WT}	6.14 ± 0.55	0.24 ± 0.05	0.76 ± 0.12	15.23 ± 5.85
PC12-LRRK2^{R1441C}	6.15 ± 0.50	0.21 ± 0.008	0.58 ± 0.05	18.24 ± 6.61
PC12-LRRK2^{G2019S}	6.80 ± 1.31	0.17 ± 0.002	0.60 ± 0.11	14.41 ± 5.98

Figure 1. Characterization of PC12 cell expressing WT or mutant LRRK2. (A) PC12-derived cells expressing myc-tagged human WT or mutant-LRRK2 were left untreated (−) or treated (+) for 48 h with 0.2 μg/mL doxycycline to induce expression of transgenic LRRK2. Cell lysates were subjected to reducing SDS/PAGE. The anti-myc antibody was used to visualize LRRK2 and anti-TH for tyrosine hydroxylase. β-actin serves as controls for equal loading of samples. (B) Dose-dependent expression of doxycyline-inducible LRRK2^{G2019S}. Cells were treated for 48 h with the indicated concentration of doxycycline and equal amounts of protein were tested in Western blot analysis with anti-myc or anti-β-actin antibodies. (C) Effect of doxycycline on DA and DOPAC+HVA concentration in PC12 cell lysates and extracellular medium after 48 h expression. At the beginning of each experiment, 10^5 PC12 cells/cm^2 were plated and after the desired incubation period, the medium was aspirated from each well and stored, and the cells were collected in metaphosphoric acid. Samples were subsequently analyzed for levels of DA and its metabolites DOPAC and HVA in cell lysates and incubation medium. Results are the means ± SEM of three experiments performed in triplicate.
doi:10.1371/journal.pone.0077198.g001

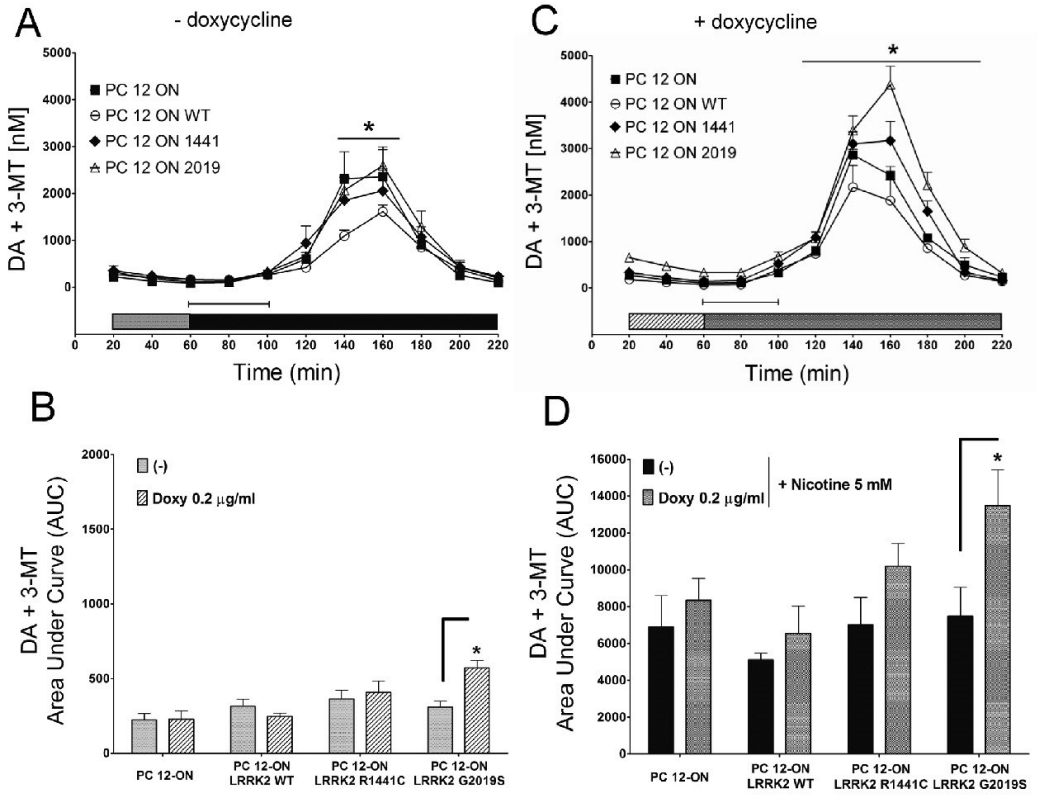

Figure 2. Effect of LRRK2 expression on dopamine (DA+3-MT) extracellular level. PC12-derived cell lines were left untreated (A) or treated (C) for 48 h with 0.2 µg/mL doxycycline. After 60 minutes of stabilization, three baseline dialysates were collected at 20-minute intervals [gray bars in panel (A), and gray bars with stripes in panel (C)]. Starting from 60 minutes, nicotine was infused for 60 minutes (capped lines). Microdialysates were continuously recovered during drug infusion and after nicotine discontinuation [black bars in panel (A), and dotted bars in panel (C)]. Values are mean + SEM and refer to dopamine concentrations in dialysates. Statistical significance was assessed using analysis of variance (ANOVA) for differences over time determined by Newman-Keules *t* test and unpaired *t*-tests. *$p<0.05$ compared with pertinent baseline values of all groups. Graphs in panel (B) and (D) represent the area under curve (AUC) values. (B) Basal dopamine concentration in dialysates of PC12 cell lines untreated (gray bars corresponding to the same color in panel A) or treated with 0.2 µg/mL doxycycline [gray bars with stripes corresponding to same color in panel (C)]. (D) Dopamine concentrations in dialysates integrated after nicotine administration in PC12 cell lines untreated [black bars corresponding to same color in panel (A)] or treated with 0.2 µg/mL of doxycycline [dotted bars corresponding to same color in panel (C)]. AUC values are mean + SEM. *$p<0.05$ vs corresponding control.
doi:10.1371/journal.pone.0077198.g002

(Figure 2B bars) or presence of doxycycline (Figure 2B barred bars), while the DA+3-MT nicotine-induced release is represented by the AUC related to points 80–220 minutes in absence (Figure 2D black bars) or presence of doxycycline (Figure 2D dotted bars). The expression of $LRRK2^{G2019S}$ induces an 85% increase ($p<0.05$) vs corresponding control in the basal level of total extracellular DA (DA+3-MT), as shown in figure 2C (20–40–60 minutes) compared to 2A (20–40–60 minutes) and quantified by the AUC in Figure 2B. In contrast, under the same experimental conditions expression of either $LRRK2^{WT}$ or $LRRK2^{R1441C}$ does not induce a significant increase in total DA extracellular levels (Figure 2A–C and quantified in 2B). Interestingly, the presence of mutant LRRK2 determines an increase in nicotine-induced DA compared to PC12-ON or $LRRK2^{WT}$ cells (Figure 2C 60–220 minutes *vs* 2A 60–220 minutes). Quantification by AUC of secreted DA indicates an increase of 22% (although not statistical significant) and 61% ($p<0.05$), respectively for $LRRK2^{R1441C}$ and $LRRK2^{G2019}$ (Figure 2D).

Under the same experimental conditions, we measured extracellular levels of DOPAC+HVA. A significant change both in the basal condition and after nicotine infusion is observed following doxycycline treatment in PC12 cells expressing $LRRK2^{WT}$ or $LRRK2^{R1441C}$ (Figure 3A–B–C–D). In particular the values are −61.4% for WT and −51.7% for $LRRK2^{R1441C}$ in doxycycline treated samples and −64.9% for WT and −45.3% for R1441C mutant by doxycycline and nicotine treatment. No significant differences were observed in PC12-ON cells or expressing the $LRRK2^{G2019S}$ mutant.

To evaluate the importance of LRRK2 kinase activity on increased DA extracellular level, we used the LRRK2 inhibitor

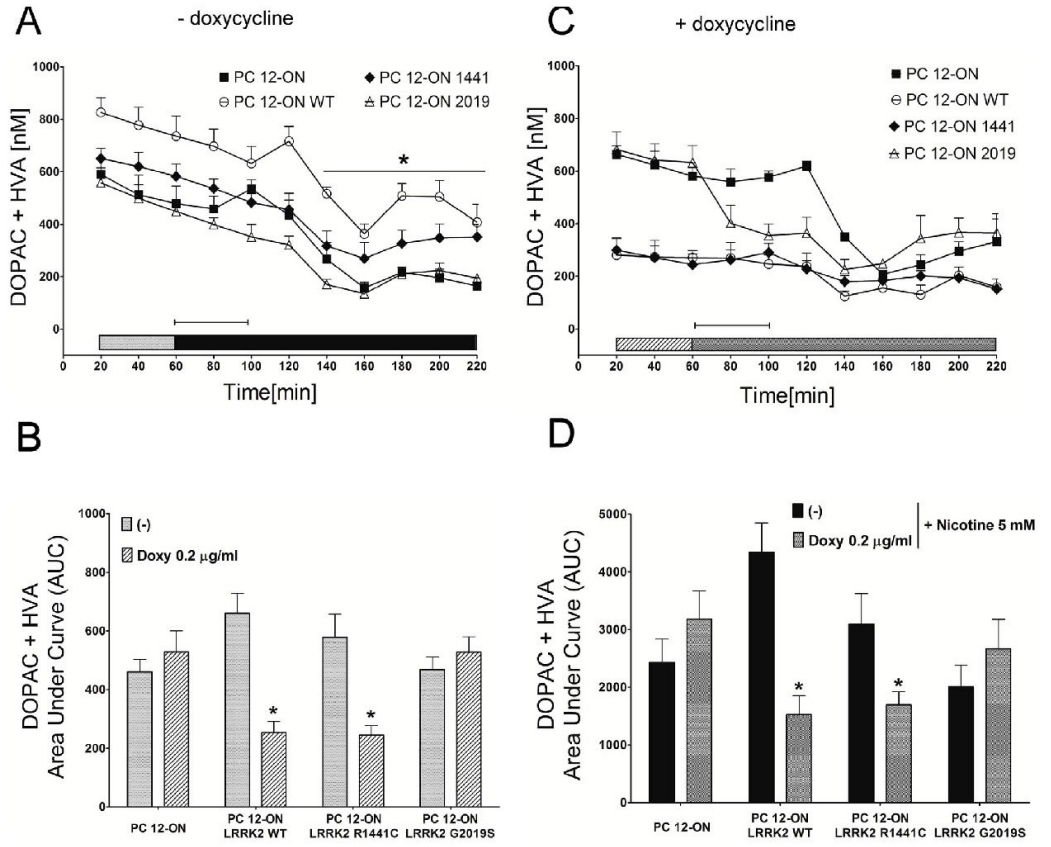

Figure 3. Effect LRRK2 expression on DOPAC+HVA concentrations. PC12-derived cell lines were left untreated (A) or treated (C) for 48 h with 0.2 µg/ml doxycycline. After 60 minutes of stabilization, three baseline dialysates were collected at 20-minute intervals [bars in panel (A), and gray bars with stripes in panel (C)]. Starting from 60 minutes, nicotine was infused for 60 minutes (capped lines). Microdialysates were continuously recovered during drug infusion and after nicotine discontinuation [black bars in panel (A), and dotted bars in panel (C)]. Values are mean + SEM and refer to DOPAC+HVA concentrations in dialysates. Statistical significance was assessed using analysis of variance (ANOVA) for differences over time determined by Newman-Keules *t* test and unpaired *t*-tests. *$p<0.05$ compared with pertinent baseline values of all groups. Graphs in panel (B) and (D) represent the area under curve (AUC) values. (B) Basal DOPAC+HVA concentration in dialysates of PC12 cell lines untreated [bars corresponding to the same color in panel (A)] or treated with 0.2 µg/mL doxycycline [bars with stripes corresponding to the same color in panel (C)]. (D) DOPAC+HVA concentrations in dialysates integrated after nicotine administration in PC12 cell lines untreated [black bars corresponding to the same color in panel (A)] or treated with 0.2 µg/ml doxycycline [dotted bars corresponding to the same color in panel (C)]. AUC values are mean + SEM. *$p<0.05$ vs corresponding control.

doi:10.1371/journal.pone.0077198.g003

GSK2578215A on PC12-ON or PC12-ON expressing the LRRK2^{G2019S}. The presence of LRRK2 inhibitor does not influence the DA extracellular level in basal conditions (20–40–60 minutes in figure 4A *vs* B or the relative AUC in Figure 4C) in both cellular types. In presence of nicotine, the inhibitor does not affect the expected increase in DA extracellular level in PC12-ON cells while it determines a reduction in PC12-ON expressing the LRRK2^{G2019S} mutant although this DA extracellular level decrease does not rich statistical significance in three independent experiments (Figure 4A from 60 to 220 minutes *vs* 4B from 60 to 220 minutes and the relative AUC in Figure 4D).

Under the same experimental conditions, the GSK2578215A inhibitor does not affect the concentration of DOPAC+HVA (Figure S1).

Vesicle Distribution in PC12 Cells Expressing LRRK2^{G2019S} Pathological Mutant

Given the dopamine secretion changes associated with LRRK2 expression, we asked whether LRRK2 might be involved in synaptic vesicle (SV) movement/distribution. Using an electron microscopy approach we analysed the vesicles distribution in PC12-ON or PC12-ON-LRRK2^{G2019S} cell lines. Expression was induced for 24 hours with 0.2 µg/mL doxycycline and cells were quickly fixed for electron microscopy. Non-induced cells served as

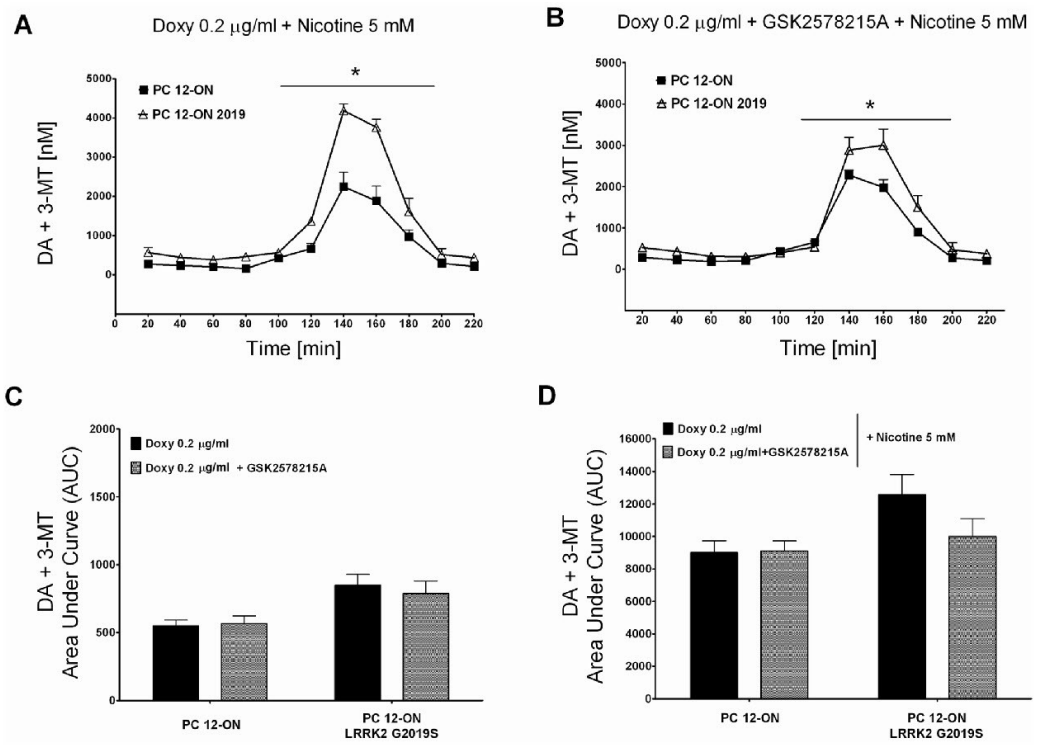

Figure 4. Effect of LRRK2 inhibitor GSK2578215A on dopamine (DA+3-MT) extracellular level. PC12-derived cell lines were left untreated (A) or treated (B) by 1 μM of GSK2578215A. After 60 minutes of stabilization, three baseline dialysates were collected at 20-minute intervals as previously described. Starting from 60 minutes, nicotine was infused for 60 minutes. Values are mean + SEM and refer to dopamine concentrations in dialysates. Statistical significance was assessed using analysis of variance (ANOVA) for differences over time determined by Newman-Keules *t* test and unpaired *t*-tests. *$p<0.05$ compared with pertinent baseline values of all groups before nicotine treatment. Graphs in panel (C) and (D) represent the area under curve (AUC) values. (C) Basal dopamine concentration in dialysates of PC12 cell lines untreated or treated with 1 μM of GSK2578215A (minutes 20–40–60 before nicotine treatment of Figure 4A *vs* B). (D) Dopamine concentrations in dialysates integrated after nicotine administration in PC12 cell lines untreated or treated with 1 μM of GSK2578215A (from minutes 80 to 220 after nicotine treatment of Figure 4A *vs* B). AUC values are mean + SEM.
doi:10.1371/journal.pone.0077198.g004

a control. Analysis of SV dimensions or relative abundance did not show significant differences between the different groups (data not shown). Conversely LRRK2 expression seemed to influence synaptic vesicle distribution in terms of shorter distance to the plasma membrane. We observed a clear increase in the relative abundance of vesicles located in close proximity to the membrane in presence of $LRRK2^{G2019S}$ mutant compared to the same cells not expressing the mutant or to PC12 ON cells either treated or untreated with doxycycline (Figure 5A–B). The level of LRRK2 expression in the different cell lines was analysed by Western blot using an aliquot of cells before fixation and it is shown in Figure 5C.

LRRK2 Increases Growth Hormone Extracellular Level in Neuronal Cells

To further evaluate the involvement of LRRK2 in the mechanisms of vesicle trafficking we generated a plasmid construct to follow secreted proteins that consists of mouse growth hormone (mGH), containing a myc-tag at the C-terminal position. GH secretion has been largely used to follow neuronal secretion, since GH is localized predominantly in vesicles in regulated secretory pathways [34,35]. We co-transfected mGH alone or together with different LRRK2 constructs in both neuronal (SH-SY5Y or PC12) or non-neuronal (HEK293) cells. 24 h after co-transfections the cell medium was changed and the level of GH secretion was evaluated collecting the extracellular medium 16 h later. As shown in figure 6A, the presence of $LRRK2^{WT}$ in SH-SY5Y determines a slight increase in extracellular GH level. This level is further increased in the presence of mutant LRRK2, with $LRRK2^{G2019S}$ inducing the maximum effect (Figure 6A–E). Total cell lysates were used to analyse the intracellular level of mGH, LRRK2 and β-actin (Figure 6A). Similar results were obtained in PC12 cells although these cells had been transfected with lower efficiency compared to SH-SY5Y (data not shown). Interestingly, the effect of LRRK2 on GH secretion was not visible performing similar experiments in kidney HEK293 cells (Figure 6B–E) suggesting a possible neuronal-specific mechanism of action for LRRK2.

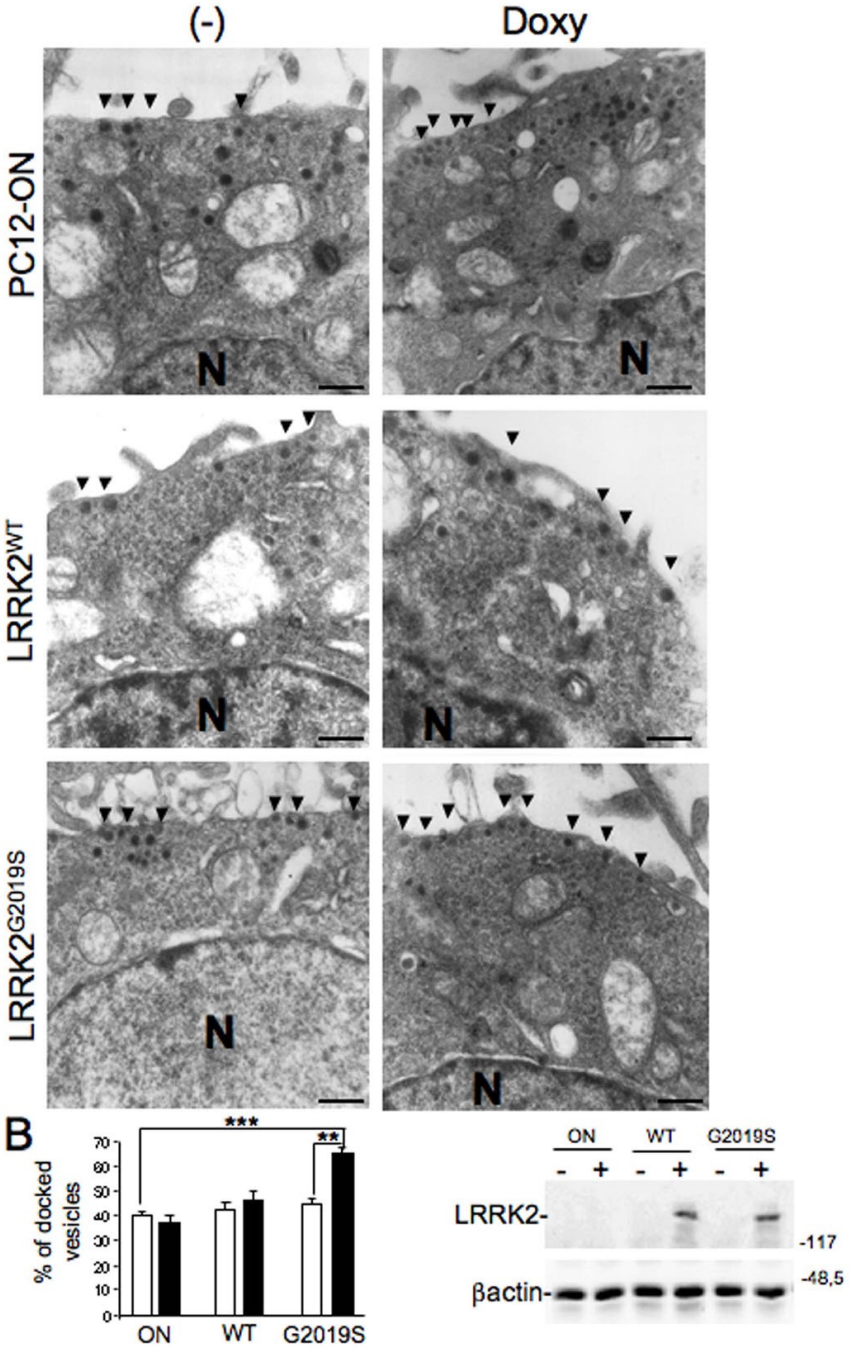

Figure 5. Effect of LRRK2^{G2019S} expression on vesicle distribution. (A) Transmission electron micrographs of PC12-ON or PC12-LRRK2^{WT} or PC12-LRRK2^{G2019S} cells untreated (−) or treated with 0.2 μg/ml doxycycline for 48 h (+). Arrows point at vesicles near the membrane. N indicates the

nucleus. Scale bars = 0,5 μM (B) Quantification of data in (A). Bars represent the mean + SEM (n = 30 cells/sample). **p<0.01 comparing cells expressing or not LRRK2^{G2019S} as indicated. (C) Control Western blot analysis using anti-myc (to detect LRRK2) and anti-βactin (as loading standard) on cells treated as in (A).
doi:10.1371/journal.pone.0077198.g005

In order to understand the role of LRRK2 kinase activity in the control of GH extracellular level we decided to use two different approaches. First we analysed the effect of two LRRK2 dead kinase mutants carrying a deletion (delta-kinase) or point mutation (D1994A). Surprisingly, the absence of kinase domain completely abolishes the LRRK2 effect on GH extracellular level, while

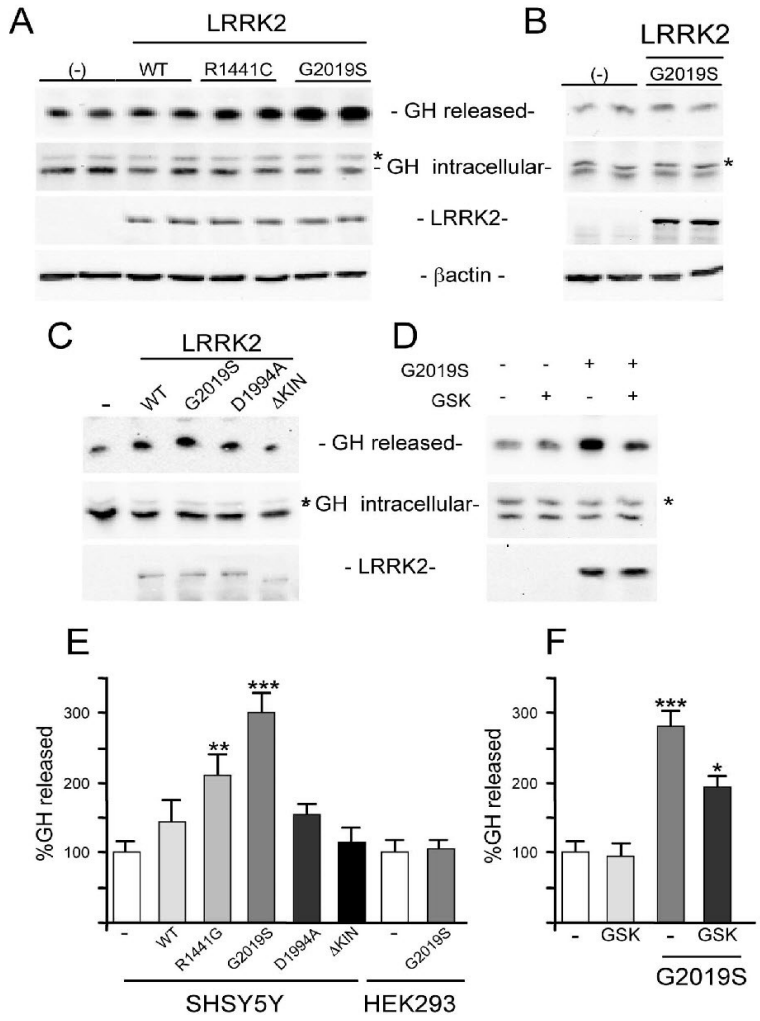

Figure 6. Effect of LRRK2 expression on released GH from neuronal and non-neuronal cells. (A) SH-SY5Y were transfected with plasmids coding for GH alone (−) or with the indicated mutant LRRK2s. Western blot on the extracellular medium (released GH) or cell protein extracts were performed using anti-myc antibodies for GH or LRRK2 and anti-β-actin as controls for equal loading of samples. The asterisk (*) indicates a non-specific band. (B) HEK293 cells were transfected with GH alone (−) or with LRRK2^{G2019S}. Western blot on the extracellular medium (released GH) or cell protein extracts were performed using Anti-myc antibody for GH or LRRK2 and anti-β-actin as controls for equal loading of samples. The asterisk (*) indicates a non-specific band. (C) Analysis of LRRK2^{D1994A} or LRRK2$^{\Delta kinase}$ on GH extracellular level in the same experimental conditions. (D) Effect of LRRK2 inhibitor on GH extracellular level in the same experimental conditions (E) Quantification by Student's *t* test of data obtained in (A–B–C). **p<0,01 and ***p<0,001 versus (−). (F) Quantification by Student's *t* test of data obtained in (D). *p<0,05 and ***p<0,001 versus (−).
doi:10.1371/journal.pone.0077198.g006

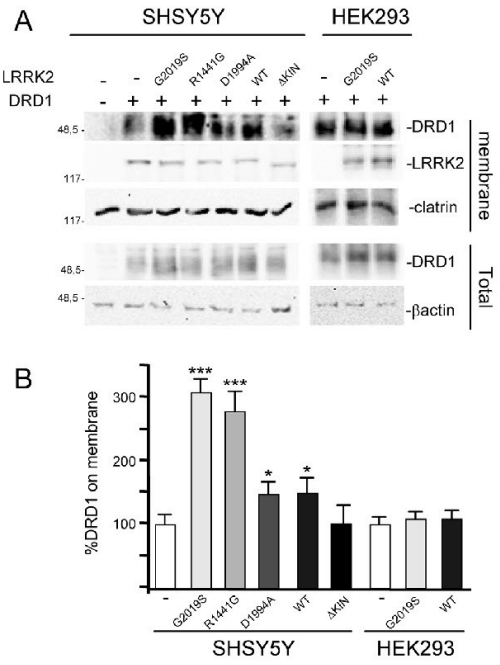

Figure 7. Effect of LRRK2 on Dopamine D1 receptor (DRD1) distribution on neuronal and non-neuronal cells. A) SH-SY5Y or HEK293 were transfected with DRD1 alone (−) or with the indicated mutant LRRK2. Western blot on the total and membrane fraction proteins were performed using anti-flag antibody for DRD1 or anti-myc for LRRK2 and anti-β-actin or clathrin as controls for equal loading of samples. Note that for SDS-PAGE analysis the protein samples were not boiled as suggested in anti-DRD1 data sheet. (B) Quantification by Student's *t* test of data obtained in (A). *p<0,05 **p<0,01 and ***p<0,001.
doi:10.1371/journal.pone.0077198.g007

$LRRK2^{D1994A}$ has an effect roughly comparable to $LRRK^{WT}$ (Figure 6C). To further evaluate the importance of LRRK2 kinase activity we used the LRRK2 inhibitor GSK2578215A. The presence of LRRK2 inhibitor significantly reduces the increase in G11 extracellular level due to $LRRK2^{G2019S}$ expression (Figure 6D–F).

LRRK2 Affects the Localization of Dopamine Receptor D1 both in Neuronal Cells and Transgenic Mouse Tissues

Vesicle trafficking is a complex process regulating multiple different cellular functions, including neurotransmitter or protein release and localization of membrane receptors. The previous results prompted us to analyse the possible effect of LRRK2 on membrane receptor localization using the membrane levels of dopamine receptor D1 (DRD1) as a read-out. DRD1is highly expressed in the prefrontal cortex, striatum and nucleus accumbens, although it is absent in dopaminergic cells where Dopamine D2 receptors are expressed [36]. We co-transfected SH-SY5Y cells with plasmid coding for DRD1 in absence or in presence of one among $LRKK2^{WT}$, $LRKK2^{G2019S}$, $LRKK2^{R1441G}$, $LRKK2^{D1994A}$ or $LRKK2^{\Delta kinase}$. 48 hours after transfection, the sub-cellular distribution of DRD1 receptors was analysed by cell fractionation. As shown in figure 7, the presence of $LRRK2^{G2019S}$ and $LRKK2^{R1441G}$, and, to a lesser extent, of $LRRK2^{WT}$ or $LRRK2^{D1994A}$ determines a significant increase in the level of membrane-associated DRD1 compared to controls with DRD1 alone, while the effect is completely abolished in presence of $LRKK2^{\Delta kinase}$. In agreement with previous findings on G11 secretion, this effect is not observed in HEK293 cells (Figure 7B, D). To extend our analysis to *in vivo* models we analysed the distribution of two neurotransmitter receptors in the striatum of transgenic $LRRK2^{G2019S}$ mice compared to non-transgenic mice. In particular, we analysed the NMDA-NR1 receptor (NR1) and DRD1 distribution in total, membrane or vesicle fractions obtained from the striatum of 5 different animals of the two genotypes. The samples were independently prepared, quantified and pooled together before SDS-PAGE loading using the same amount of protein. As shown in Figure 8A the expression of $LRRK2^{G2019S}$ leads to a significant increase of DRD1 in membrane fraction paralleling a significant decrease in vesicle fraction, with no significant differences in total protein extracts between the two genotypes (Figure 8B). No significant differences in the different fractions were observed for NR1, clathrin or sec8, a member of the exocyst complex.

Discussion

In neurons, vesicle trafficking mediates neurotransmitter or protein release and uptake, localization of membrane receptors, changes in plasma membrane composition at the cell surface and, not least, organelle biogenesis, thus underlying virtually all functions of the nervous system. The transport, binding and fusion of secretory vesicles with the cell surface are tightly regulated and their dysregulation has been implicated in PD and other neurological disorders [37]. There are two exocytosis pathways, constitutive and regulated, by which secretory proteins are released from cells. Regulated exocytosis is triggered by signals originating outside the cell, usually through a rise in Ca^{2+} concentration at release sites; however, the regulated pathway also exhibits basal or unstimulated secretion, which is distinct from constitutive secretion [38]. Moreover, there is now a general consensus that synaptic vesicles formation relies predominantly on the endocytic pathway [39] strongly suggesting a prominent role of endocytosis in the control of neurotransmitter extracellular level or membrane receptor level. Neurons and neuroendocrine cells (for example, PC12 cells) have both constitutive and regulated exocytosis, while most non-neuronal cells have only constitutive secretion. Chromaffin PC12 cells have been extensively used as cellular model of dopaminergic neurons to study vesicle trafficking under basal or stimulated conditions [40]. In fact, PC12 cells mimic many features of central DA neurons; they are characterized by the presence of catecholamine synthesizing enzymes (i.e. tyrosine hydroxylase) [41], catecholamine storage granules of about 0.2–0.5 μm [41,42] and DA receptors, as well as by DA uptake mechanisms. Like dopaminergic neurons, PC12 cells also contain the type A isoform of monoamine oxidase (MAO) [43]. Finally, we and other researchers have demonstrated that PC12 cells release catecholamines in response to different stimulations [28,30,44]. Moreover, PC12 cells together with SH-SY5Y neuronal cells have been largely used to analyse the LRRK2 physio-pathological functions [6,26,45,46].

In this study, we highlight an important cellular function of LRRK2 in the regulation of vesicle trafficking. We demonstrate that, under different experimental conditions, the presence of PD-linked mutant LRRK2 determines an increase in DA extracellular level in short-time dynamic experiments in PC12 cells, an increase

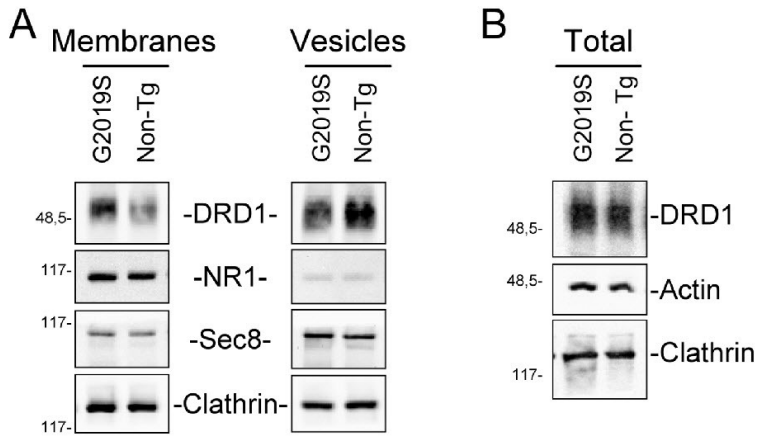

Figure 8. Effect of LRRK2 on Dopamine D1 receptor (DRD1) distribution on the striatum of G2019S LRRK2 or non-transgenic mice. The total, membrane or vesicle fractions were purified from 5 different LRRK2^{G2019S} transgenic mice or relative control (No Tg). Each of the five fractions were quantified and pooled together. A) Analysis of DRD1 level on protein extracts from membrane or vesicle fraction obtained from striatum of No Tg or LRRK2^{G2019S} transgenic mice. The western blot was performed using anti-DRD1, anti-NR1, anti-Sec8, or anti-clathrin antibodies. Note that for DRD1 analysis the samples were not boiled for the SDS-PAGE analysis as recommended in the antibody data sheet. B) Analysis of DRD1 level on total protein extracts obtained from striatum of No Tg or LRRK2^{G2019S} transgenic mice. The Western blot was performed using anti-DRD1, anti-actin or anti-clathrin antibodies. Note that for DRD1 analysis the samples were not boiled for the SDS-PAGE analysis.
doi:10.1371/journal.pone.0077198.g008

in GII release in SH-SY5Y cells and an increase of DRD1 on cell membrane of both SH-SY5Y cells and striatum of LRRK2^{G2019S} transgenic mice. The content of intracellular DA, DOPAC and HVA and DA, 3-MT, DOPAC and HVA in culture medium is similar in all the LRRK2-containing clones, whether or not expression of the protein has been induced (Figure 1C). This result suggests that LRRK2 expression does not interfere with basal dopamine metabolism. An alternative explanation is that long time sampling of extracellular content (48 h) may mask small/significant differences in DA secretion and metabolism among different PC12 clones since catecholamine medium content is the result of several biological phenomena including secretion, reuptake and enzymatic oxidative metabolism, but as well as the outcome of chemical events such as autoxidation of hydroxyl groups [28,30]. However, short-time dynamic experiments performed using *in vitro* microdialysis demonstrate a basal increase of DA secretion in cells expressing LRRK2^{G2019S} and a nicotine-induced increase of extracellular DA in those expressing both mutated LRRK2 genes (Figure 2A–B). Interestingly, these results on PC12 cells match that of LRRK2^{G2019S} transgenic rat model [23], in which temporally induced, but not constitutive, over-expression of LRRK2^{G2019S} determines an increased DA extracellular level and an increased motor activity, probably due to an impairment in dopamine reuptake by dopamine transporter [23]. In our PC12 cells, LRRK2 expression negatively affects the DA enzymatic metabolism, resulting in a decrease of DOPAC+HVA in basal microdialysate samples with the exception of the LRRK2^{G2019S} cells and the same trend is emphasized by nicotine treatment. This difference may be explained by the increased DA secretion in LRRK2^{G2019S}-expressing cells with the consequent reuptake and rise of the substrate available for intracellular MAO-A enzymes.

The expression of LRRK2^{G2019S} also affects the vesicle distribution in PC12 cells in terms of shortest distance from cell membranes. Although our ultrastructural analysis does not discriminate univocally the three different SV classes [47], it has generally been assumed that the vesicles closest to release sites (in a range of 100 nm) and the docked vesicles represent the readily releasable pool (RRP) and thus are recruited first during synapse activity [48]. Thus, our electron microscopy results may suggest that the increase in extracellular DA level either in basal conditions or after nicotine stimulation may be due to alteration in vesicle distribution inside the cells.

The increase in DA level in the extracellular medium of PC12 expressing LRRK2^{G2019S} is comparable to the biological effect detectable in SH-SY5Y cells using GII or DRD1 as read-out in the presence of LRRK2 pathological mutants (Figure 6–7). To date, the role of kinase activity in LRRK2 physio-pathological function is still controversial because different pathological or risk factor mutants exist with unchanged or reduced kinase activity (for review see Greggio et al. 2009) and because in different experimental models the kinase dead LRRK2 mutants behave as the pathological mutants [49]. Under our experimental conditions, the LRRK2^{D1994A} mutant protein shows smaller but consistent effect on both DRD1 membrane level and secreted GII compared to pathological mutants despite the fact that LRRK2^{D1994A} has a robust reduction in kinase activity [6,26]. In agreement with this result, the LRRK2 inhibitor GSK2578215A reduces but does not fully eliminate the LRRK2^{G2019S} effect either on DA or GII extracellular level. Taken together, our results seem to suggest that LRRK2 may primarily act as a regulatory scaffolding protein, where the LRRK2 kinase activity may further support this function. The absence of biological effect of LRRK2 lacking the kinase domain (LRRK2$^{\Delta KIN}$) on both GII and DRD1 readouts may be in part explained by a destabilization of the protein due to the large amino acid deletion.

Interestingly, the LRRK2 biological effects, in our experimental conditions, seem to be neuronal specific, since no increase in GII extracellular level or DRD1 membrane level was observed in

HEK293 cell when mutant LRRK2 is present. Neuronal-specific mechanisms of vesicle trafficking are well described [38] and this aspect could explain at least partially the neuron specific toxicity of mutant LRRK2. This view is supported by experiments *in vivo*, showing that the LRRK2 effects on DRD1 localization in neuronal cells is observed in the striatum of G2019S transgenic mice. The transgene expression determines an increase of DRD1 in the plasma membrane fraction that correlates with a decrease in the vesicle fraction. This effect is possibly specific for this receptor since it is not detectable for NMDA-NR1 receptor. It is generally accepted that membrane receptors show different turnover rate and different endocytic pathways. For instance, NMDARs are considered to be relatively stable once delivered to the cell surface of mature neurons, especially when compared with AMPARs that, even under basal conditions, cycle much more rapidly to and from the surface [50]. On the other hand, DRD1s internalize rapidly following agonist-induced activation [51]. Thus, the LRRK2 protein does not seem to exert a general control in secretion but rather accurately modulates the vesicle turnover.

The amount of secreted neurotransmitter or plasma membrane protein at steady state level is the sum of the transport reaching the cell surface from biosynthetic pathways, the leaving of the surface via the endocytic pathway, and the returning to plasma membrane from the intracellular endosomal pools; consequently, a change in any of these parameters could be responsible for the differences that we observe in DA or GH release and DRD1 membrane localization. For instance, LRRK2 has been implicated to different extents in vesicle trafficking either directly throughout endocytosis regulation [24,25,49] or indirectly throughout interaction with actin or tubulin [12,52] that in turn may affect vesicle movement among the cytoskeleton. The dysregulation on vesicle trafficking may have important consequences on neuronal toxicity. It is believed that inter-related processes like oxidative stress, excitotoxicity, inflammation, mitochondrial dysfunction and altered proteolysis are involved in the cascade of events that will lead to DA neuron death [53]. In this respect, the increase in neurotransmitter levels in the inter-synaptic space or the increase in membrane receptors in neuronal plasma membrane due to the expression of mutant LRRK2 could alter the normal neuronal physiology that in turn may lead to neuronal toxicity. In this respect, the increased neurotransmitter levels in the inter-synaptic space or the increase in membrane receptors in neuronal plasma membrane due to the expression of mutant LRRK2 could alter the normal neuronal physiology that in turn may lead to neuronal toxicity. For instance, a dysregulation in DA level has been extensively studied as prominent PD etiological factor for the neurotoxic properties of DA metabolites [54,55].

Supporting Information

Figure S1 Effect of LRRK2 inhibitor GSK2578215A on DOPAC+HVA concentrations. PC12-derived cell lines were left untreated (A) or treated (B) with 1 μM of GSK2578215A. After 60 minutes of stabilization, three baseline dialysates were collected at 20-minute intervals as previously described. Starting from 60 minutes, nicotine was infused for 60 minutes. Microdialysates were continuously recovered during drug infusion and after nicotine discontinuation. Values are mean ± SEM and refer to DOPAC+HVA concentrations in dialysates. Statistical significance was assessed using analysis of variance (ANOVA) for differences over time determined by Newman-Keules *t* test and unpaired *t*-tests. *$p<0.05$ compared with pertinent baseline values of all groups before nicotine treatment. Graphs in panel (C) and (D) represent the area under curve (AUC) values. (C) Basal DOPAC+HVA concentrations in dialysates of PC12 cell lines untreated or treated with 1 μM of GSK2578215A (minutes 20–40–60 before nicotine treatment of Figure S1A *vs* B). (D) DOPAC+HVA in dialysates integrated after nicotine administration in PC12 cell lines untreated or treated with 1 μM of GSK2578215A (from minutes 80 to 220 after nicotine treatment of Figure S1A *vs* B). AUC values are mean ± SEM.
(TIF)

Acknowledgments

We would like to acknowledge all the people from the laboratory that critically read the manuscript. Thanks are due to Salvatore Marceddu for Electron Microscopy analysis and Giustina Casu for proofreading the manuscript for English language.

This paper is dedicated to Prof. Giuseppe Rotilio on the occasion of his 72nd birthday.

Author Contributions

Conceived and designed the experiments: CI CC RM PAS. Performed the experiments: RM MGDG YS GS YX MG GR AB. Analyzed the data: CI CC RM PAS. Contributed reagents/materials/analysis tools: TMD VLD MTC. Wrote the paper: CI CC PAS RM MTC.

References

1. Biskup S, Gerlach M, Kupsch A, Reichmann H, Riederer P, et al. (2006) Genes associated with Parkinson syndrome. J Neurol 253 Suppl 5: 8–17.
2. Paisan-Ruiz C, Jain S, Evans EW, Gilks WP, Simon J, et al. (2004) Cloning of the gene containing mutations that cause PARK8-linked Parkinson's disease. Neuron 44: 595–600.
3. Zimprich A, Biskup S, Leitner P, Lichtner P, Farrer M, et al. (2004) Mutations in LRRK2 cause autosomal-dominant parkinsonism with pleomorphic pathology. Neuron 44: 601–607.
4. Marin I, van Egmond WN, van Haastert PJ (2008) The Roco protein family: a functional perspective. Faseb J 22: 3103–3110.
5. Healy DG, Falchi M, O'Sullivan SS, Bonifati V, Durr A, et al. (2008) Phenotype, genotype, and worldwide genetic penetrance of LRRK2-associated Parkinson's disease: a case-control study. Lancet Neurol 7: 583–590.
6. Smith WW, Pei Z, Jiang H, Dawson VL, Dawson TM, et al. (2006) Kinase activity of mutant LRRK2 mediates neuronal toxicity. Nat Neurosci 9: 1231–1233.
7. West AB, Moore DJ, Biskup S, Bugayenko A, Smith WW, et al. (2005) Parkinson's disease-associated mutations in leucine-rich repeat kinase 2 augment kinase activity. Proc Natl Acad Sci U S A 102: 16842–16847.
8. Greggio E, Cookson MR (2009) Leucine-rich repeat kinase 2 mutations and Parkinson's disease: three questions. ASN Neuro 1.
9. Bonifati V (2006) The pleomorphic pathology of inherited Parkinson's disease: lessons from LRRK2. Curr Neurol Neurosci Rep 6: 355–357.
10. Gehrke S, Imai Y, Sokol N, Lu B (2010) Pathogenic LRRK2 negatively regulates microRNA-mediated translational repression. Nature 466: 637–641.
11. Imai Y, Gehrke S, Wang HQ, Takahashi R, Hasegawa K, et al. (2008) Phosphorylation of 4E-BP by LRRK2 affects the maintenance of dopaminergic neurons in Drosophila. Embo J 27: 2432–2443.
12. Parisiadou L, Xie C, Cho HJ, Lin X, Gu XL, et al. (2009) Phosphorylation of ezrin/radixin/moesin proteins by LRRK2 promotes the rearrangement of actin cytoskeleton in neuronal morphogenesis. J Neurosci 29: 13971–13980.
13. Gillardon F (2009) Leucine-rich repeat kinase 2 phosphorylates brain tubulin-beta isoforms and modulates microtubule stability–a point of convergence in parkinsonian neurodegeneration? J Neurochem 110: 1514–1522.
14. Melrose HL, Dachsel JC, Behrouz B, Lincoln SJ, Yue M, et al. (2010) Impaired dopaminergic neurotransmission and microtubule-associated protein tau alterations in human LRRK2 transgenic mice. Neurobiol Dis 40: 503–517.
15. Tong Y, Giaime E, Yamaguchi H, Ichimura T, Liu Y, et al. (2012) Loss of leucine-rich repeat kinase 2 causes age-dependent bi-phasic alterations of the autophagy pathway. Mol Neurodegener 7: 2.
16. Ramonet D, Daher JP, Lin BM, Stafa K, Kim J, et al. (2011) Dopaminergic neuronal loss, reduced neurite complexity and autophagic abnormalities in transgenic mice expressing G2019S mutant LRRK2. PLoS One 6: e18568.
17. Liu Z, Lee J, Krummey S, Lu W, Cai H, et al. (2011) The kinase LRRK2 is a regulator of the transcription factor NFAT that modulates the severity of inflammatory bowel disease. Nat Immunol 12: 1063–1070.

18. Sanna G, Del Giudice MG, Crosio C, Iaccarino C (2012) LRRK2 and vesicle trafficking. Biochem Soc Trans 40: 1117–1122.
19. Biskup S, Moore DJ, Celsi F, Higashi S, West AB, et al. (2006) Localization of LRRK2 to membranous and vesicular structures in mammalian brain. Ann Neurol 60: 557–569.
20. Hatano T, Kubo S, Imai S, Maeda M, Ishikawa K, et al. (2007) Leucine-rich repeat kinase 2 associates with lipid rafts. Hum Mol Genet 16: 678–690.
21. Li Y, Liu W, Oo TF, Wang L, Tang Y, et al. (2009) Mutant LRRK2(R1441G) BAC transgenic mice recapitulate cardinal features of Parkinson's disease. Nat Neurosci 12: 826–828.
22. Li X, Patel JC, Wang J, Avshalumov MV, Nicholson C, et al. (2010) Enhanced striatal dopamine transmission and motor performance with LRRK2 overexpression in mice is eliminated by familial Parkinson's disease mutation G2019S. J Neurosci 30: 1788–1797.
23. Zhou H, Huang C, Tong J, Hong WC, Liu YJ, et al. (2011) Temporal expression of mutant LRRK2 in adult rats impairs dopamine reuptake. Int J Biol Sci 7: 753–761.
24. Piccoli G, Condliffe SB, Bauer M, Giesert F, Boldt K, et al. (2011) LRRK2 controls synaptic vesicle storage and mobilization within the recycling pool. J Neurosci 31: 2225–2237.
25. Shin N, Jeong H, Kwon J, Heo HY, Kwon JJ, et al. (2008) LRRK2 regulates synaptic vesicle endocytosis. Exp Cell Res 314: 2053–2065.
26. Iaccarino C, Crosio C, Vitale C, Sanna G, Carri MT, et al. (2007) Apoptotic mechanisms in mutant LRRK2-mediated cell death. Hum Mol Genet 16: 1319–1326.
27. Migheli R, Godani C, Sciola L, Delogu MR, Serra PA, et al. (1999) Enhancing effect of manganese on L-DOPA-induced apoptosis in PC12 cells: role of oxidative stress. J Neurochem 73: 1155–1163.
28. Serra PA, Migheli R, Rocchitta G, Taras MG, Mura MP, et al. (2003) Role of the nitric oxide/cyclic GMP pathway and ascorbic acid in 3-morpholinosydnonimine (SIN-1)-induced increases in dopamine secretion from PC12 cells. A microdialysis in vitro study. Neurosci Lett 353: 5–8.
29. Migheli R, Puggioni G, Dedola S, Rocchitta G, Calia G, et al. (2008) Novel integrated microdialysis-amperometric system for in vitro detection of dopamine secreted from PC12 cells: design, construction, and validation. Anal Biochem 380: 323–330.
30. Serra PA, Rocchitta G, Delogu MR, Migheli R, Taras MG, et al. (2003) Role of the nitric oxide/cyclic GMP pathway and extracellular environment in the nitric oxide donor-induced increase in dopamine secretion from PC12 cells: a microdialysis in vitro study. J Neurochem 86: 1403–1413.
31. Xiong Y, Yuan C, Chen R, Dawson TM, Dawson VL (2012) ArfGAP1 Is a GTPase Activating Protein for LRRK2: Reciprocal Regulation of ArfGAP1 by LRRK2. J Neurosci 32: 3877–3886.
32. Iaccarino C, Mura ME, Esposito S, Carta F, Sanna G, et al. (2011) Bcl2-A1 interacts with pro-caspase-3: implications for amyotrophic lateral sclerosis. Neurobiol Dis 43: 642–650.
33. Bradberry CW, Sprouse JS, Sheldon PW, Aghajanian GK, Roth RH (1991) In vitro microdialysis: a novel technique for stimulated neurotransmitter release measurements. J Neurosci Methods 36: 85–90.
34. Wick PF, Senter RA, Parsels LA, Uhler MD, Holz RW (1993) Transient transfection studies of secretion in bovine chromaffin cells and PC12 cells. Generation of kainate-sensitive chromaffin cells. J Biol Chem 268: 10983–10989.
35. Lee HW, Park JW, Sandagsuren EU, Kim KB, Yoo JJ, et al. (2006) Overexpression of APP stimulates basal and constitutive exocytosis in PC12 cells. Neurosci Lett 436: 245–249.
36. Missale C, Nash SR, Robinson SW, Jaber M, Caron MG (1998) Dopamine receptors: from structure to function. Physiol Rev 78: 189–225.
37. Esposito G, Ana Clara F, Verstreken P (2012) Synaptic vesicle trafficking and Parkinson's disease. Dev Neurobiol 72: 134–144.
38. Chijsen WE, Leenders AG (2005) Differential signaling in presynaptic neurotransmitter release. Cell Mol Life Sci 62: 937–954.
39. Buckley KM, Melikian HE, Provoda CJ, Waring MT (2000) Regulation of neuronal function by protein trafficking: a role for the endosomal pathway. J Physiol 525 Pt 1: 11–19.
40. Martin TF, Grishanin RN (2003) PC12 cells as a model for studies of regulated secretion in neuronal and endocrine cells. Methods Cell Biol 71: 267–286.
41. Markey KA, Kondo H, Shenkman L, Goldstein M (1980) Purification and characterization of tyrosine hydroxylase from a clonal pheochromocytoma cell line. Mol Pharmacol 17: 79–85.
42. Roda LG, Nolan JA, Kim SU, Hogue-Angeletti RA (1980) Isolation and characterization of chromaffin granules from a pheochromocytoma (PC 12) cell line. Exp Cell Res 126: 103–109.
43. Finberg JP, Youdim MB (1983) Selective MAO A and B inhibitors: their mechanism of action and pharmacology. Neuropharmacology 22: 441–446.
44. Fujita K, Lazarovici P, Guroff G (1989) Regulation of the differentiation of PC12 pheochromocytoma cells. Environ Health Perspect 80: 127–142.
45. Greggio E, Jain S, Kingsbury A, Bandopadhyay R, Lewis P, et al. (2006) Kinase activity is required for the toxic effects of mutant LRRK2/dardarin. Neurobiol Dis 23: 329–341.
46. Heo HY, Kim KS, Seol W (2010) Coordinate Regulation of Neurite Outgrowth by LRRK2 and Its Interactor, Rab5. Exp Neurobiol 19: 97–105.
47. Rizzoli SO, Betz WJ (2005) Synaptic vesicle pools. Nat Rev Neurosci 6: 57–69.
48. Rizzoli SO, Betz WJ (2004) The structural organization of the readily releasable pool of synaptic vesicles. Science 303: 2037–2039.
49. Matta S, Van Kolen K, da Cunha R, van den Bogaart G, Mandemakers W, et al. (2012) LRRK2 Controls an EndoA Phosphorylation Cycle in Synaptic Endocytosis. Neuron 75: 1008–1021.
50. Groc L, Choquet D (2006) AMPA and NMDA glutamate receptor trafficking: multiple roads for reaching and leaving the synapse. Cell Tissue Res 326: 423–438.
51. Kotowski SJ, Hopf FW, Seif T, Bonci A, von Zastrow M (2011) Endocytosis promotes rapid dopaminergic signaling. Neuron 71: 278–290.
52. Kawakami F, Yabata T, Ohta E, Maekawa T, Shimada N, et al. (2012) LRRK2 phosphorylates tubulin-associated tau but not the free molecule: LRRK2-mediated regulation of the tau-tubulin association and neurite outgrowth. PLoS One 7: e30834.
53. Schapira AH, Jenner P (2011) Etiology and pathogenesis of Parkinson's disease. Mov Disord 26: 1049–1055.
54. Jiang Y, Pei L, Li S, Wang M, Liu F (2008) Extracellular dopamine induces the oxidative toxicity of SH-SY5Y cells. Synapse 62: 797–803.
55. Stokes AH, Lewis DY, Lash LH, Jerome WG 3rd, Grant KW, et al. (2000) Dopamine toxicity in neuroblastoma cells: role of glutathione depletion by L-BSO and apoptosis. Brain Res 858: 1–8.

CHAPTER 5

REFERENCES

1. Biskup S, Gerlach M, Kupsch A, Reichmann H, Riederer P, Vieregge P, et al. Genes associated with Parkinson syndrome. Journal of neurology. 2008;255 Suppl 5:8-17. Epub 2008/09/20.

2. Dauer W, Przedborski S. Parkinson's disease: mechanisms and models. Neuron. 2003;39(6):889-909. Epub 2003/09/16.

3. Gibb WR, Lees AJ. The relevance of the Lewy body to the pathogenesis of idiopathic Parkinson's disease. Journal of neurology, neurosurgery, and psychiatry. 1988;51(6):745-52. Epub 1988/06/01.

4. Forno LS. Neuropathology of Parkinson's disease. Journal of neuropathology and experimental neurology. 1996;55(3):259-72. Epub 1996/03/01.

5. Spillantini MG, Crowther RA, Jakes R, Hasegawa M, Goedert M. alpha-Synuclein in filamentous inclusions of Lewy bodies from Parkinson's disease and dementia with lewy bodies. Proceedings of the National Academy of Sciences of the United States of America. 1998;95(11):6469-73. Epub 1998/05/30.

6. Pappolla MA. Lewy bodies of Parkinson's disease. Immune electron microscopic demonstration of neurofilament antigens in constituent filaments. Archives of pathology & laboratory medicine. 1986;110(12):1160-3. Epub 1986/12/01.

7. Stacy M, Jankovic J. Differential diagnosis of Parkinson's disease and the parkinsonism plus syndromes. Neurologic clinics. 1992;10(2):341-59. Epub 1992/05/01.

8. Ahlskog JE. Diagnosis and differential diagnosis of Parkinson's disease and parkinsonism. Parkinsonism & related disorders. 2000;7(1):63-70. Epub 2000/09/29.

9. Gelb DJ, Oliver E, Gilman S. Diagnostic criteria for Parkinson disease. Archives of neurology. 1999;56(1):33-9. Epub 1999/01/29.

10. Poewe W, Antonini A, Zijlmans JC, Burkhard PR, Vingerhoets F. Levodopa in the treatment of Parkinson's disease: an old drug still going strong. Clinical interventions in aging. 2010;5:229-38. Epub 2010/09/21.

11. Penney JB, Jr., Young AB. Speculations on the functional anatomy of basal ganglia disorders. Annual review of neuroscience. 1983;6:73-94. Epub 1983/01/01.

12. Farley IJ, Price KS, Hornykiewicz O. Dopamine in thelimbic regions of the human brain: normal and abnormal. Advances in biochemical psychopharmacology. 1977;16:57-64. Epub 1977/01/01.

13. Hornykiewicz O. Parkinson's disease: from brain homogenate to treatment. Federation proceedings. 1973;32(2):183-90. Epub 1973/02/01.

14. Neve KA. The dopamine receptors. 2nd ed. New York, NY: Humana Press; 2010. xii, 647 p. p.

15. Giros B, Sokoloff P, Martres MP, Riou JF, Emorine LJ, Schwartz JC. Alternative splicing directs the expression of two D2 dopamine receptor isoforms. Nature. 1989;342(6252):923-6. Epub 1989/12/21.

16. Callier S, Snapyan M, Le Crom S, Prou D, Vincent JD, Vernier P. Evolution and cell biology of dopamine receptors in vertebrates. Biology of the cell / under the auspices of the European Cell Biology Organization. 2003;95(7):489-502. Epub 2003/11/05.

17. Ritter SL, Hall RA. Fine-tuning of GPCR activity by receptor-interacting proteins. Nature reviews Molecular cell biology. 2009;10(12):819-30. Epub 2009/11/26.

18. Kitada T, Asakawa S, Hattori N, Matsumine H, Yamamura Y, Minoshima S, et al. Mutations in the parkin gene cause autosomal recessive juvenile parkinsonism. Nature. 1998;392(6676):605-8. Epub 1998/04/29.

19. Thomas B, Beal MF. Parkinson's disease. Human molecular genetics. 2007;16 Spec No. 2:R183-94. Epub 2007/10/04.

20. Gasser T. Genetics of Parkinson's disease. Dialogues in clinical neuroscience. 2004;6(3):295-301. Epub 2004/09/01.

21. R K. Parkinson's Disease, genetic type. 2004 [updated August 2004August 2004].

22. Langston JW, Ballard P, Tetrud JW, Irwin I. Chronic Parkinsonism in humans due to a product of meperidine-analog synthesis. Science. 1983;219(4587):979-80. Epub 1983/02/25.

23. Irwin I, DeLanney LE, Langston JW. MPTP and aging. Studies in the C57BL/6 mouse. Advances in neurology. 1993;60:197-206. Epub 1993/01/01.

24. Ovadia A, Zhang Z, Gash DM. Increased susceptibility to MPTP toxicity in middle-aged rhesus monkeys. Neurobiology of aging. 1995;16(6):931-7. Epub 1995/11/01.

25. Liu Y, Roghani A, Edwards RH. Gene transfer of a reserpine-sensitive mechanism of resistance to N-methyl-4-phenylpyridinium. Proceedings of the National Academy of Sciences of the United States of America. 1992;89(19):9074-8. Epub 1992/10/01.

26. Ramsay RR, Dadgar J, Trevor A, Singer TP. Energy-driven uptake of N-methyl-4-phenylpyridine by brain mitochondria mediates the neurotoxicity of MPTP. Life sciences. 1986;39(7):581-8. Epub 1986/08/18.

27. Klaidman LK, Adams JD, Jr., Leung AC, Kim SS, Cadenas E. Redox cycling of MPP+: evidence for a new mechanism involving hydride transfer with xanthine oxidase, aldehyde dehydrogenase, and lipoamide dehydrogenase. Free radical biology & medicine. 1993;15(2):169-79. Epub 1993/08/01.

28. Wirdefeldt K, Adami HO, Cole P, Trichopoulos D, Mandel J. Epidemiology and etiology of Parkinson's disease: a review of the evidence. European journal of epidemiology. 2011;26 Suppl 1:S1-58. Epub 2011/06/03.

29. Cohen G. Oxy-radical toxicity in catecholamine neurons. Neurotoxicology. 1984;5(1):77-82. Epub 1984/01/01.

30. Sandy MS, Armstrong M, Tanner CM, Daly AK, Di Monte DA, Langston JW, et al. CYP2D6 allelic frequencies in young-onset Parkinson's disease. Neurology. 1996;47(1):225-30. Epub 1996/07/01.

31. Nagatsu T. Isoquinoline neurotoxins in the brain and Parkinson's disease. Neuroscience research. 1997;29(2):99-111. Epub 1997/11/14.

32. Priyadarshi A, Khuder SA, Schaub EA, Priyadarshi SS. Environmental risk factors and Parkinson's disease: a metaanalysis. Environmental research. 2001;86(2):122-7. Epub 2001/07/05.

33. Poskanzer DC, Schwab RS. Cohort Analysis of Parkinson's Syndrome: Evidence for a Single Etiology Related to Subclinical Infection About 1920. Journal of chronic diseases. 1963;16:961-73. Epub 1963/09/01.

34. Gamboa ET, Wolf A, Yahr MD, Harter DH, Duffy PE, Barden H, et al. Influenza virus antigen in postencephalitic parkinsonism brain. Detection by immunofluorescence. Archives of neurology. 1974;31(4):228-32. Epub 1974/10/01.

35. Pirkevi C, Lesage S, Brice A, Basak AN. From genes to proteins in mendelian Parkinson's disease: an overview. Anat Rec (Hoboken). 2009;292(12):1893-901. Epub 2009/11/28.

36. Cookson MR. The role of leucine-rich repeat kinase 2 (LRRK2) in Parkinson's disease. Nature reviews Neuroscience. 2010;11(12):791-7. Epub 2010/11/23.

37. Seol W. Biochemical and molecular features of LRRK2 and its pathophysiological roles in Parkinson's disease. BMB reports. 2010;43(4):233-44. Epub 2010/04/29.

38. Larsen KE, Schmitz Y, Troyer MD, Mosharov E, Dietrich P, Quazi AZ, et al. Alpha-synuclein overexpression in PC12 and chromaffin cells impairs catecholamine release by interfering with a late step in exocytosis. The Journal of neuroscience : the official journal of the Society for Neuroscience. 2006;26(46):11915-22. Epub 2006/11/17.

39. Lashuel HA, Petre BM, Wall J, Simon M, Nowak RJ, Walz T, et al. Alpha-synuclein, especially the Parkinson's disease-associated mutants, forms pore-like annular and tubular protofibrils. Journal of molecular biology. 2002;322(5):1089-102. Epub 2002/10/09.

40. Moore DJ. Parkin: a multifaceted ubiquitin ligase. Biochemical Society transactions. 2006;34(Pt 5):749-53. Epub 2006/10/21.

41. Mizuno Y, Hattori N, Kubo S, Sato S, Nishioka K, Hatano T, et al. Progress in the pathogenesis and genetics of Parkinson's disease. Philosophical transactions of the Royal Society of London Series B, Biological sciences. 2008;363(1500):2215-27. Epub 2008/04/23.

42. Gandhi S, Wood NW. Molecular pathogenesis of Parkinson's disease. Human molecular genetics. 2005;14 Spec No. 2:2749-55. Epub 2005/11/10.

43. Pridgeon JW, Olzmann JA, Chin LS, Li L. PINK1 protects against oxidative stress by phosphorylating mitochondrial chaperone TRAP1. PLoS biology. 2007;5(7):e172. Epub 2007/06/21.

44. Plun-Favreau H, Klupsch K, Moisoi N, Gandhi S, Kjaer S, Frith D, et al. The mitochondrial protease HtrA2 is regulated by Parkinson's disease-associated kinase PINK1. Nature cell biology. 2007;9(11):1243-52. Epub 2007/10/02.

45. Wang X, Winter D, Ashrafi G, Schlehe J, Wong YL, Selkoe D, et al. PINK1 and Parkin target Miro for phosphorylation and degradation to arrest mitochondrial motility. Cell. 2011;147(4):893-906. Epub 2011/11/15.

46. Geisler S, Holmstrom KM, Skujat D, Fiesel FC, Rothfuss OC, Kahle PJ, et al. PINK1/Parkin-mediated mitophagy is dependent on VDAC1 and p62/SQSTM1. Nature cell biology. 2010;12(2):119-31. Epub 2010/01/26.

47. Narendra DP, Jin SM, Tanaka A, Suen DF, Gautier CA, Shen J, et al. PINK1 is selectively stabilized on impaired mitochondria to activate Parkin. PLoS biology. 2010;8(1):e1000298. Epub 2010/02/04.

48. Surmeier DJ, Guzman JN, Sanchez-Padilla J, Goldberg JA. What causes the death of dopaminergic neurons in Parkinson's disease? Progress in brain research. 2010;183:59-77. Epub 2010/08/11.

49. Madian AG, Hindupur J, Hulleman JD, Diaz-Maldonado N, Mishra VR, Guigard E, et al. Effect of single amino acid substitution on oxidative modifications of the Parkinson's disease-related protein, DJ-1. Molecular & cellular proteomics : MCP. 2012;11(2):M111 010892. Epub 2011/11/23.

50. Funayama M, Hasegawa K, Kowa H, Saito M, Tsuji S, Obata F. A new locus for Parkinson's disease (PARK8) maps to chromosome 12p11.2-q13.1. Annals of neurology. 2002;51(3):296-301. Epub 2002/03/14.

51. Haubenberger D, Bonelli S, Hotzy C, Leitner P, Lichtner P, Samal D, et al. A novel LRRK2 mutation in an Austrian cohort of patients with Parkinson's disease. Movement disorders : official journal of the Movement Disorder Society. 2007;22(11):1640-3. Epub 2007/05/25.

52. Paisan-Ruiz C, Jain S, Evans EW, Gilks WP, Simon J, van der Brug M, et al. Cloning of the gene containing mutations that cause PARK8-linked Parkinson's disease. Neuron. 2004;44(4):595-600. Epub 2004/11/16.

53. Kumar A, Cookson MR. Role of LRRK2 kinase dysfunction in Parkinson disease. Expert reviews in molecular medicine. 2011;13:e20. Epub 2011/06/17.

54. Li C, Beal MF. Leucine-rich repeat kinase 2: a new player with a familiar theme for Parkinson's disease pathogenesis. Proceedings of the National Academy of Sciences of the United States of America. 2005;102(46):16535-6. Epub 2005/11/09.

55. Rideout HJ, Stefanis L. The Neurobiology of LRRK2 and its Role in the Pathogenesis of Parkinson's Disease. Neurochemical research. 2013. Epub 2013/06/05.

56. Tewari R, Bailes E, Bunting KA, Coates JC. Armadillo-repeat protein functions: questions for little creatures. Trends in cell biology. 2010;20(8):470-81. Epub 2010/08/07.

57. Mosavi LK, Cammett TJ, Desrosiers DC, Peng ZY. The ankyrin repeat as molecular architecture for protein recognition. Protein science : a publication of the Protein Society. 2004;13(6):1435-48. Epub 2004/05/21.

58. Mata IF, Wedemeyer WJ, Farrer MJ, Taylor JP, Gallo KA. LRRK2 in Parkinson's disease: protein domains and functional insights. Trends in neurosciences. 2006;29(5):286-93. Epub 2006/04/18.

59. Anand VS, Braithwaite SP. LRRK2 in Parkinson's disease: biochemical functions. The FEBS journal. 2009;276(22):6428-35. Epub 2009/10/07.

60. Greggio E, Zambrano I, Kaganovich A, Beilina A, Taymans JM, Daniels V, et al. The Parkinson disease-associated leucine-rich repeat kinase 2 (LRRK2) is a dimer that undergoes intramolecular autophosphorylation. The Journal of biological chemistry. 2008;283(24):16906-14. Epub 2008/04/10.

61. Biskup S, Moore DJ, Celsi F, Higashi S, West AB, Andrabi SA, et al. Localization of LRRK2 to membranous and vesicular structures in mammalian brain. Annals of neurology. 2006;60(5):557-69. Epub 2006/11/23.

62. West AB, Moore DJ, Biskup S, Bugayenko A, Smith WW, Ross CA, et al. Parkinson's disease-associated mutations in leucine-rich repeat kinase 2 augment kinase activity. Proceedings of the National Academy of Sciences of the United States of America. 2005;102(46):16842-7. Epub 2005/11/05.

63. Smith WW, Pei Z, Jiang H, Moore DJ, Liang Y, West AB, et al. Leucine-rich repeat kinase 2 (LRRK2) interacts with parkin, and mutant LRRK2 induces neuronal degeneration. Proceedings of the National Academy of Sciences of the United States of America. 2005;102(51):18676-81. Epub 2005/12/15.

64. Dachsel JC, Wider C, Vilarino-Guell C, Aasly JO, Rajput A, Rajput AH, et al. Death-associated protein kinase 1 variation and Parkinson's disease. European journal of neurology : the official journal of the European Federation of Neurological Societies. 2011;18(8):1090-3. Epub 2011/07/14.

65. Gandhi PN, Chen SG, Wilson-Delfosse AL. Leucine-rich repeat kinase 2 (LRRK2): a key player in the pathogenesis of Parkinson's disease. Journal of neuroscience research. 2009;87(6):1283-95. Epub 2008/11/26.

66. Melrose H. Update on the functional biology of Lrrk2. Future neurology. 2008;3(6):669-81. Epub 2009/02/20.

67. Ozelius LJ, Senthil G, Saunders-Pullman R, Ohmann E, Deligtisch A, Tagliati M, et al. LRRK2 G2019S as a cause of Parkinson's disease in Ashkenazi Jews. The New England journal of medicine. 2006;354(4):424-5. Epub 2006/01/27.

68. Cossu G, van Doeselaar M, Deriu M, Melis M, Molari A, Di Fonzo A, et al. LRRK2 mutations and Parkinson's disease in Sardinia--A Mediterranean genetic isolate. Parkinsonism & related disorders. 2007;13(1):17-21. Epub 2006/10/27.

69. MacLeod D, Dowman J, Hammond R, Leete T, Inoue K, Abeliovich A. The familial Parkinsonism gene LRRK2 regulates neurite process morphology. Neuron. 2006;52(4):587-93. Epub 2006/11/23.

70. Parisiadou L, Cai H. LRRK2 function on actin and microtubule dynamics in Parkinson disease. Communicative & integrative biology. 2010;3(5):396-400. Epub 2010/11/09.

71. Plowey ED, Cherra SJ, 3rd, Liu YJ, Chu CT. Role of autophagy in G2019S-LRRK2-associated neurite shortening in differentiated SH-SY5Y cells. Journal of neurochemistry. 2008;105(3):1048-56. Epub 2008/01/10.

72. Sakaguchi-Nakashima A, Meir JY, Jin Y, Matsumoto K, Hisamoto N. LRK-1, a C. elegans PARK8-related kinase, regulates axonal-dendritic polarity of SV proteins. Current biology : CB. 2007;17(7):592-8. Epub 2007/03/10.

73. Gillardon F. Leucine-rich repeat kinase 2 phosphorylates brain tubulin-beta isoforms and modulates microtubule stability--a point of convergence in parkinsonian neurodegeneration? Journal of neurochemistry. 2009;110(5):1514-22. Epub 2009/06/24.

74. Ho CC, Rideout HJ, Ribe E, Troy CM, Dauer WT. The Parkinson disease protein leucine-rich repeat kinase 2 transduces death signals via Fas-associated protein with death domain and caspase-8 in a cellular model of neurodegeneration. The Journal of neuroscience : the official journal of the Society for Neuroscience. 2009;29(4):1011-6. Epub 2009/01/30.

75. Iaccarino C, Crosio C, Vitale C, Sanna G, Carri MT, Barone P. Apoptotic mechanisms in mutant LRRK2-mediated cell death. Human molecular genetics. 2007;16(11):1319-26. Epub 2007/04/06.

76. Greggio E, Jain S, Kingsbury A, Bandopadhyay R, Lewis P, Kaganovich A, et al. Kinase activity is required for the toxic effects of mutant LRRK2/dardarin. Neurobiology of disease. 2006;23(2):329-41. Epub 2006/06/06.

77. Qing H, Zhang Y, Deng Y, McGeer EG, McGeer PL. Lrrk2 interaction with alpha-synuclein in diffuse Lewy body disease. Biochemical and biophysical research communications. 2009;390(4):1229-34. Epub 2009/11/03.

78. Qing H, Wong W, McGeer EG, McGeer PL. Lrrk2 phosphorylates alpha synuclein at serine 129: Parkinson disease implications. Biochemical and biophysical research communications. 2009;387(1):149-52. Epub 2009/07/07.

79. Kondo K, Obitsu S, Teshima R. alpha-Synuclein aggregation and transmission are enhanced by leucine-rich repeat kinase 2 in human neuroblastoma SH-SY5Y cells. Biological & pharmaceutical bulletin. 2011;34(7):1078-83. Epub 2011/07/02.

80. Lin X, Parisiadou L, Gu XL, Wang L, Shim H, Sun L, et al. Leucine-rich repeat kinase 2 regulates the progression of neuropathology induced by Parkinson's-disease-related mutant alpha-synuclein. Neuron. 2009;64(6):807-27. Epub 2010/01/13.

81. Andres-Mateos E, Mejias R, Sasaki M, Li X, Lin BM, Biskup S, et al. Unexpected lack of hypersensitivity in LRRK2 knock-out mice to MPTP (1-methyl-4-phenyl-1,2,3,6-tetrahydropyridine). The Journal of neuroscience : the official journal of the Society for Neuroscience. 2009;29(50):15846-50. Epub 2009/12/18.

82. Tong Y, Yamaguchi H, Giaime E, Boyle S, Kopan R, Kelleher RJ, 3rd, et al. Loss of leucine-rich repeat kinase 2 causes impairment of protein degradation pathways, accumulation of alpha-synuclein, and apoptotic cell death in aged mice. Proceedings of the National Academy of Sciences of the United States of America. 2010;107(21):9879-84. Epub 2010/05/12.

83. Li X, Patel JC, Wang J, Avshalumov MV, Nicholson C, Buxbaum JD, et al. Enhanced striatal dopamine transmission and motor performance with LRRK2 overexpression in mice is eliminated by familial Parkinson's disease mutation G2019S. The Journal of neuroscience : the official journal of the Society for Neuroscience. 2010;30(5):1788-97. Epub 2010/02/05.

84. Ramonet D, Daher JP, Lin BM, Stafa K, Kim J, Banerjee R, et al. Dopaminergic neuronal loss, reduced neurite complexity and autophagic abnormalities in transgenic mice expressing G2019S mutant LRRK2. PloS one. 2011;6(4):e18568. Epub 2011/04/16.

85. Melrose HL, Dachsel JC, Behrouz B, Lincoln SJ, Yue M, Hinkle KM, et al. Impaired dopaminergic neurotransmission and microtubule-associated protein tau alterations in human LRRK2 transgenic mice. Neurobiology of disease. 2010;40(3):503-17. Epub 2010/07/28.

86. Li Y, Liu W, Oo TF, Wang L, Tang Y, Jackson-Lewis V, et al. Mutant LRRK2(R1441G) BAC transgenic mice recapitulate cardinal features of Parkinson's disease. Nature neuroscience. 2009;12(7):826-8. Epub 2009/06/09.

87. Lee BD, Shin JH, VanKampen J, Petrucelli L, West AB, Ko HS, et al. Inhibitors of leucine-rich repeat kinase-2 protect against models of Parkinson's disease. Nature medicine. 2010;16(9):998-1000. Epub 2010/08/24.

88. Dusonchet J, Kochubey O, Stafa K, Young SM, Jr., Zufferey R, Moore DJ, et al. A rat model of progressive nigral neurodegeneration induced by the Parkinson's disease-associated G2019S mutation in LRRK2. The Journal of neuroscience : the official journal of the Society for Neuroscience. 2011;31(3):907-12. Epub 2011/01/21.

89. Yue Z, Lachenmayer ML. Genetic LRRK2 models of Parkinson's disease: Dissecting the pathogenic pathway and exploring clinical applications. Movement disorders : official journal of the Movement Disorder Society. 2011;26(8):1386-97. Epub 2011/05/04.

90. Kramer T, Lo Monte F, Goring S, Okala Amombo GM, Schmidt B. Small molecule kinase inhibitors for LRRK2 and their application to Parkinson's disease models. ACS chemical neuroscience. 2012;3(3):151-60. Epub 2012/08/04.

91. Hatano T, Kubo S, Imai S, Maeda M, Ishikawa K, Mizuno Y, et al. Leucine-rich repeat kinase 2 associates with lipid rafts. Human molecular genetics. 2007;16(6):678-90. Epub 2007/03/08.

92. Brown DA, London E. Functions of lipid rafts in biological membranes. Annual review of cell and developmental biology. 1998;14:111-36. Epub 1999/01/19.

93. Gil C, Soler-Jover A, Blasi J, Aguilera J. Synaptic proteins and SNARE complexes are localized in lipid rafts from rat brain synaptosomes. Biochemical and biophysical research communications. 2005;329(1):117-24. Epub 2005/02/22.

94. Thiele C, Hannah MJ, Fahrenholz F, Huttner WB. Cholesterol binds to synaptophysin and is required for biogenesis of synaptic vesicles. Nature cell biology. 2000;2(1):42-9. Epub 2000/01/06.

95. Jaleel M, Nichols RJ, Deak M, Campbell DG, Gillardon F, Knebel A, et al. LRRK2 phosphorylates moesin at threonine-558: characterization of how Parkinson's disease mutants affect kinase activity. The Biochemical journal. 2007;405(2):307-17. Epub 2007/04/24.

96. Shin N, Jeong H, Kwon J, Heo HY, Kwon JJ, Yun HJ, et al. LRRK2 regulates synaptic vesicle endocytosis. Experimental cell research. 2008;314(10):2055-65. Epub 2008/05/01.

97. Piccoli G, Condliffe SB, Bauer M, Giesert F, Boldt K, De Astis S, et al. LRRK2 controls synaptic vesicle storage and mobilization within the recycling pool. The Journal of neuroscience : the official journal of the Society for Neuroscience. 2011;31(6):2225-37. Epub 2011/02/11.

98. Meixner A, Boldt K, Van Troys M, Askenazi M, Gloeckner CJ, Bauer M, et al. A QUICK screen for Lrrk2 interaction partners--leucine-rich repeat kinase 2 is involved in actin cytoskeleton dynamics. Molecular & cellular proteomics : MCP. 2011;10(1):M110 001172. Epub 2010/09/30.

99. Matta S, Van Kolen K, da Cunha R, van den Bogaart G, Mandemakers W, Miskiewicz K, et al. LRRK2 controls an EndoA phosphorylation cycle in synaptic endocytosis. Neuron. 2012;75(6):1008-21. Epub 2012/09/25.

100. Xiong Y, Yuan C, Chen R, Dawson TM, Dawson VL. ArfGAP1 is a GTPase activating protein for LRRK2: reciprocal regulation of ArfGAP1 by LRRK2. The Journal of neuroscience : the official journal of the Society for Neuroscience. 2012;32(11):3877-86. Epub 2012/03/17.

101. Haebig K, Gloeckner CJ, Miralles MG, Gillardon F, Schulte C, Riess O, et al. ARHGEF7 (Beta-PIX) acts as guanine nucleotide exchange factor for leucine-rich repeat kinase 2. PloS one. 2010;5(10):e13762. Epub 2010/11/05.

102. Nichols RJ, Dzamko N, Morrice NA, Campbell DG, Deak M, Ordureau A, et al. 14-3-3 binding to LRRK2 is disrupted by multiple Parkinson's disease-associated mutations and regulates cytoplasmic localization. The Biochemical journal. 2010;430(3):393-404. Epub 2010/07/21.

103. Jahn R, Fasshauer D. Molecular machines governing exocytosis of synaptic vesicles. Nature. 2012;490(7419):201-7. Epub 2012/10/13.

104. Carney DS, Davies BA, Horazdovsky BF. Vps9 domain-containing proteins: activators of Rab5 GTPases from yeast to neurons. Trends in cell biology. 2006;16(1):27-35. Epub 2005/12/07.

105. Stafa K, Trancikova A, Webber PJ, Glauser L, West AB, Moore DJ. GTPase activity and neuronal toxicity of Parkinson's disease-associated LRRK2 is regulated by ArfGAP1. PLoS genetics. 2012;8(2):e1002526. Epub 2012/03/01.

106. Donaldson JG, Jackson CL. ARF family G proteins and their regulators: roles in membrane transport, development and disease. Nature reviews Molecular cell biology. 2011;12(6):362-75. Epub 2011/05/19.

107. Hehnly H, Stamnes M. Regulating cytoskeleton-based vesicle motility. FEBS letters. 2007;581(11):2112-8. Epub 2007/03/06.

108. Parisiadou L, Xie C, Cho HJ, Lin X, Gu XL, Long CX, et al. Phosphorylation of ezrin/radixin/moesin proteins by LRRK2 promotes the rearrangement of actin cytoskeleton in neuronal morphogenesis. The Journal of neuroscience : the official journal of the Society for Neuroscience. 2009;29(44):13971-80. Epub 2009/11/06.

109. Sanna G, Del Giudice MG, Crosio C, Iaccarino C. LRRK2 and vesicle trafficking. Biochemical Society transactions. 2012;40(5):1117-22. Epub 2012/09/20.

110. Bosgraaf L, Van Haastert PJ. Roc, a Ras/GTPase domain in complex proteins. Biochimica et biophysica acta. 2003;1643(1-3):5-10. Epub 2003/12/05.

111. Civiero L, Bubacco L. Human leucine-rich repeat kinase 1 and 2: intersecting or unrelated functions? Biochemical Society transactions. 2012;40(5):1095-101. Epub 2012/09/20.

112. Civiero L, Vancraenenbroeck R, Belluzzi E, Beilina A, Lobbestael E, Reyniers L, et al. Biochemical characterization of highly purified leucine-rich repeat kinases 1 and 2 demonstrates formation of homodimers. PloS one. 2012;7(8):e43472. Epub 2012/09/07.

113. Dachsel JC, Nishioka K, Vilarino-Guell C, Lincoln SJ, Soto-Ortolaza AI, Kachergus J, et al. Heterodimerization of Lrrk1-Lrrk2: Implications for LRRK2-associated Parkinson disease. Mechanisms of ageing and development. 2010;131(3):210-4. Epub 2010/02/11.

114. Greggio E, Lewis PA, van der Brug MP, Ahmad R, Kaganovich A, Ding J, et al. Mutations in LRRK2/dardarin associated with Parkinson disease are more toxic than equivalent mutations in the homologous kinase LRRK1. Journal of neurochemistry. 2007;102(1):93-102. Epub 2007/03/31.

115. Biskup S, Moore DJ, Rea A, Lorenz-Deperieux B, Coombes CE, Dawson VL, et al. Dynamic and redundant regulation of LRRK2 and LRRK1 expression. BMC neuroscience. 2007;8:102. Epub 2007/11/30.

116. Giesert F, Hofmann A, Burger A, Zerle J, Kloos K, Hafen U, et al. Expression analysis of Lrrk1, Lrrk2 and Lrrk2 splice variants in mice. PloS one. 2013;8(5):e63778. Epub 2013/05/16.

117. Hanafusa H, Ishikawa K, Kedashiro S, Saigo T, Iemura S, Natsume T, et al. Leucine-rich repeat kinase LRRK1 regulates endosomal trafficking of the EGF receptor. Nature communications. 2011;2:158. Epub 2011/01/20.

118. Davies P, Hinkle KM, Sukar NN, Sepulveda B, Mesias R, Serrano G, et al. Comprehensive characterization and optimization of anti-LRRK2 (leucine-rich repeat kinase 2) monoclonal antibodies. The Biochemical journal. 2013;453(1):101-13. Epub 2013/04/09.

119. Migheli R, Godani C, Sciola L, Delogu MR, Serra PA, Zangani D, et al. Enhancing effect of manganese on L-DOPA-induced apoptosis in PC12 cells: role of oxidative stress. Journal of neurochemistry. 1999;73(3):1155-63. Epub 1999/08/26.

120. Migheli R, Puggioni G, Dedola S, Rocchitta G, Calia G, Bazzu G, et al. Novel integrated microdialysis-amperometric system for in vitro detection of dopamine secreted from PC12 cells: design, construction, and validation. Analytical biochemistry. 2008;380(2):323-30. Epub 2008/06/26.

121. Serra PA, Rocchitta G, Delogu MR, Migheli R, Taras MG, Mura MP, et al. Role of the nitric oxide/cyclic GMP pathway and extracellular environment in the nitric oxide donor-induced increase in dopamine secretion from PC12 cells: a microdialysis in vitro study. Journal of neurochemistry. 2003;86(6):1403-13. Epub 2003/09/03.

122. Missale C, Nash SR, Robinson SW, Jaber M, Caron MG. Dopamine receptors: from structure to function. Physiological reviews. 1998;78(1):189-225. Epub 1998/02/11.

123. Michaelis M, Bliss J, Arnold SC, Hinsch N, Rothweiler F, Deubzer HE, et al. Cisplatin-resistant neuroblastoma cells express enhanced levels of epidermal growth factor receptor (EGFR) and are sensitive to treatment with EGFR-specific toxins. Clinical cancer research : an official journal of the American Association for Cancer Research. 2008;14(20):6531-7. Epub 2008/10/18.

124. Klein CL, Rovelli G, Springer W, Schall C, Gasser T, Kahle PJ. Homo- and heterodimerization of ROCO kinases: LRRK2 kinase inhibition by the LRRK2 ROCO fragment. Journal of neurochemistry. 2009;111(3):703-15. Epub 2009/08/29.

125. Esposito G, Ana Clara F, Verstreken P. Synaptic vesicle trafficking and Parkinson's disease. Developmental neurobiology. 2012;72(1):134-44. Epub 2011/05/13.

126. Ghijsen WE, Leenders AG. Differential signaling in presynaptic neurotransmitter release. Cellular and molecular life sciences : CMLS. 2005;62(9):937-54. Epub 2005/03/12.

127. Buckley KM, Melikian HE, Provoda CJ, Waring MT. Regulation of neuronal function by protein trafficking: a role for the endosomal pathway. The Journal of physiology. 2000;525 Pt 1:11-9. Epub 2000/05/16.

128. Martin TF, Grishanin RN. PC12 cells as a model for studies of regulated secretion in neuronal and endocrine cells. Methods in cell biology. 2003;71:267-86. Epub 2003/07/30.

129. Markey KA, Kondo H, Shenkman L, Goldstein M. Purification and characterization of tyrosine hydroxylase from a clonal pheochromocytoma cell line. Molecular pharmacology. 1980;17(1):79-85. Epub 1980/01/01.

130. Roda LG, Nolan JA, Kim SU, Hogue-Angeletti RA. Isolation and characterization of chromaffin granules from a pheochromocytoma (PC 12) cell line. Experimental cell research. 1980;128(1):103-9. Epub 1980/07/01.

131. Finberg JP, Youdim MB. Selective MAO A and B inhibitors: their mechanism of action and pharmacology. Neuropharmacology. 1983;22(3 Spec No):441-6. Epub 1983/03/01.

132. Fujita K, Lazarovici P, Guroff G. Regulation of the differentiation of PC12 pheochromocytoma cells. Environmental health perspectives. 1989;80:127-42. Epub 1989/03/01.

133. Smith WW, Pei Z, Jiang H, Dawson VL, Dawson TM, Ross CA. Kinase activity of mutant LRRK2 mediates neuronal toxicity. Nature neuroscience. 2006;9(10):1231-3. Epub 2006/09/19.

134. Heo HY, Kim KS, Seol W. Coordinate Regulation of Neurite Outgrowth by LRRK2 and Its Interactor, Rab5. Experimental neurobiology. 2010;19(2):97-105. Epub 2010/09/01.

135. Zhou H, Huang C, Tong J, Hong WC, Liu YJ, Xia XG. Temporal expression of mutant LRRK2 in adult rats impairs dopamine reuptake. International journal of biological sciences. 2011;7(6):753-61. Epub 2011/06/24.

136. Rizzoli SO, Betz WJ. Synaptic vesicle pools. Nature reviews Neuroscience. 2005;6(1):57-69. Epub 2004/12/22.

137. Rizzoli SO, Betz WJ. The structural organization of the readily releasable pool of synaptic vesicles. Science. 2004;303(5666):2037-9. Epub 2004/03/27.

138. Sossi V, de la Fuente-Fernandez R, Nandhagopal R, Schulzer M, McKenzie J, Ruth TJ, et al. Dopamine turnover increases in asymptomatic LRRK2 mutations carriers. Movement disorders : official journal of the Movement Disorder Society. 2010;25(16):2717-23. Epub 2010/10/13.

139. Smith AD, Castro SL, Zigmond MJ. Stress-induced Parkinson's disease: a working hypothesis. Physiology & behavior. 2002;77(4-5):527-31. Epub 2003/01/16.

140. Zigmond MJ, Hastings TG, Perez RG. Increased dopamine turnover after partial loss of dopaminergic neurons: compensation or toxicity? Parkinsonism & related disorders. 2002;8(6):389-93. Epub 2002/09/10.

141. Greggio E, Cookson MR. Leucine-rich repeat kinase 2 mutations and Parkinson's disease: three questions. ASN neuro. 2009;1(1). Epub 2009/07/03.

142. Groc L, Choquet D. AMPA and NMDA glutamate receptor trafficking: multiple roads for reaching and leaving the synapse. Cell and tissue research. 2006;326(2):423-38. Epub 2006/07/19.

143. Kotowski SJ, Hopf FW, Seif T, Bonci A, von Zastrow M. Endocytosis promotes rapid dopaminergic signaling. Neuron. 2011;71(2):278-90. Epub 2011/07/28.

144. Kawakami F, Yabata T, Ohta E, Maekawa T, Shimada N, Suzuki M, et al. LRRK2 phosphorylates tubulin-associated tau but not the free molecule: LRRK2-mediated regulation of the tau-tubulin association and neurite outgrowth. PloS one. 2012;7(1):e30834. Epub 2012/02/04.

145. Schapira AH, Jenner P. Etiology and pathogenesis of Parkinson's disease. Movement disorders : official journal of the Movement Disorder Society. 2011;26(6):1049-55. Epub 2011/06/01.

146. Jiang Y, Pei L, Li S, Wang M, Liu F. Extracellular dopamine induces the oxidative toxicity of SH-SY5Y cells. Synapse. 2008;62(11):797-803. Epub 2008/08/23.

147. Stokes AH, Lewis DY, Lash LH, Jerome WG, 3rd, Grant KW, Aschner M, et al. Dopamine toxicity in neuroblastoma cells: role of glutathione depletion by L-BSO and apoptosis. Brain research. 2000;858(1):1-8. Epub 2000/03/04.

148. Lewis PA. The function of ROCO proteins in health and disease. Biology of the cell / under the auspices of the European Cell Biology Organization. 2009;101(3):183-91. Epub 2009/01/21.

149. Haugarvoll K, Toft M, Ross OA, White LR, Aasly JO, Farrer MJ. Variants in the LRRK1 gene and susceptibility to Parkinson's disease in Norway. Neuroscience letters. 2007;416(3):299-301. Epub 2007/02/28.

150. Taylor JP, Hulihan MM, Kachergus JM, Melrose HL, Lincoln SJ, Hinkle KM, et al. Leucine-rich repeat kinase 1: a paralog of LRRK2 and a candidate gene for Parkinson's disease. Neurogenetics. 2007;8(2):95-102. Epub 2007/01/17.

151. Lichtenberg M, Mansilla A, Zecchini VR, Fleming A, Rubinsztein DC. The Parkinson's disease protein LRRK2 impairs proteasome substrate clearance without affecting proteasome catalytic activity. Cell death & disease. 2011;2:e196. Epub 2011/08/26.

ABBREVIATION LIST

- 3-MT - 3-methoxytyramine
- AD – Autosomal Dominant
- AIMs - Abnormal Involuntary Movements
- AR – Autosomal Recessive
- ArfGAP1 - ADP-ribosylation factor GTPase-activating protein 1
- AUC – Area Under the Curve
- CNS - central nervous system
- COMT - catechyl-O-metyl-transferase
- COR – Carboxy Terminal of Roc
- DAR – DopAmine Receptors
- DAT – Dopamine Transporter
- DOPAC - 3,4-Dihydroxyphenylacetic acid
- Dox – Doxycicline
- EGF – Epidermal Growth Factor
- EGFR - epidermal growth factor receptor
- EGF-Rh – EGF Rhodamine (conjugated)
- EM – Electron Microscopy
- ER - endoplasmic reticulum
- ERM - ezrin/radixin/moesin
- GEFs - guanine nucleotide exchange factors
- GH – Growth Hormone
- GNEF: Guanine Nucleotide Exchange Factor
- GPCRs - G protein-coupled receptors
- GRKs - GPCR kinases
- HVA - homovanillic acid
- KD – Knock Down
- KIN – kinase
- LB – Lewy bodies
- L-dopa - Levodopa
- LRR – Leucine Rich Repeat
- LRRK1 - Leucine-Rich Repeat Kinase 1.
- LRRK2 – Leucine Rich Repeat Kinase 2
- LV – Lentiviral
- MAO B - monoamine-oxidase B
- mGH - murine growth hormone
- MPTP - 1-methyl-4-phenyl-1, 2, 3, 6,-tetrahydropyridine
- MS: Mass Spectrometry

- NR1 - NMDA-NR1 receptor
- OE: OverExpression
- P: Phosphorylation/Phosphate
- PBS-T - PBS 1x containing 0.1% Triton
- PD - Parkinson Disease
- PINK1 - PTEN-induced kinase 1
- PVDF - polyvinylidenedifluoride
- RP recycling Pool
- RRP - Readily Releasable Pool
- SNARE - Soluble N-ethylmaleimide-sensitive fusion protein-Attachment protein Receptor
- SNCA – Alpha Synuclein
- SNpc – Substantia Nigra Pars Compacta
- SV - Synaptic Vesicle
- TRAP1 - TNF receptor-associated protein 1
- UCHL-1 - Ubiquitin carboxyl-terminal esterase L1
- WB: Western Blot
- WT – Wild Type
- Y2H: Yeast Two Hybrid
- α-Syn – Alpha Synuclein